Patrick Launeau

Quantitative Image Analysis off Minerals and Rocks

Fabric analysis

- Shape preferred orientation (SPO) vs. strain quantification.
- Intercepts in digital images : a tool to analyze interconnection of grains in rocks vs. inertia tensor of individualized grains
- SPO vs Spatial distribution (Fry)
- Ellipsoid of SPO and strain by combining 3 ⊥ images.

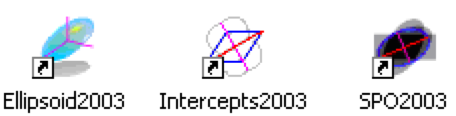

Patrick Launeau

Quantitative Image Analysis off Minerals and Rocks

Fabric analysis

- Shape preferred orientation (SPO) vs. strain quantification.
- Intercepts in digital images : a tool to analyze interconnection of grains in rocks vs. inertia tensor of individualized grains
- SPO vs Spatial distribution (Fry)
- Ellipsoid of SPO and strain by combining 3 ⊥ images.

Ellipsoid2003 Intercepts2003 SPO2003

Passive / active deformation

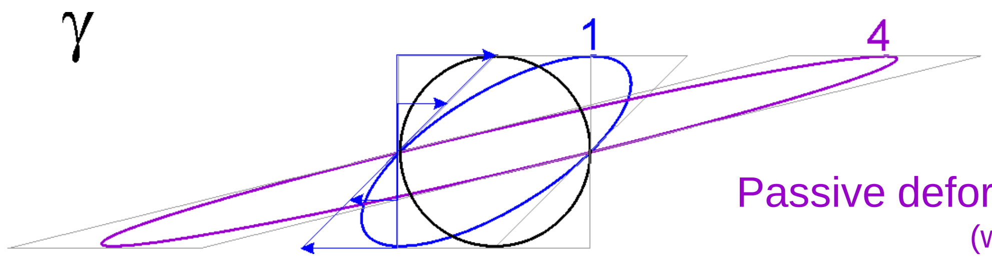

Passive deformation of an enclave
(with elongation of the shape)

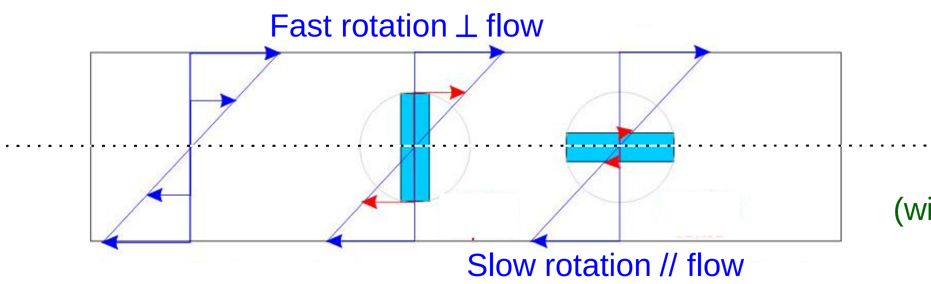

Preferred Orientation of rigid objects
(with out any change of the shape)

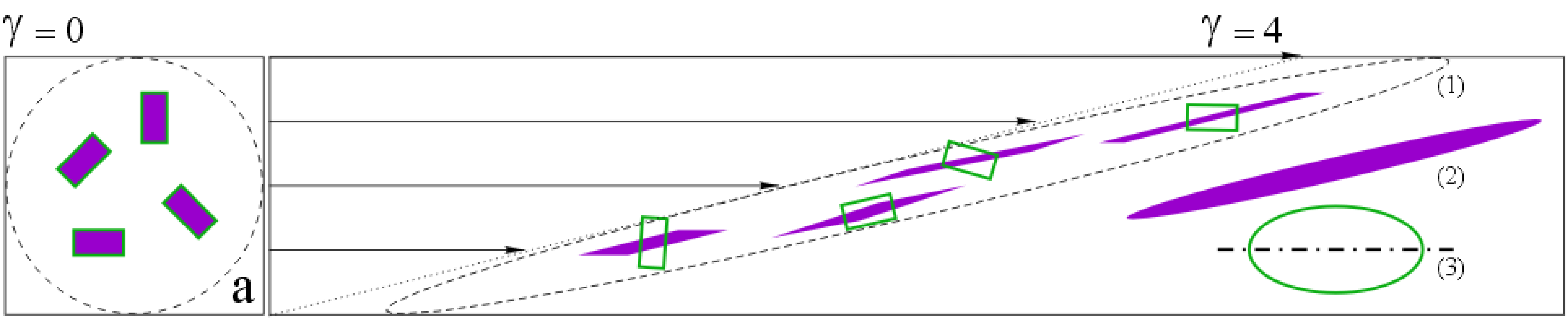

P. Launeau (2004) "Mise en évidence des écoulements magmatiques par analyse d'images 2-D des distributions 3-D d'Orientations Préférentielles de Formes". *Bull. Soc. Géol. Fr* , 175, 331-350

In a more realistic magma flow …

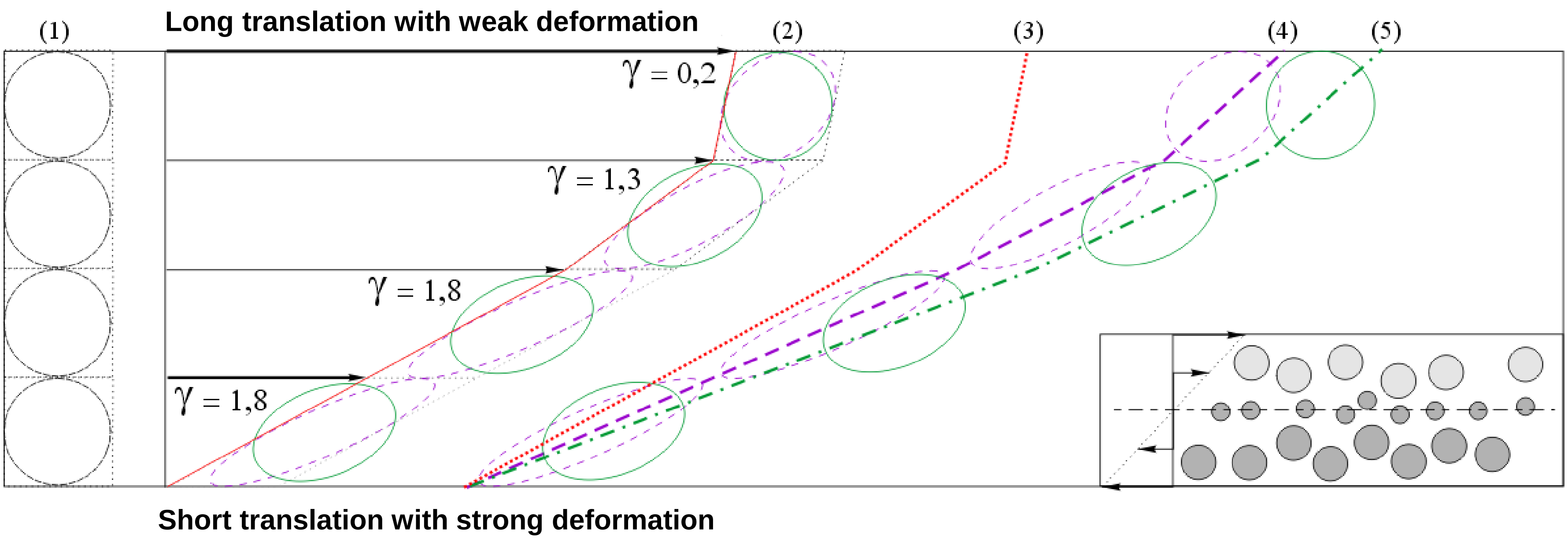

(1) Initial position of a magma bubble
(2) Final position of its vertical section in red, its shape in purple, the preferred orientation of its microlithes in green
(3) Alignment of the initial vertical sections of the magma bubbles
(4) Alignment of the ellipses of magma deformed passively
(5) Alignment of the ellipses of crystal preferred orientation

P. Launeau (2004) "Mise en évidence des écoulements magmatiques par analyse d'images 2-D des distributions 3-D d'Orientations Préférentielles de Formes". *Bull. Soc. Géol. Fr* , 175, 331-350

Preferred Orientation (PO)

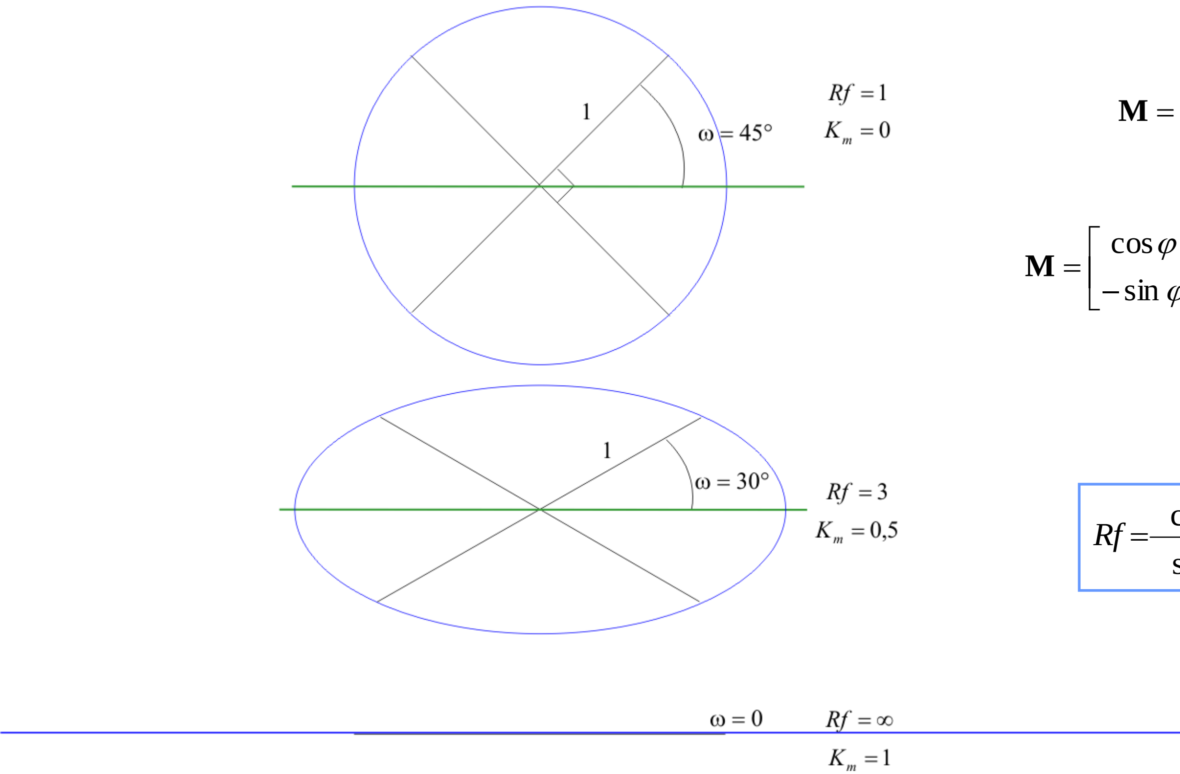

Cosines directions (Harvey & Laxton, 1980)

$$\mathbf{M} = \frac{1}{N}\begin{bmatrix} \sum \cos^2 \varphi_i & \sum \cos\varphi_i \sin\varphi_i \\ \sum \sin\varphi_i \cos\varphi_i & \sum \sin^2 \varphi_i \end{bmatrix}$$

$$\mathbf{M} = \begin{bmatrix} \cos\varphi & \sin\varphi \\ -\sin\varphi & \cos\varphi \end{bmatrix} \cdot \begin{bmatrix} \sqrt{Rf} & 0 \\ 0 & 1/\sqrt{Rf} \end{bmatrix} \cdot \begin{bmatrix} \cos\varphi & -\sin\varphi \\ \sin\varphi & \cos\varphi \end{bmatrix}$$

$$\boxed{Rf = \frac{\cos^2 \omega}{\sin^2 \omega} = \frac{1}{\tan^2 \omega}} \qquad K_m = \frac{Rf - 1}{Rf + 1}$$

P. Launeau (2004) "Mise en évidence des écoulements magmatiques par analyse d'images 2-D des distributions 3-D d'Orientations Préférentielles de Formes". *Bull. Soc. Géol. Fr* , 175, 331-350

Shape Preferred Orientation (SPO)

SPO → of shapes with long and short axes

A n=2 a=5,9926 cm b=3,9318 cm R=1,524 [1,729]n [1,734]b , 89,99°
K=0,398, Kn=0,498 {0,799}, Kb=0,501 {0,795}

R=1,5 $\sqrt{Rf}=1{,}7$

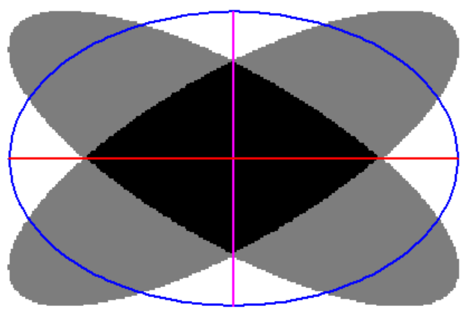

$R \leq \sqrt{Rf}$ when $r \geq 10$

$R < \sqrt{Rf}$ when $1 < r < 10$

ω+π/2 R=3 $\sqrt{Rf}=\infty$

ω

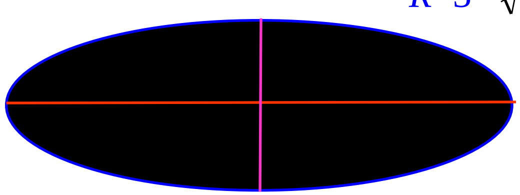

$$R = \frac{d(\omega)}{d(\omega + \pi/2)}$$

Normalization to k

$$k = \frac{r^2 - 1}{r^2 + 1}$$

$$K_n = K / k$$

$$R_n = \sqrt{\frac{1 + K_n}{1 - K_n}}$$

r $K = \frac{R^2 - 1}{R^2 + 1}$

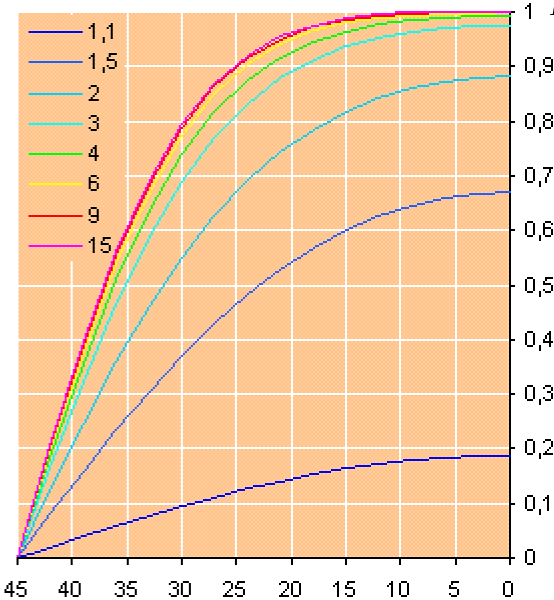

P. Launeau (2004) "Mise en évidence des écoulements magmatiques par analyse d'images 2-D des distributions 3-D d'Orientations Préférentielles de Formes". *Bull. Soc. Géol. Fr* , 175, 331-350

Quantitative Image Analysis of Minerals and Rocks

http://www.sciences.univ-nantes.fr/lpgnantes/SPO

2D magma flow

SPO with strain record
(passive deformation)

SPO without strain record
(active deformation)

Jeffery 1922

$$\tan\beta' = r \cdot \tan\left[\frac{r \cdot \gamma}{r^2+1} + \arctan\left(\frac{\tan\beta}{r}\right)\right]$$

$$\gamma_c = \frac{\pi}{\sqrt{1-k^2}} \qquad k = \frac{r^2-1}{r^2+1}$$

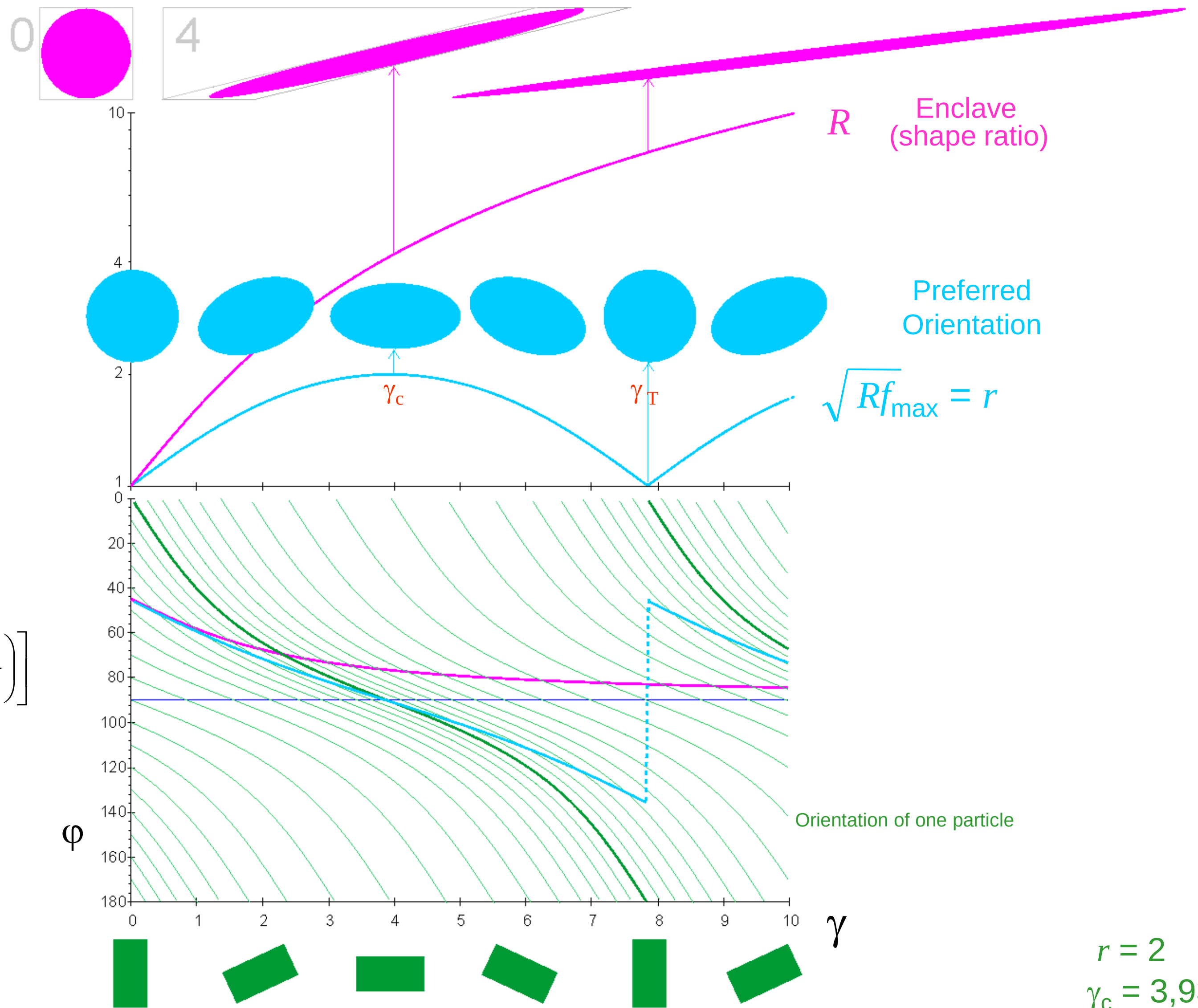

$r = 2$
$\gamma_c = 3,93$

P. Launeau (2004) "Mise en évidence des écoulements magmatiques par analyse d'images 2-D des distributions 3-D d'Orientations Préférentielles de Formes". *Bull. Soc. Géol. Fr* , 175, 331-350

Simple shear in 3D

3D

Jeffery (1922), Reed and Tryggvason (1974) et Willis (1977)

$$\tan\beta' = r \cdot \tan\left[\frac{r \cdot \gamma}{r^2+1} + \arctan\left(\frac{\tan\beta}{r}\right)\right] \qquad \tan^2\psi' = \tan^2\psi \cdot \left(\frac{r \cdot \cos^2\beta + \sin^2\beta}{r \cdot \cos^2\beta' + \sin^2\beta'}\right)$$

$r = 1,5$

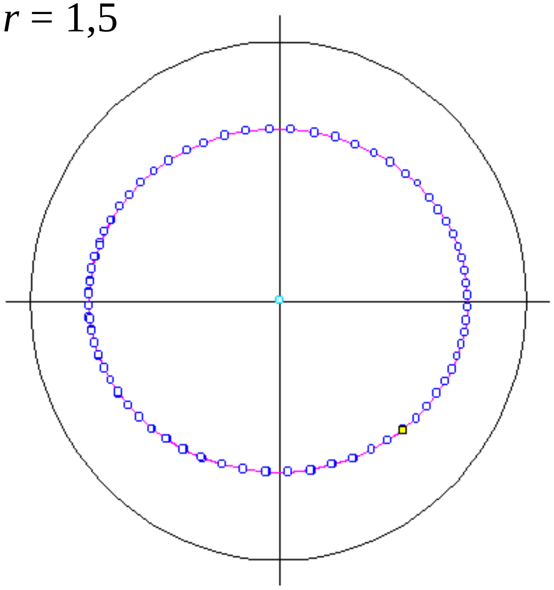

1,5 : 1 : 1

$r = 2,5$

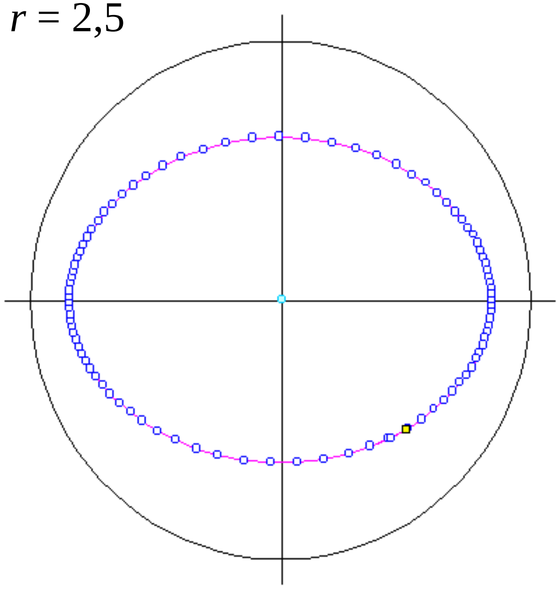

2,5 : 1 : 1

P. Launeau (2004) "Mise en évidence des écoulements magmatiques par analyse d'images 2-D des distributions 3-D d'Orientations Préférentielles de Formes". *Bull. Soc. Géol. Fr* , 175, 331-350

UMR 6112
PLANÉTOLOGIE & GÉODYNAMIQUE

Quantitative Image Analysis of Minerals and Rocks

http://www.sciences.univ-nantes.fr/lpgnantes/SPO

3D magma flow

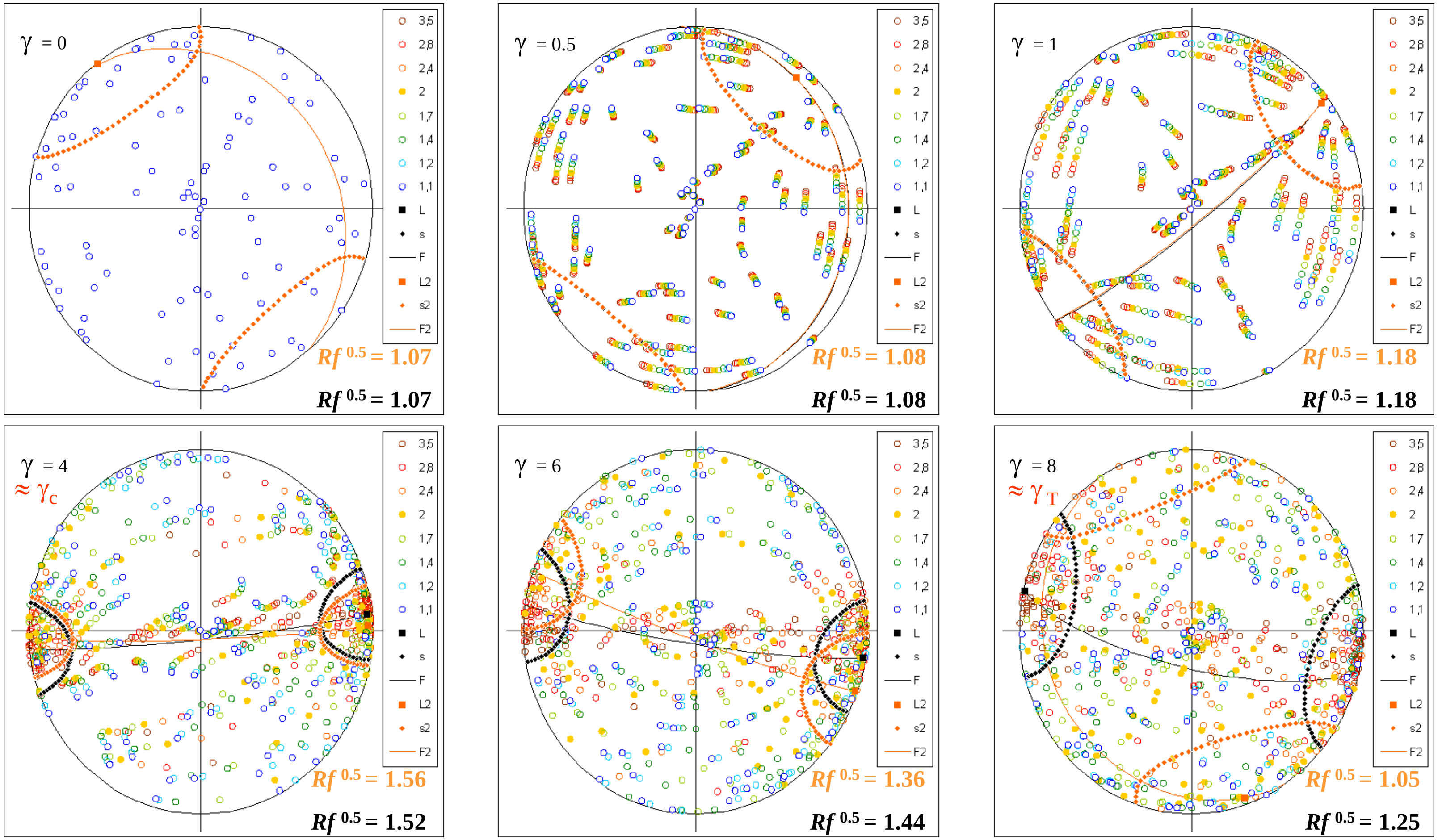

Ellipsoid 2:1:1 $r_{a/c} = 2$

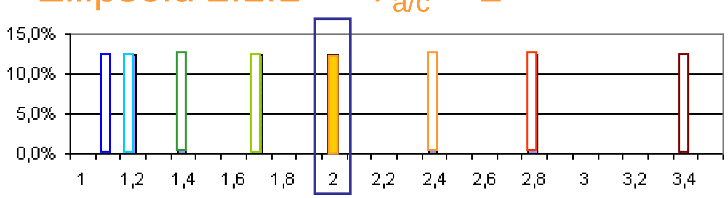

The PO of one class of aspect ratio is cyclic

The PO of standard CSD is not cyclic

Jeffery (1922), Reed and Tryggvason (1974) et Willis (1977)

$$\tan\beta' = r \cdot \tan\left[\frac{r \cdot \gamma}{r^2+1} + \arctan\left(\frac{\tan\beta}{r}\right)\right]$$

$$\tan^2\psi' = \tan^2\psi \cdot \left(\frac{r \cdot \cos^2\beta + \sin^2\beta}{r \cdot \cos^2\beta' + \sin^2\beta'}\right)$$

Ellipsoid 2:1:1

$r_{a/c} = 2$

SPO with strong initial SPO tend toward a weak SPO along a magma flow

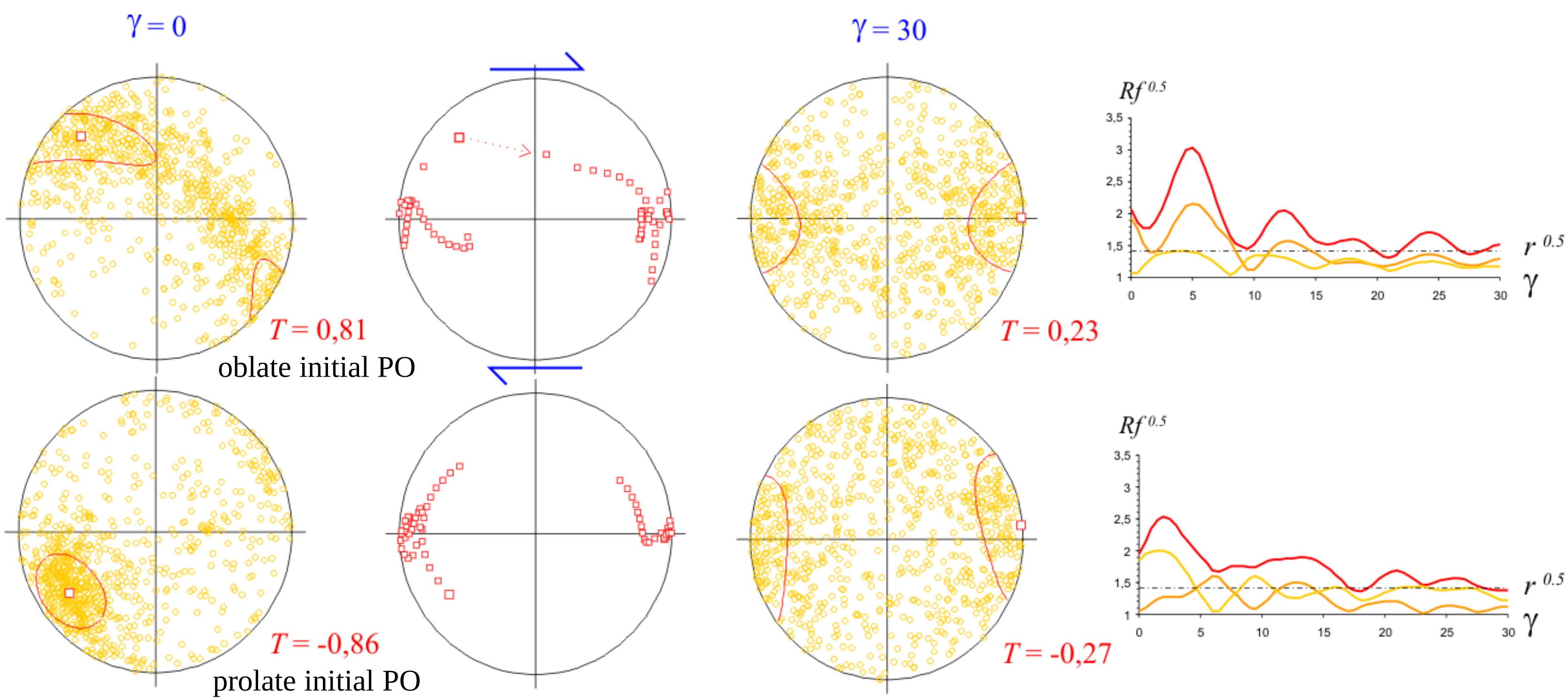

P. Launeau (2004) "Mise en évidence des écoulements magmatiques par analyse d'images 2-D des distributions 3-D d'Orientations Préférentielles de Formes". *Bull. Soc. Géol. Fr* , 175, 331-350

Passive / active deformation

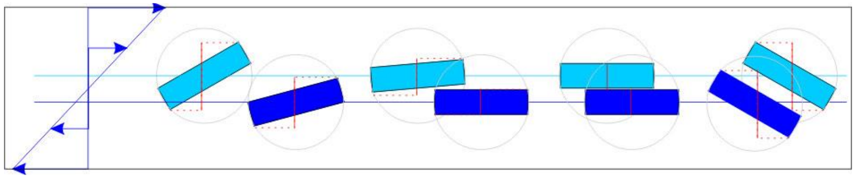

Particle interactions may reduce the object rotation

P. Launeau (2004) "Mise en évidence des écoulements magmatiques par analyse d'images 2-D des distributions 3-D d'Orientations Préférentielles de Formes". *Bull. Soc. Géol. Fr* , 175, 331-350

Patrick Launeau

Quantitative Image Analysis off Minerals and Rocks

Fabric analysis

- Shape preferred orientation (SPO) vs. strain quantification.
- Intercepts in digital images : a tool to analyze interconnection of grains in rocks vs. inertia tensor of individualized grains
- SPO vs Spatial distribution (Fry)
- Ellipsoid of SPO and strain by combining 3 ⊥ images.

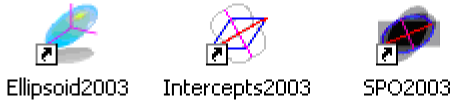

Image analysis

First hypothesis :

do we have isolated crystals or aggregates ?

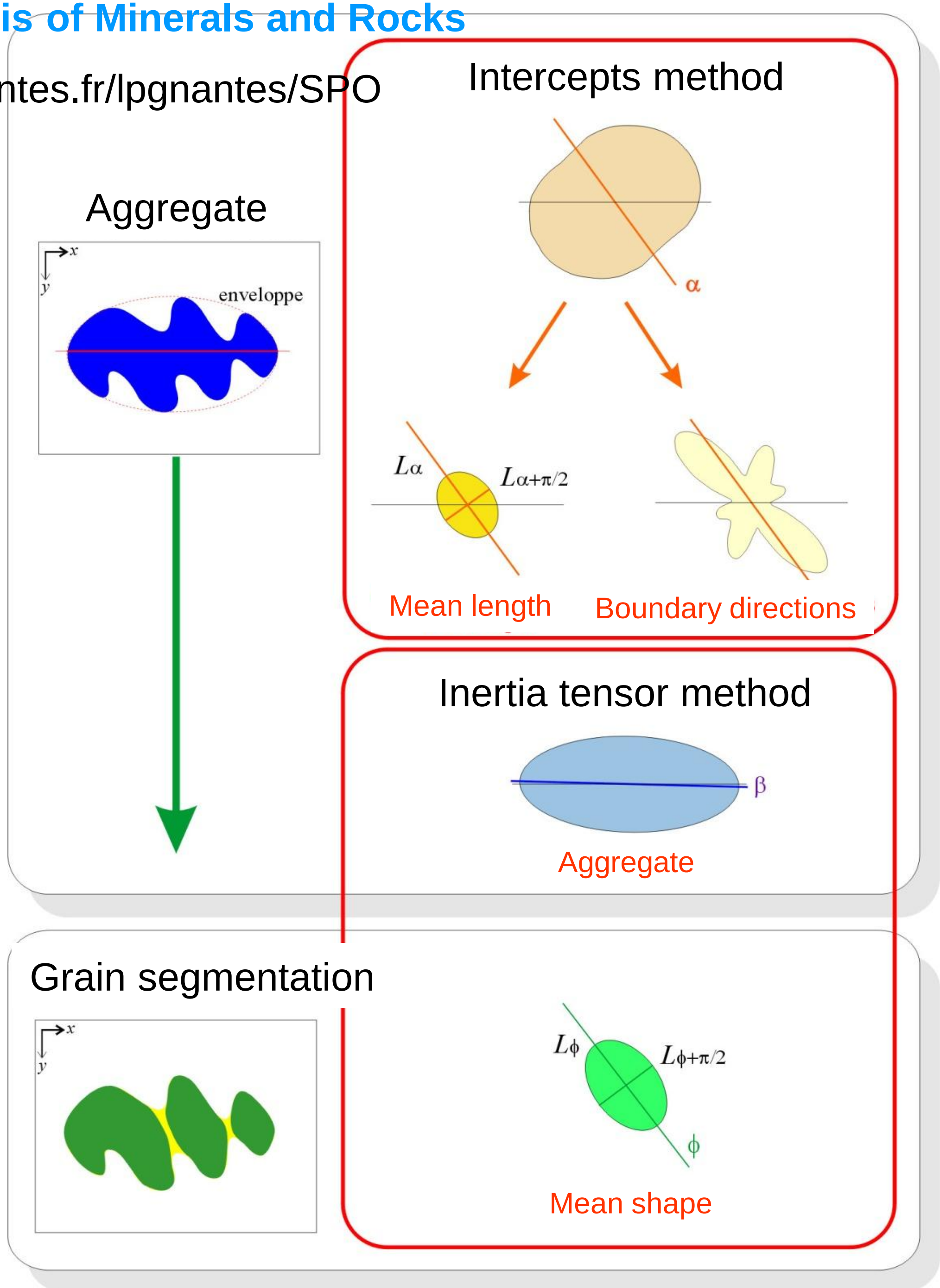

P. Launeau (2004) "Mise en évidence des écoulements magmatiques par analyse d'images 2-D des distributions 3-D d'Orientations Préférentielles de Formes". *Bull. Soc. Géol. Fr* , 175, 331-350

Shape analysis with inertia tensor

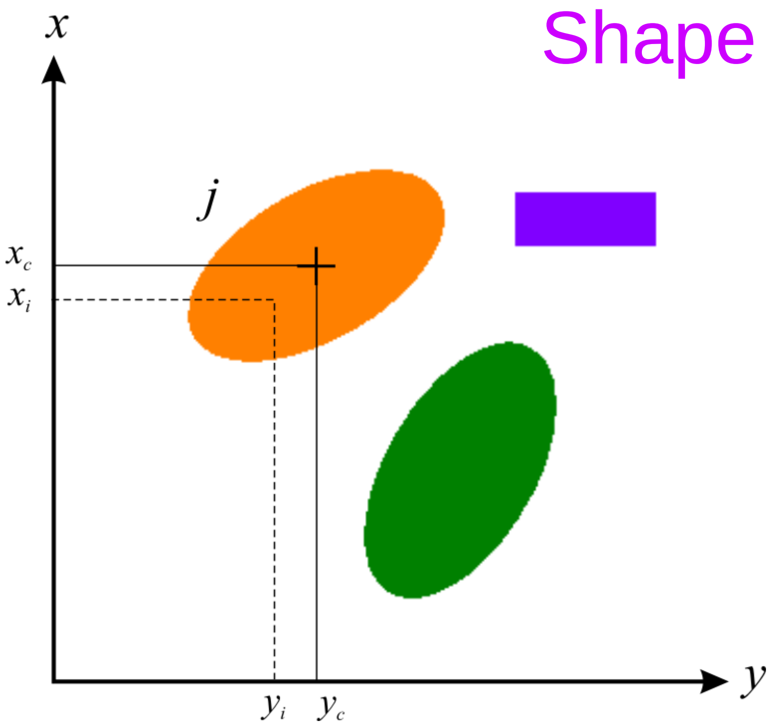

Case of 1 object

$$x_c = \frac{1}{A}\sum_i x_i$$

$$y_c = \frac{1}{A}\sum_i y_i$$

$$m_{xxj} = \frac{1}{A}\sum_i (x_i - x_c)^2$$

$$m_{xyj} = \frac{1}{A}\sum_i (x_i - x_c)(y_i - y_c)$$

$$m_{yyj} = \frac{1}{A}\sum_i (y_i - y_c)^2$$

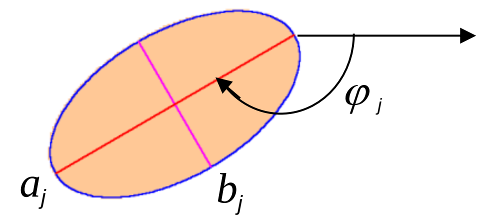

$$r_j = \frac{a_j}{b_j}$$

$$\mathbf{M}_j = \begin{vmatrix} m_{xxj} & m_{xyj} \\ m_{xyj} & m_{yyj} \end{vmatrix}$$

$$\mathbf{M}_j = \begin{bmatrix} \cos\varphi_j & \sin\varphi_j \\ -\sin\varphi_j & \cos\varphi_j \end{bmatrix} \cdot \begin{bmatrix} a_j^2/4 & 0 \\ 0 & b_j^2/4 \end{bmatrix} \cdot \begin{bmatrix} \cos\varphi_j & -\sin\varphi_j \\ \sin\varphi_j & \cos\varphi_j \end{bmatrix}$$

Rink, M. (1976). – A computerized quantitative image analysis procedure for investigating features and an adapted image process. *Journal of Microscopy*, 107: 267-286

Case of *N* objects

$$\mathbf{M} = \frac{1}{N}\sum_j \mathbf{M}_j = \frac{1}{N}\begin{vmatrix} \sum_j m_{xxj} & \sum_j m_{xyj} \\ \sum_j m_{xyj} & \sum_j m_{yyj} \end{vmatrix}$$

$$R = \frac{a}{b} = \sqrt{\frac{\rho_1}{\rho_2}}$$

P. Launeau (2004) "Mise en évidence des écoulements magmatiques par analyse d'images 2-D des distributions 3-D d'Orientations Préférentielles de Formes". *Bull. Soc. Géol. Fr* , 175, 331-350

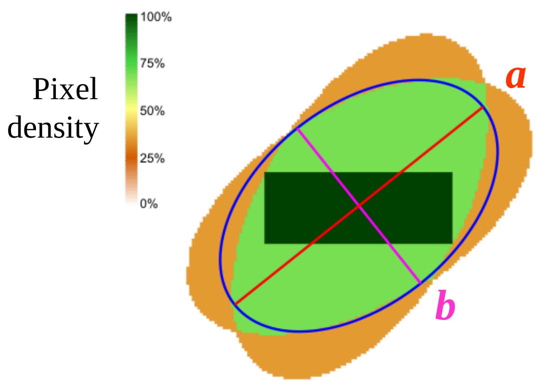

Stack of object piled on their gravity centre

Other shape parameters …

Inertia tensor ellipse

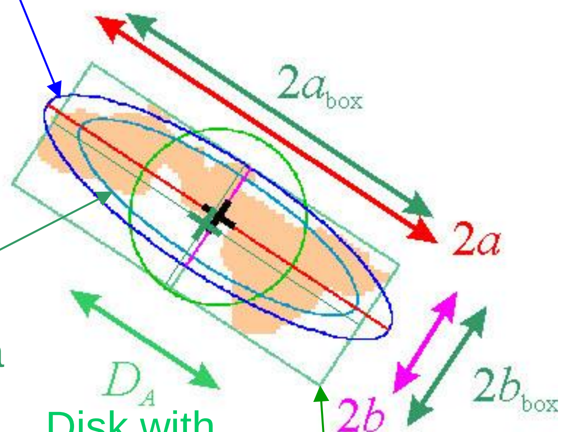

Ellipse with identical surface area

Disk with identical surface area

Rectangular box

Shape n°

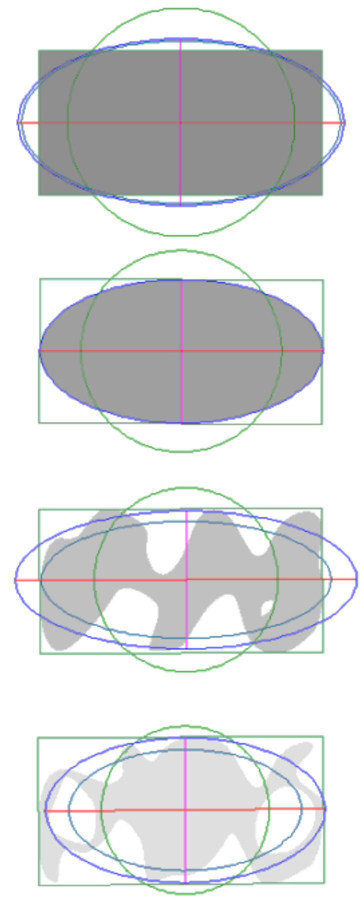

1 : rectangle

r = 2

2 : ellipse

r = 2

3 : *“centrifugal” shape*

r = 2,4

4 : *“centripetal” shape*

r = 2

P. Launeau (2004) "Mise en évidence des écoulements magmatiques par analyse d’images 2-D des distributions 3-D d’Orientations Préférentielles de Formes". *Bull. Soc. Géol. Fr* , 175, 331-350

Quantitative Image Analysis of Minerals and Rocks

http://www.sciences.univ-nantes.fr/lpgnantes/SPO

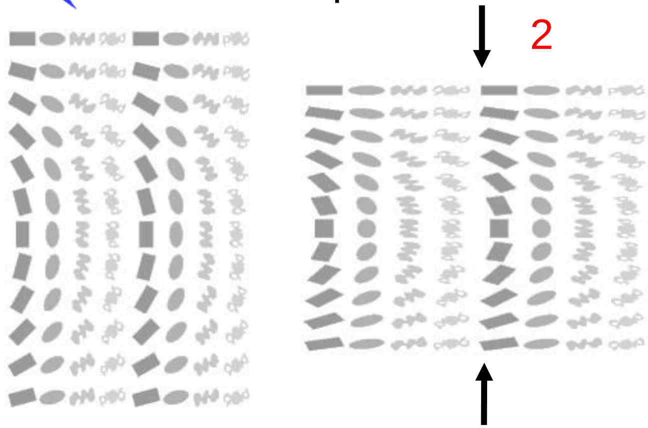

Passive Deformation

no viscosity contrast

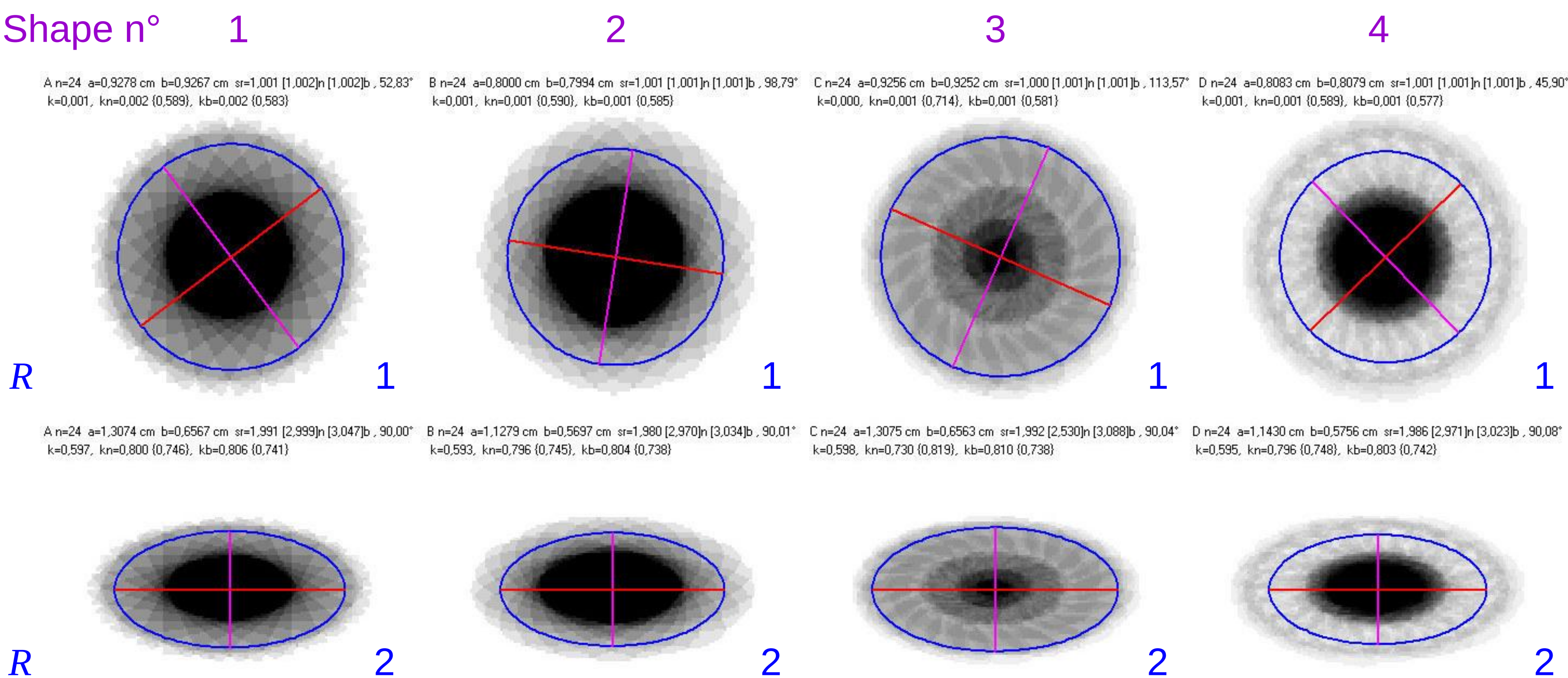

P. Launeau (2004) "Mise en évidence des écoulements magmatiques par analyse d'images 2-D des distributions 3-D d'Orientations Préférentielles de Formes". *Bull. Soc. Géol. Fr* , 175, 331-350

Active Deformation

rigid body rotation

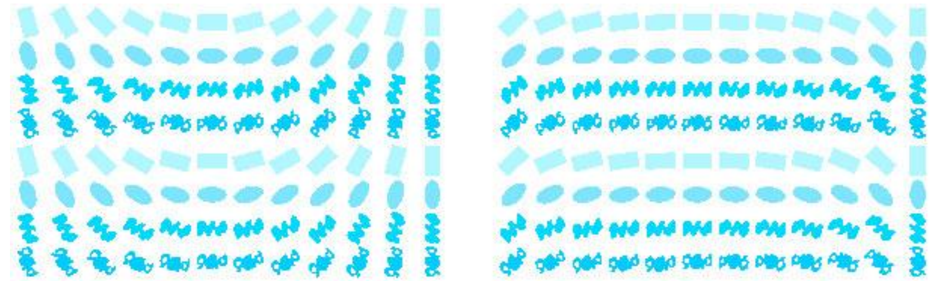

P.K. Harvey et C.C. Ferguson, 1978

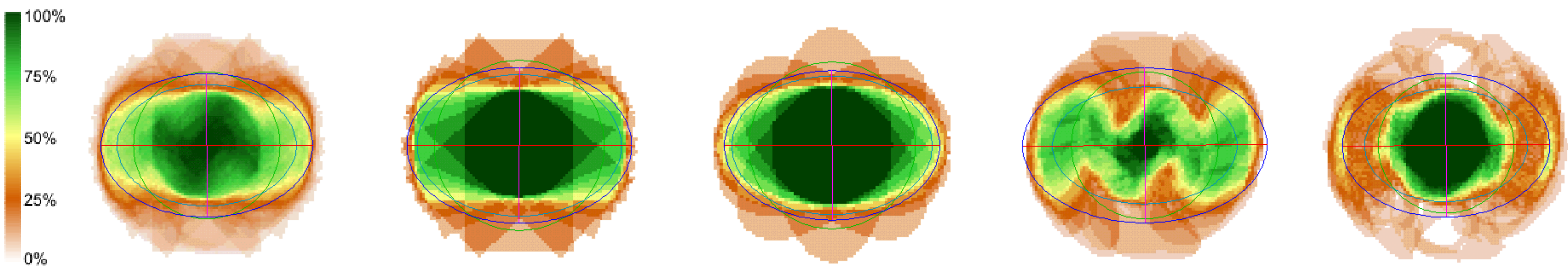

Shape n°	1234	1	2	3	4
$R\gamma_c$	1,48	1,44	1,44	1,57	1,44
R_n	1,99	1,95	1,98	1,99	1,99
r	2	2	2	2,4	2

P. Launeau (2004) "Mise en évidence des écoulements magmatiques par analyse d'images 2-D des distributions 3-D d'Orientations Préférentielles de Formes". *Bull. Soc. Géol. Fr* , 175, 331-350

Case of 1 object

Shape analysis with the intercepts

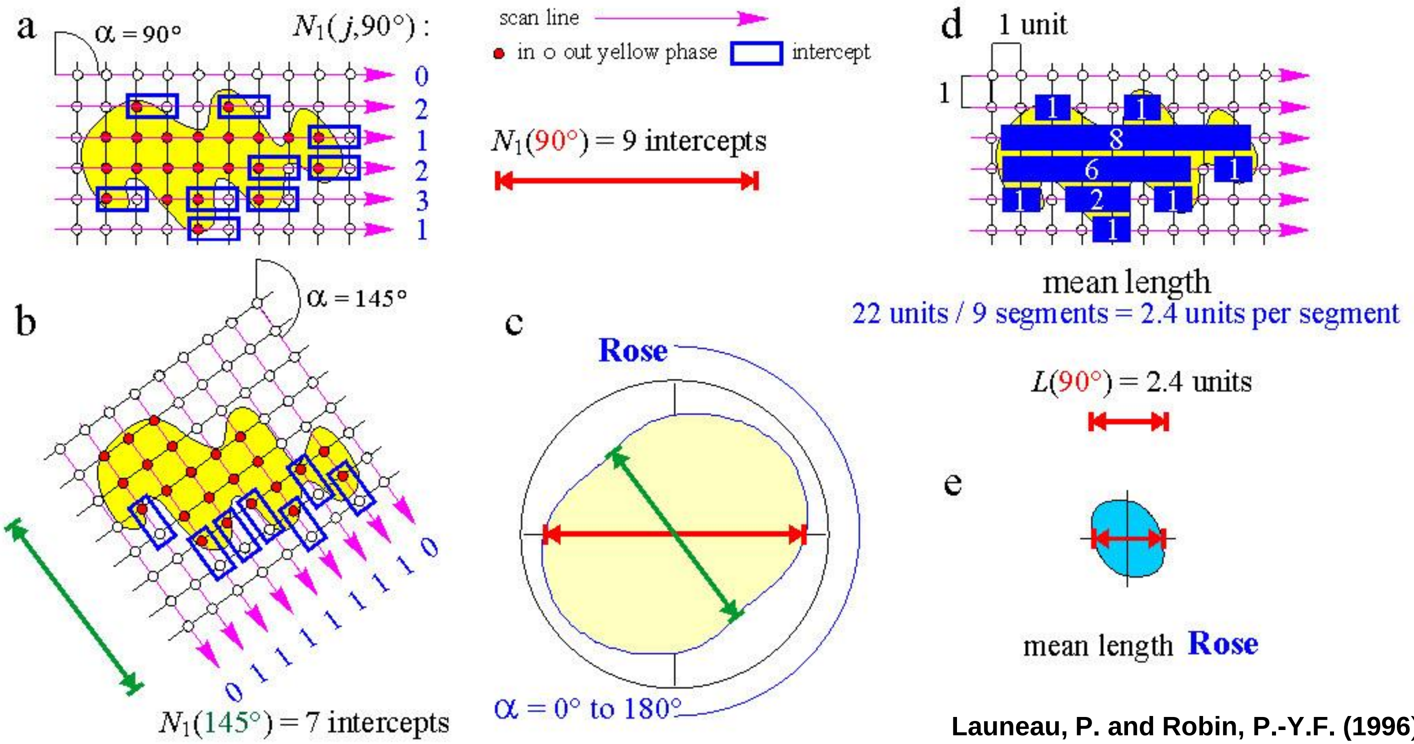

Launeau, P. and Robin, P.-Y.F. (1996). – Fabric analysis using the intercept method. *Tectonophysics* 267, 91-119

UMR 6112
PLANÉTOLOGIE & GÉODYNAMIQUE

Quantitative Image Analysis of Minerals and Rocks

http://www.sciences.univ-nantes.fr/lpgnantes/SPO

Case of 1 object

Shape analysis with the intercepts

Theoretical shapes of roses

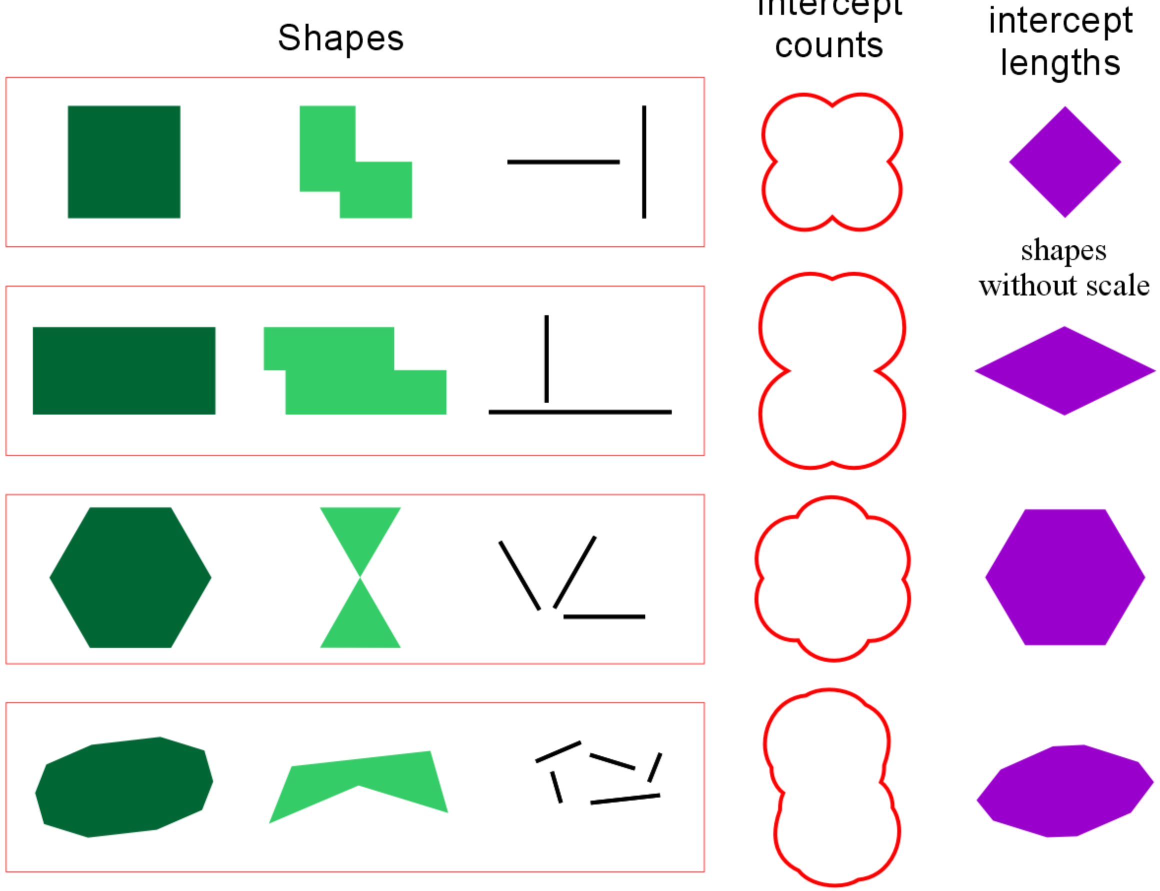

Launeau, P. and Robin, P.-Y.F. (1996). –
Fabric analysis using the intercept method.
Tectonophysics 267, 91-119

Case of *N* objects

Shape analysis with the intercepts

A n=2 a=5,9926 cm b=3,9318 cm R=1,524 [1,729]n [1,734]b , 89,99°
K=0,398, Kn=0,498 {0,799}, Kb=0,501 {0,795}

$r = 3 \quad R = 1{,}52$

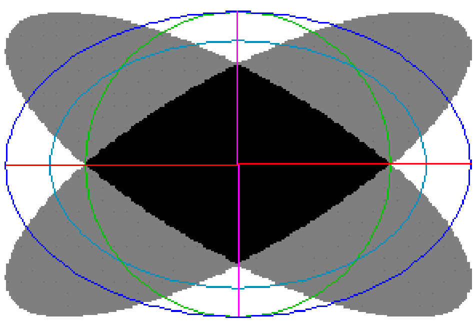

A a=3,9357 cm b=2,5886 cm R=1,520 , 90,12°

(1) 84°

$R = 1{,}52$

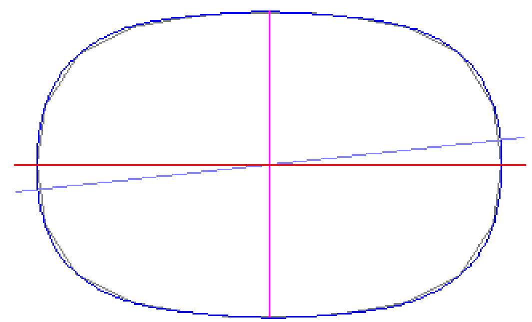

A a=11,9422 cm b=7,8547 cm R=1,520 , 90,12°

(1) 60°
(2) 120°

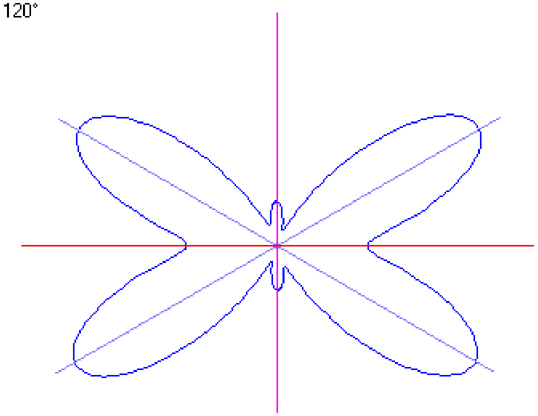

Inertia tensor

Lengths of intercepts

Boundaries directions

A n=2 a=0,4883 cm b=0,3171 cm R=1,540 [1,732]n [1,746]b , 89,82°
K=0,407, Kn=0,500 {0,814}, Kb=0,506 {0,804}

$r = 3 \quad R = 1{,}54$

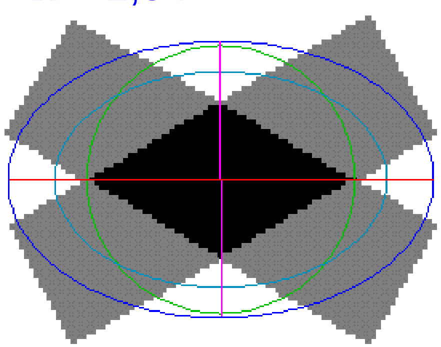

A a=0,2599 cm b=0,1990 cm R=1,306 , 89,98°

(1) 61°
(2) 117°

$R = 1{,}30$

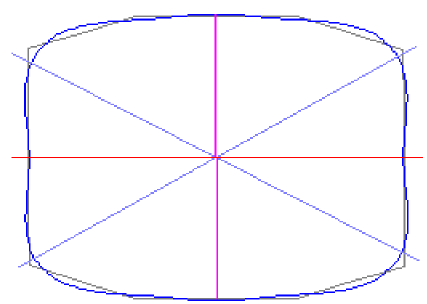

A a=0,9649 cm b=0,7434 cm R=1,298 , 89,98°

(1) 23°
(2) 63°
(3) 117°
(4) 158°

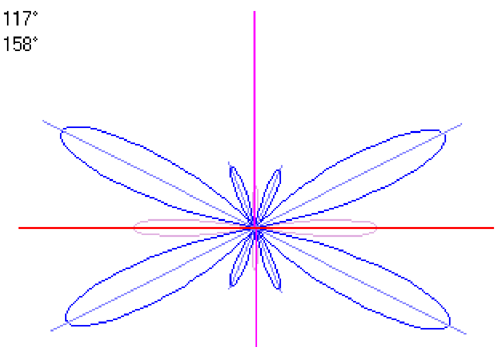

Intercepts are sensitive to the boundary

Launeau, P. and Robin, P.-Y.F. (1996). – Fabric analysis using the intercept method. *Tectonophysics* 267, 91-119

SPO of objects with any boundary geometry

Inertia tensor

intercepts

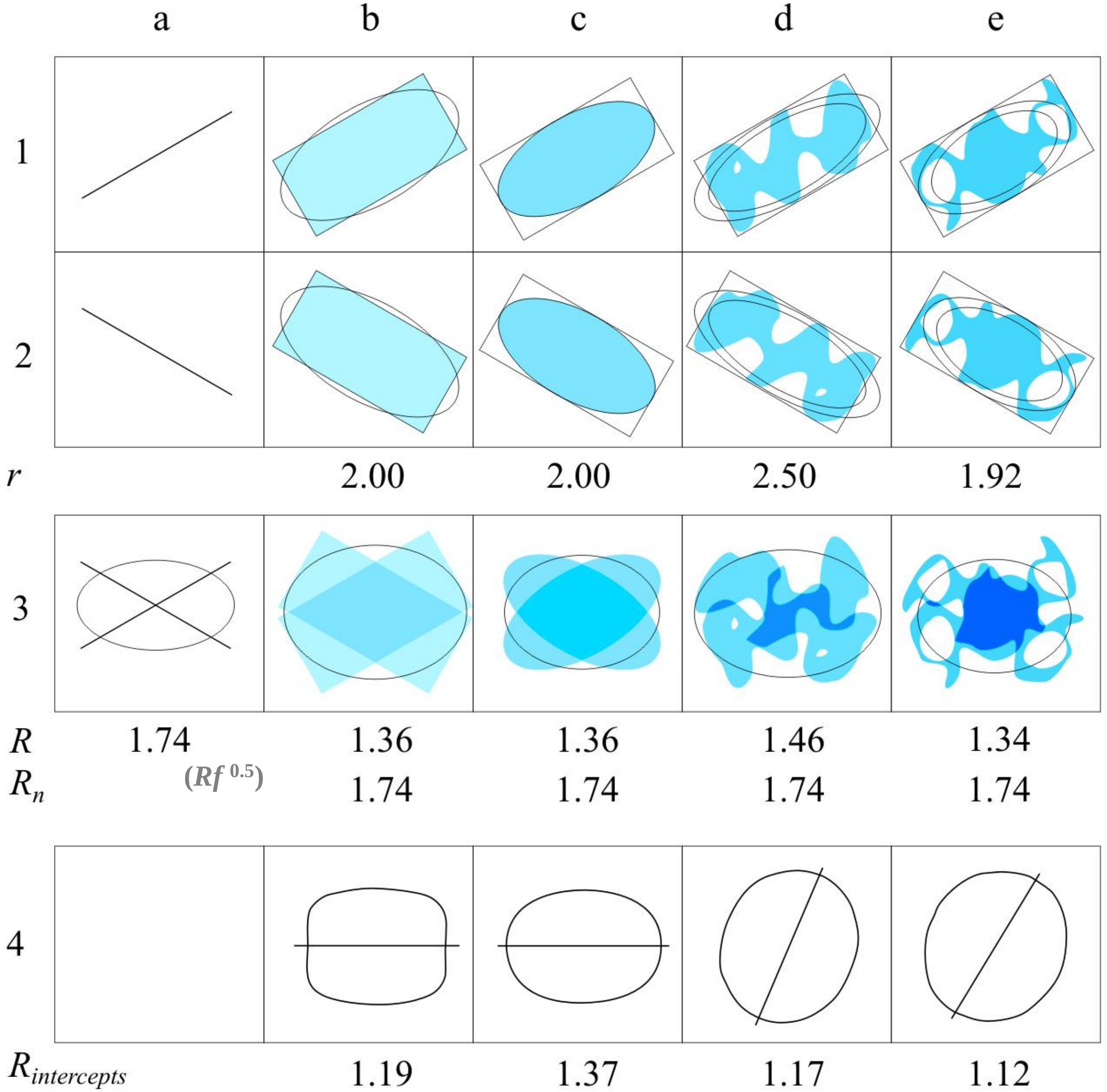

P. Launeau (2004) "Mise en évidence des écoulements magmatiques par analyse d'images 2-D des distributions 3-D d'Orientations Préférentielles de Formes". *Bull. Soc. Géol. Fr* , 175, 331-350

Quantitative Image Analysis of Minerals and Rocks

http://www.sciences.univ-nantes.fr/lpgnantes/SPO

P. Launeau (2004) "Mise en évidence des écoulements magmatiques par analyse d'images 2-D des distributions 3-D d'Orientations Préférentielles de Formes". *Bull. Soc. Géol. Fr* , 175, 331-350

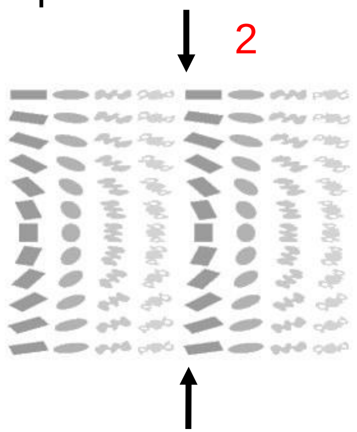

Passive Deformation

no viscosity contrast

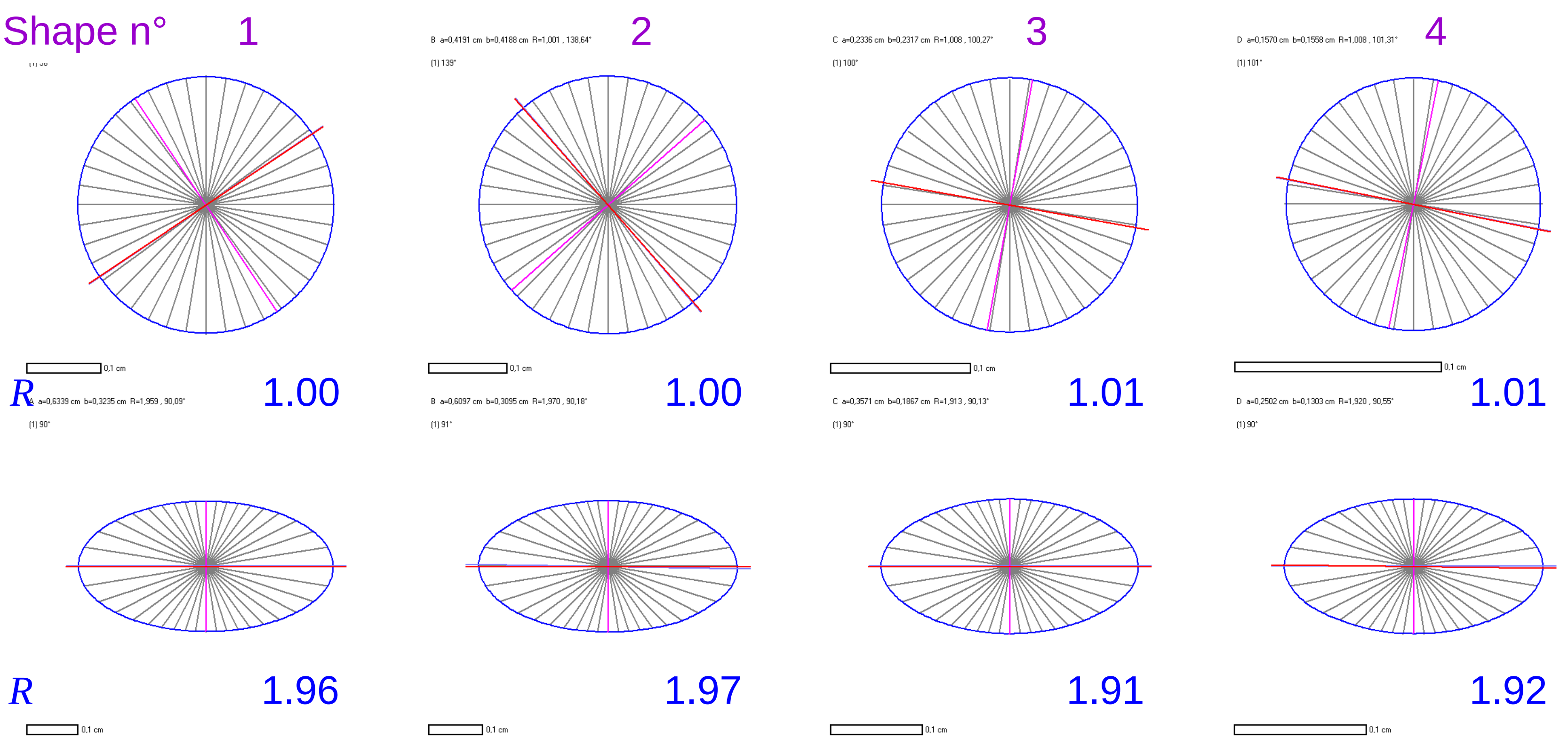

Passive / Active Deformation

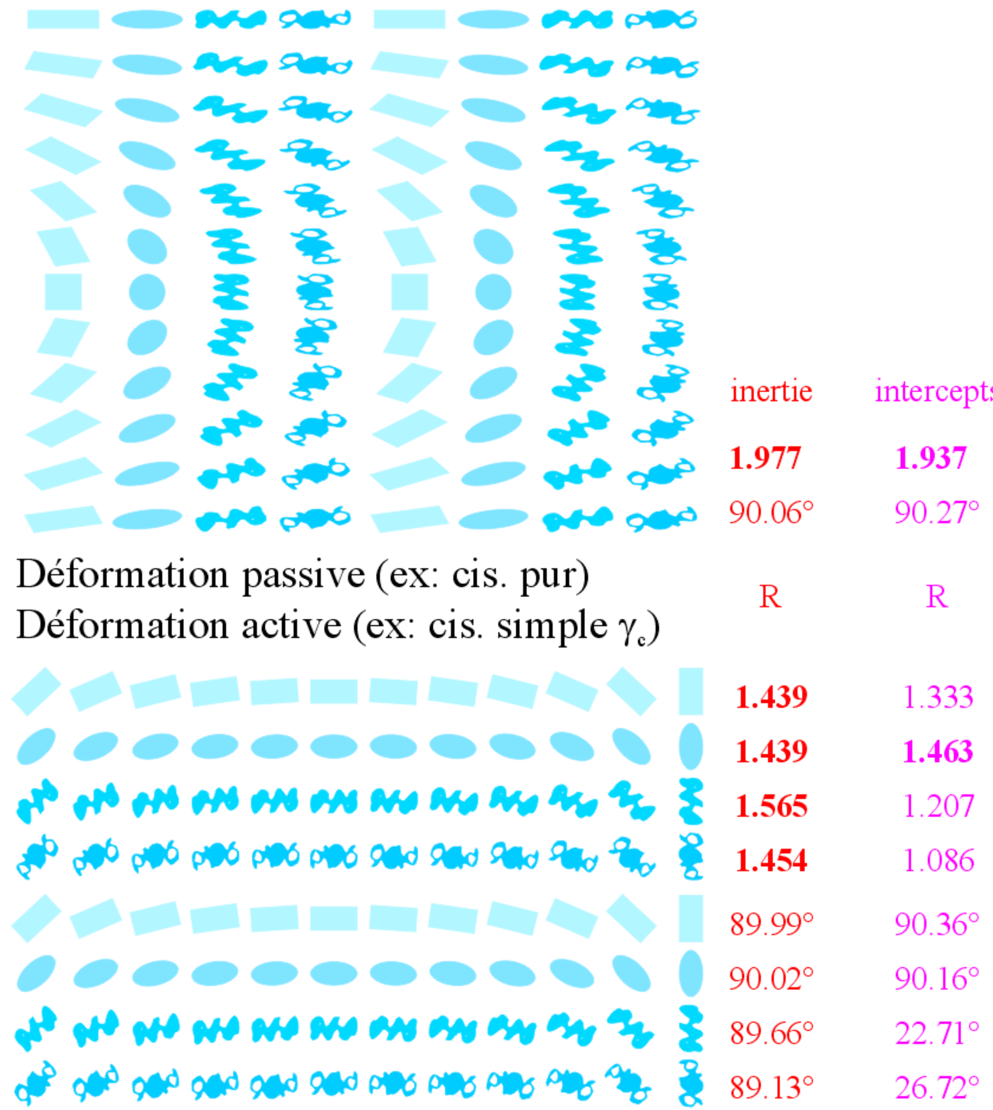

P. Launeau (2004) "Mise en évidence des écoulements magmatiques par analyse d'images 2-D des distributions 3-D d'Orientations Préférentielles de Formes". *Bull. Soc. Géol. Fr* , 175, 331-350

Application to digital images

Connexity

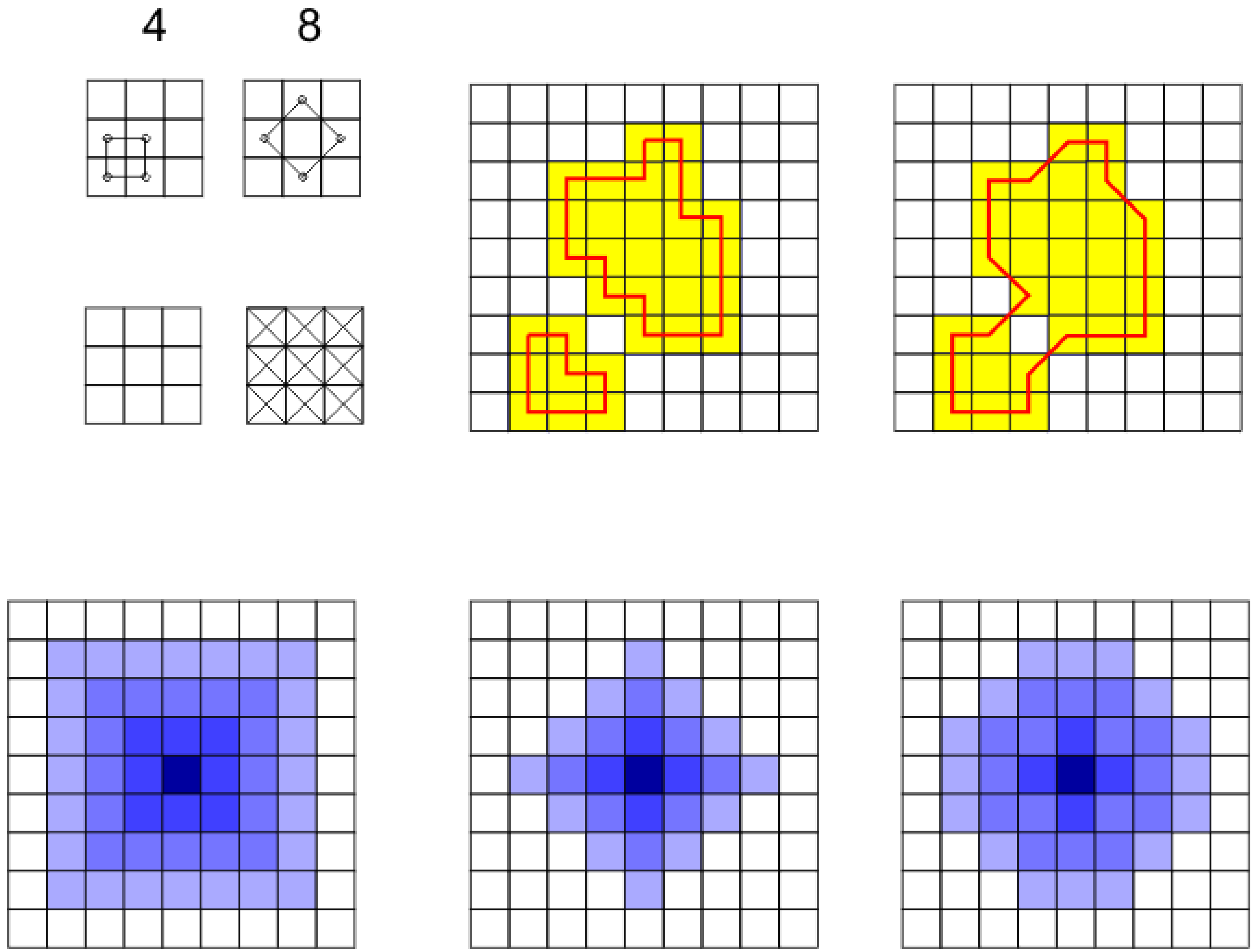

UMR 6112
PLANÉTOLOGIE &
GÉODYNAMIQUE

Inertia tensor

Scanning of one object

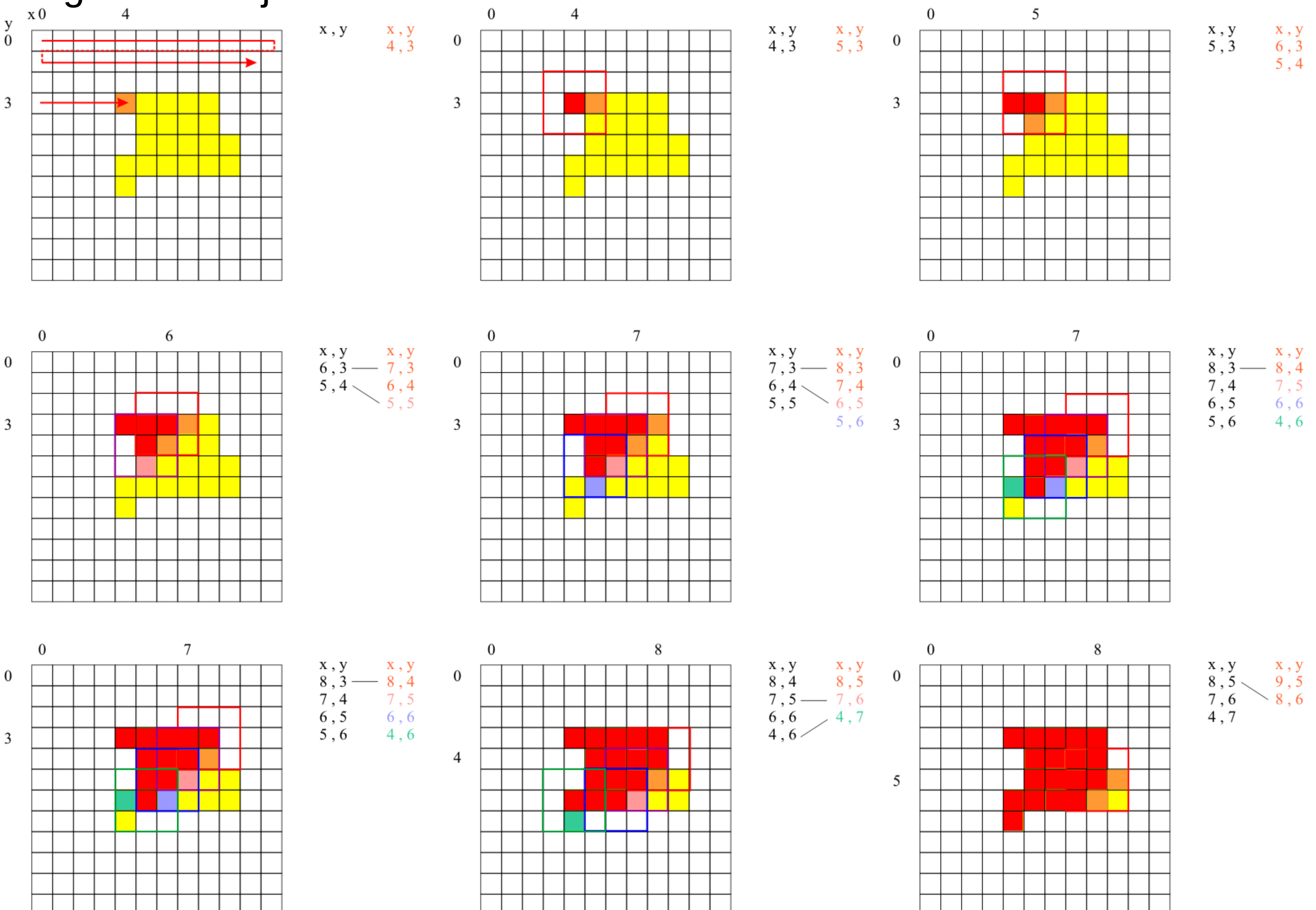

Quantitative Image Analysis of Minerals and Rocks

http://www.sciences.univ-nantes.fr/lpgnantes/SPO

Density of intercept count

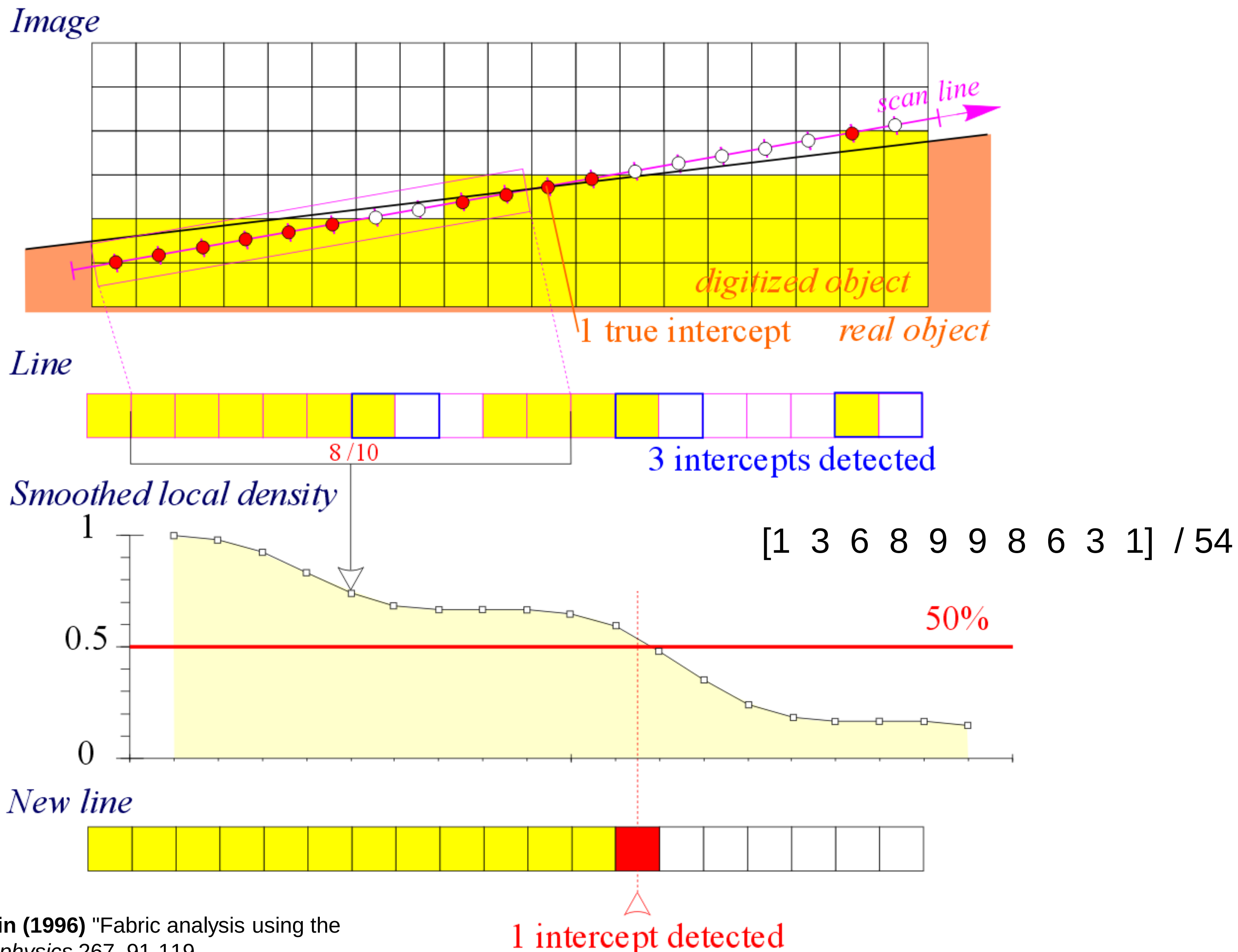

P. Launeau and P-Y. Robin (1996) "Fabric analysis using the intercept method". *Tectonophysics* 267, 91-119

1 – resampling along any line direction in grey level

2 – smoothing sampled line with [1 3 6 8 9 9 8 6 3 1] / 54
minimized over counts of intercepts

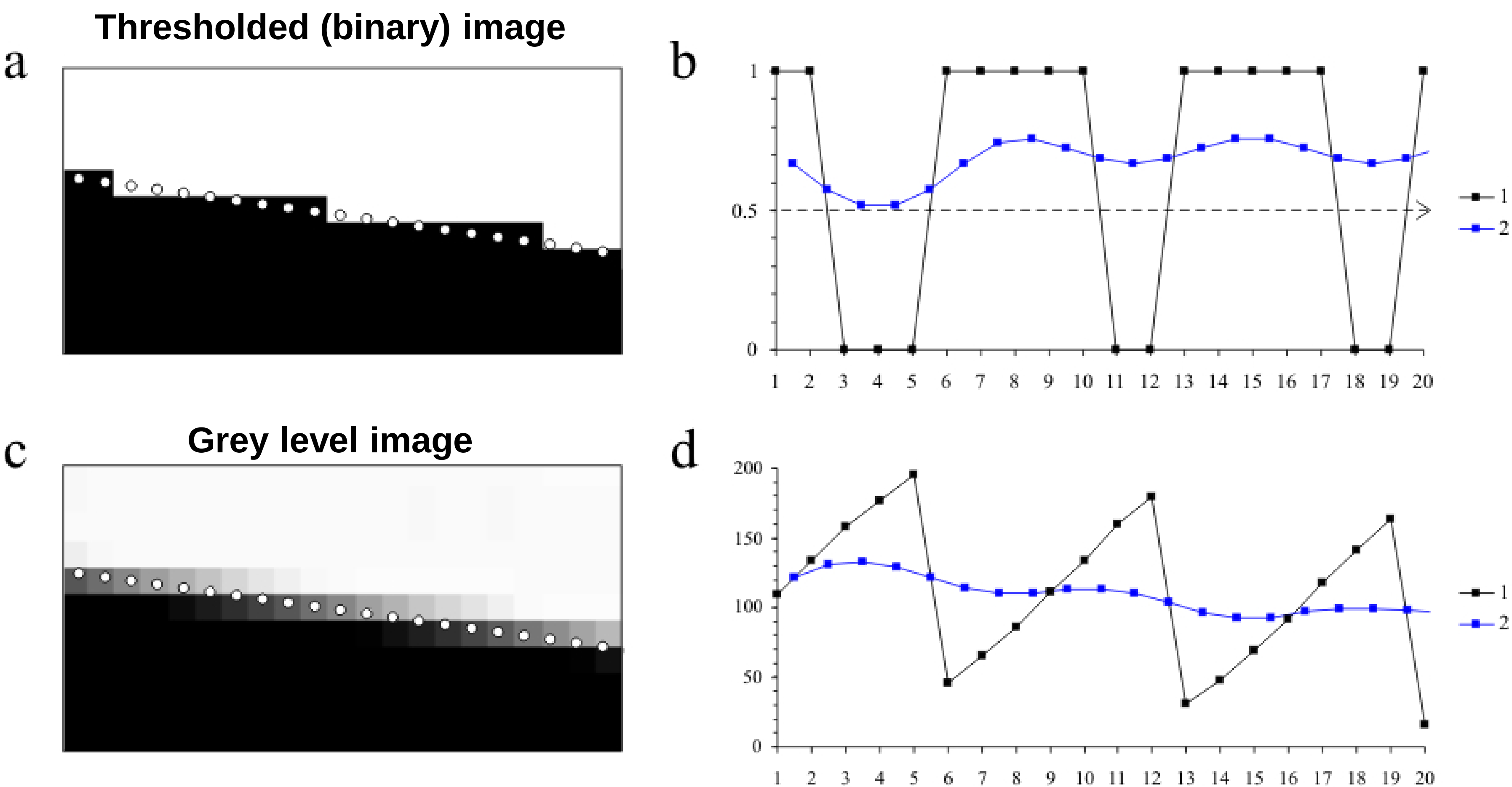

Launeau P., Archanjo C. J., Picard D., Arbaret L., Robin P.Y. (2010). Two- and three-dimensional shape fabric analysis by the intercept method in grey levels. Tectonophysics, Volume 492, Issues 1-4, 20 September 2010, Pages 230-239

Intercept detection *i* in grey levels

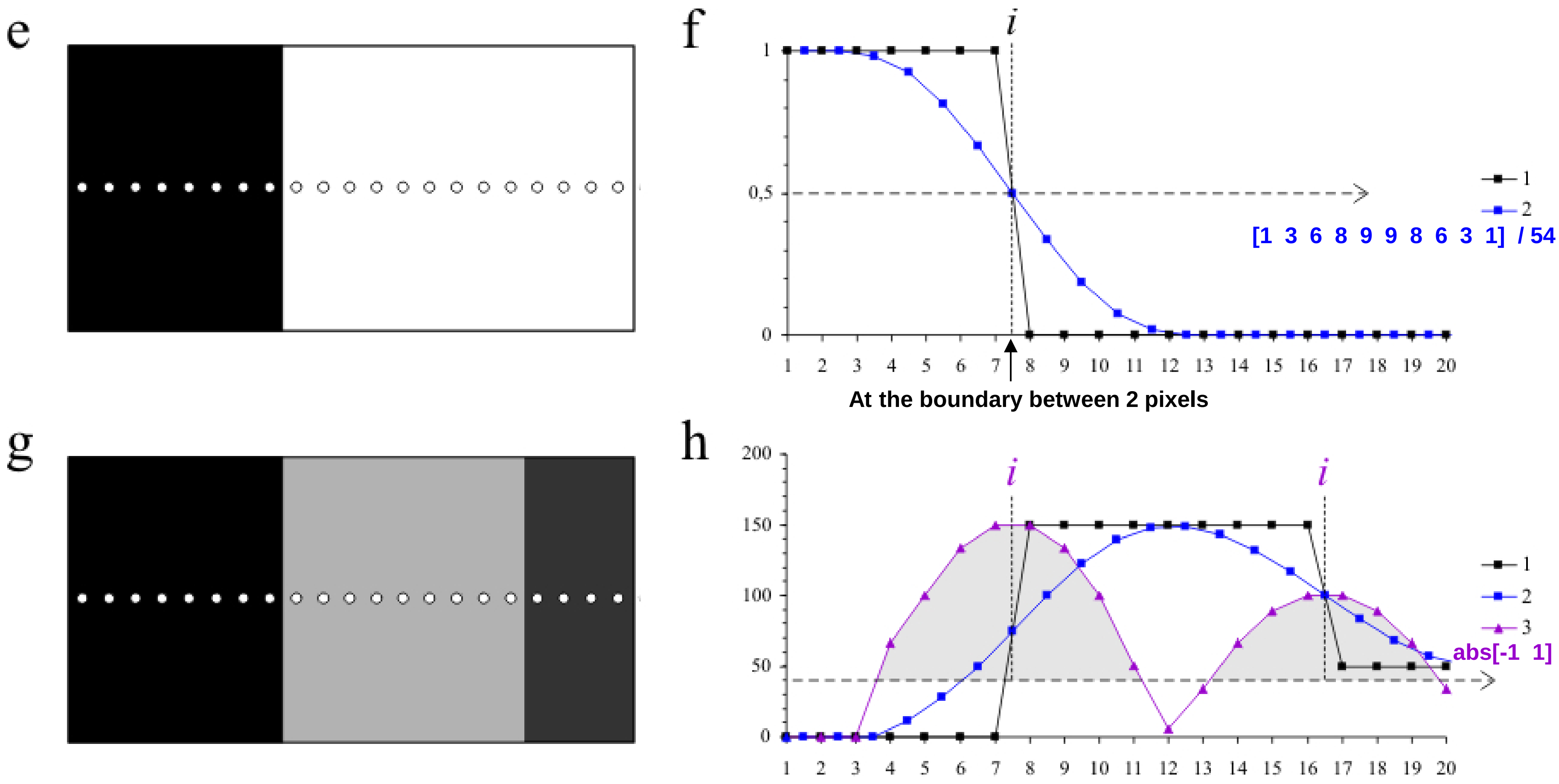

Launeau P., Archanjo C. J., Picard D., Arbaret L., Robin P.Y. (2010). Two- and three-dimensional shape fabric analysis by the intercept method in grey levels. Tectonophysics, Volume 492, Issues 1-4, 20 September 2010, Pages 230-239

Intercept detection *i* in grey levels (sp. case)

In case of one grey phase with dark boundaries the intercepts detection occures only from a dark pixel to a bright pixel to avoid double detection on both sides of each boundary

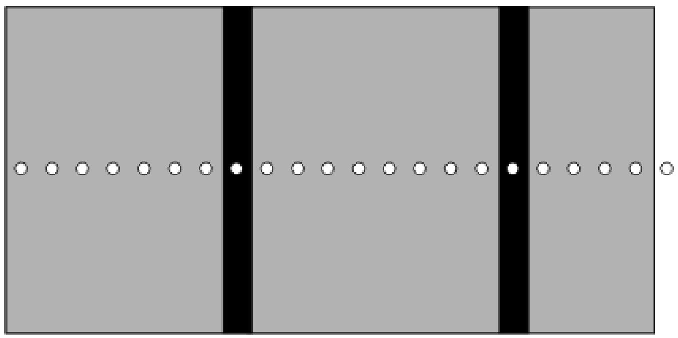

[1 3 6 8 9 9 8 6 3 1] / 54

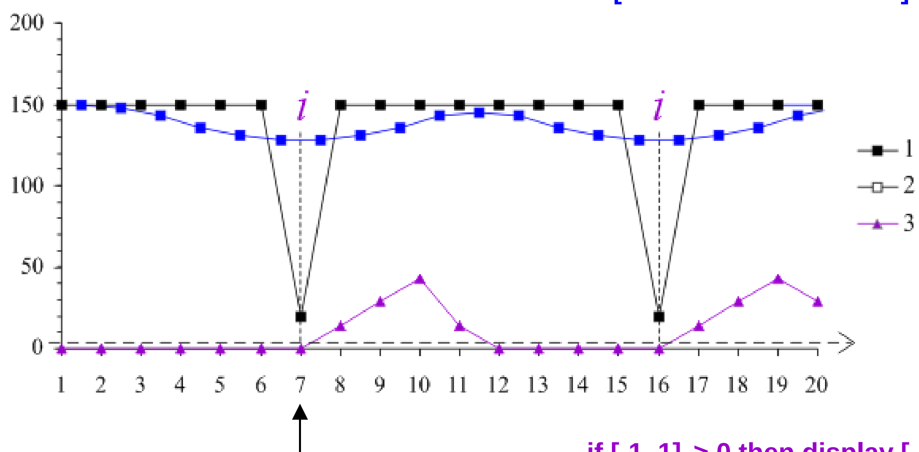

if [-1 1] > 0 then display [-1 1]

Launeau P., Archanjo C. J., Picard D., Arbaret L., Robin P.Y. (2010). Two- and three-dimensional shape fabric analysis by the intercept method in grey levels. Tectonophysics, Volume 492, Issues 1-4, 20 September 2010, Pages 230-239

Fourier series of intercepts

Hilliard, J. E., 1962. Specification and measurement of microstructural anisotropy. Trans. of the Metallurgical Society of AIME, 224: 1201-1211.

$$N_1(\alpha) = \sum_j N_1(j,\alpha)$$

Fourier series of intercepts counts : $A_{2m} = \frac{2}{K} \sum_{k=0}^{K-1} N_L(k\delta\alpha) \cos 2mk\delta\alpha \,, \quad B_{2m} = \frac{2}{K} \sum_{k=0}^{K-1} N_L(k\delta\alpha) \sin 2mk\delta\alpha$

phase $\tan 2m\varphi_{2m} = \frac{B_{2m}}{A_{2m}}$, power $C_{2m}^2 = A_{2m}^2 + B_{2m}^2$

Power spectrum of intercepts

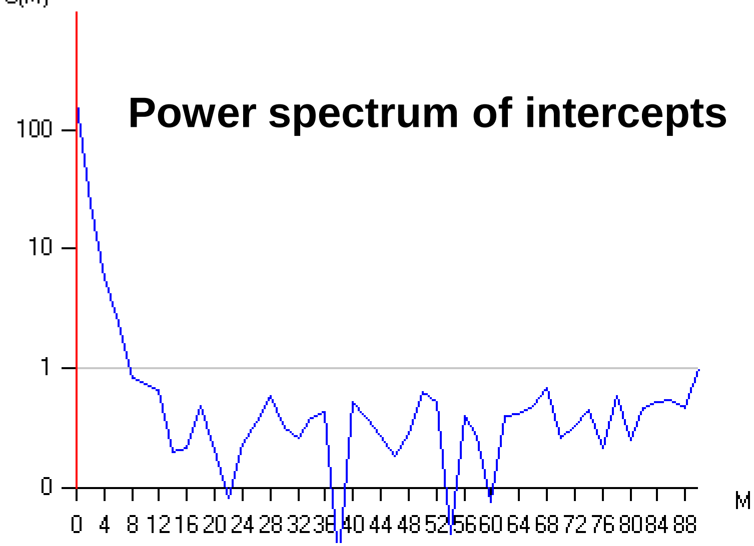

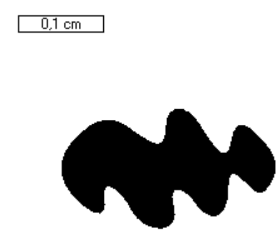

P. Launeau and P-Y. Robin (1996) "Fabric analysis using the intercept method". *Tectonophysics* 267, 91-119

Fourier series : rose of intercepts

$$N_1(\alpha) = \sum_j N_1(j,\alpha)$$

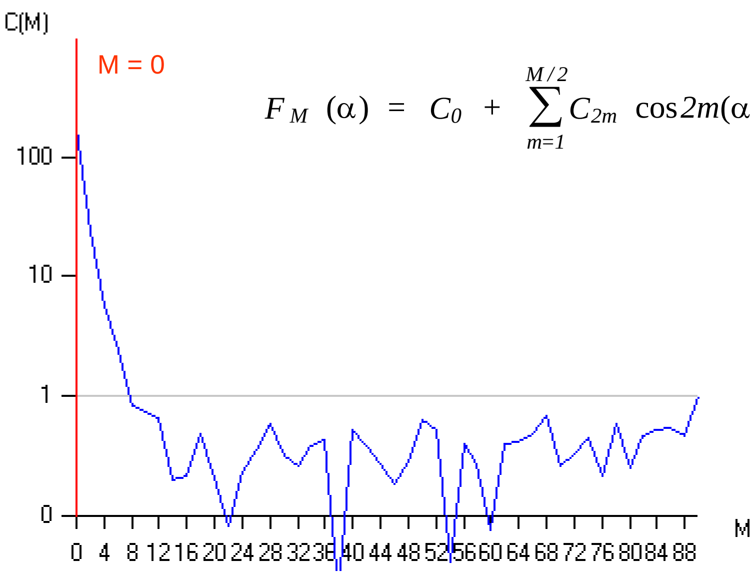

$$F_M(\alpha) = C_0 + \sum_{m=1}^{M/2} C_{2m} \cos 2m(\alpha - \varphi_{2m})$$

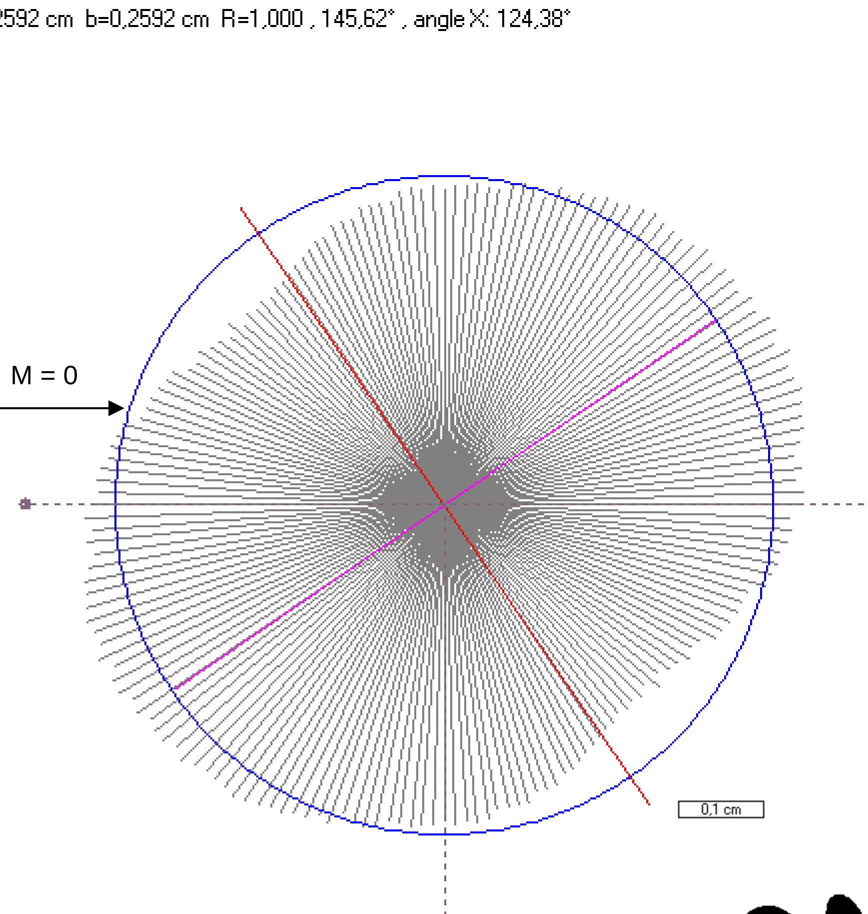

$$F_M(\alpha) = C_0 + \sum_{m=1}^{M/2} \left(A_{2m} \cos 2m\alpha + B_{2m} \sin 2m\alpha \right)$$

P. Launeau and P-Y. Robin (1996) "Fabric analysis using the intercept method". *Tectonophysics* 267, 91-119

Fourier series : rose of intercepts

$$N_1(\alpha) = \sum_j N_1(j,\alpha)$$

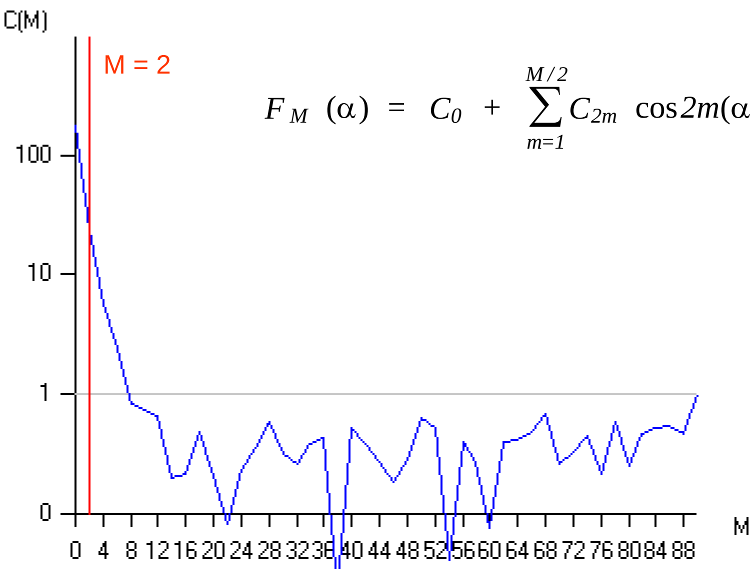

$$F_M(\alpha) = C_0 + \sum_{m=1}^{M/2} C_{2m} \cos 2m(\alpha - \varphi_{2m})$$

M = 8 →

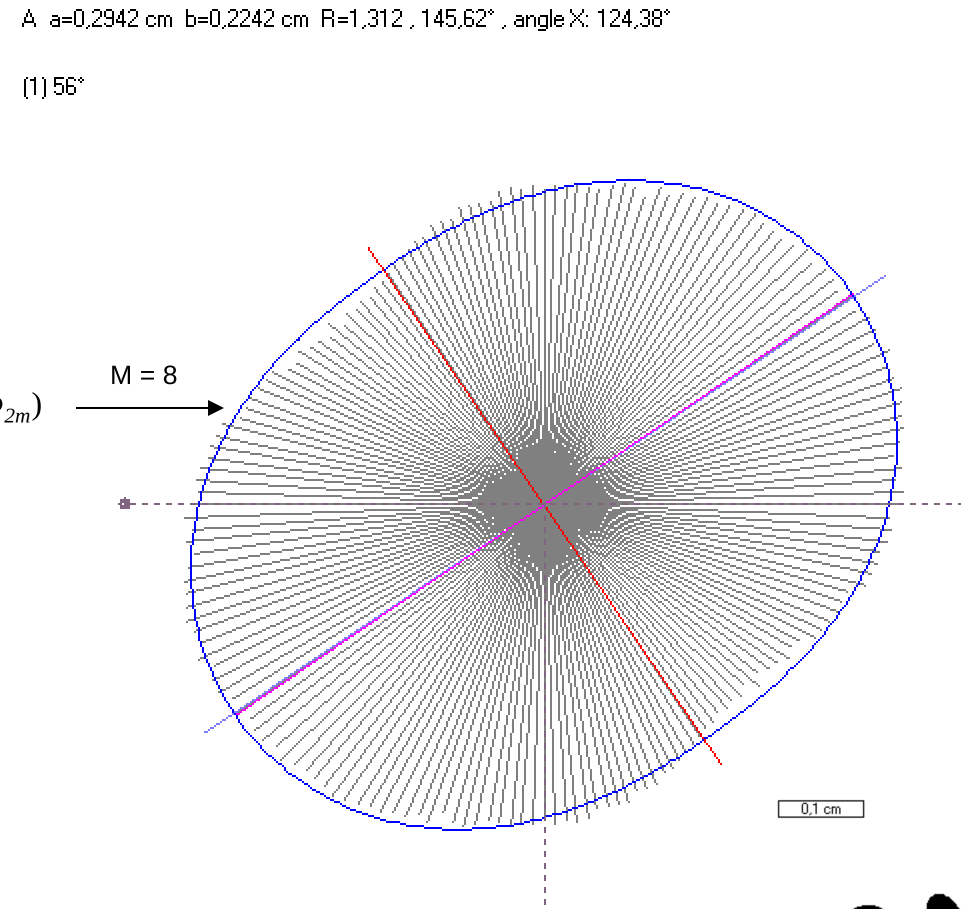

$$F_M(\alpha) = C_0 + \sum_{m=1}^{M/2} \left(A_{2m} \cos 2m\alpha + B_{2m} \sin 2m\alpha\right)$$

P. Launeau and P-Y. Robin (1996) "Fabric analysis using the intercept method". *Tectonophysics* 267, 91-119

Fourier series : rose of intercepts

$$N_1(\alpha) = \sum_j N_1(j,\alpha)$$

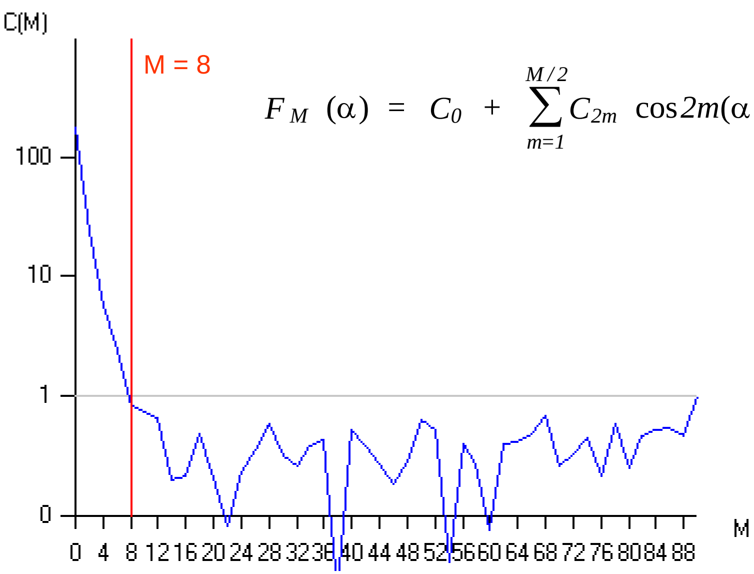

$$F_M(\alpha) = C_0 + \sum_{m=1}^{M/2} C_{2m} \cos 2m(\alpha - \varphi_{2m})$$

M = 8 →

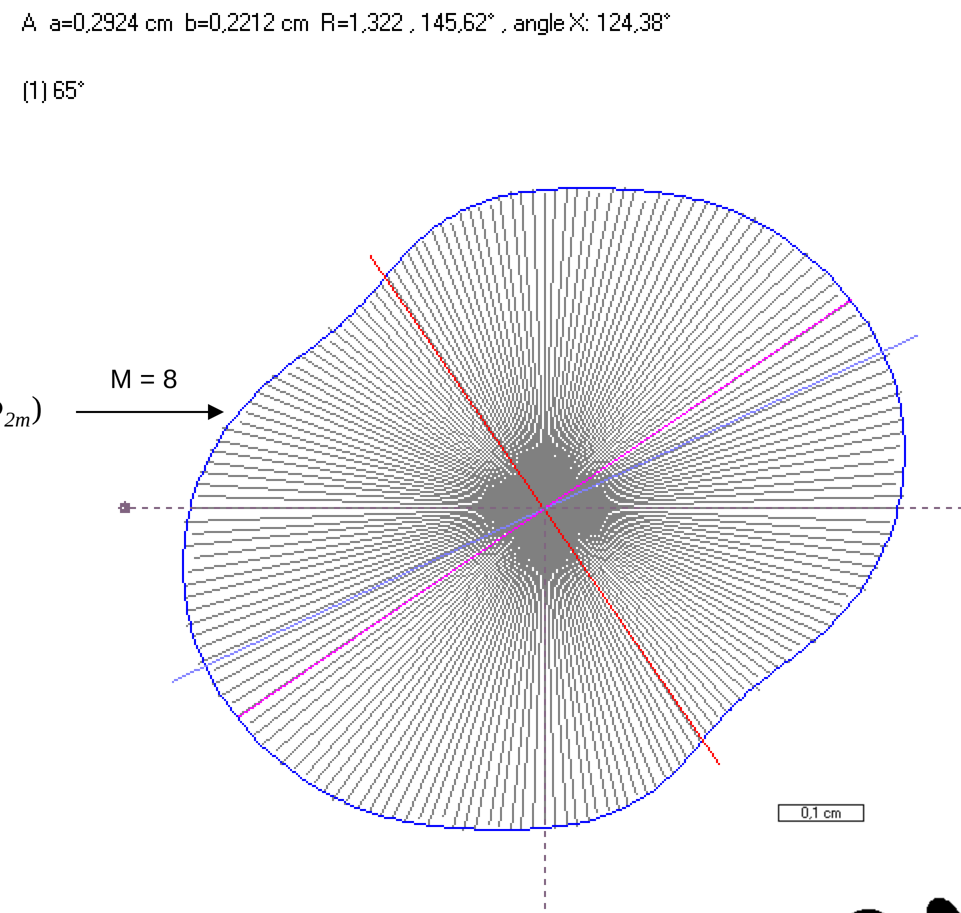

$$F_M(\alpha) = C_0 + \sum_{m=1}^{M/2} \left(A_{2m} \cos 2m\alpha + B_{2m} \sin 2m\alpha\right)$$

P. Launeau and P-Y. Robin (1996) "Fabric analysis using the intercept method". *Tectonophysics* 267, 91-119

Fourier series : rose of traverses (mean length)

$$N_1(\alpha) = \sum_j N_1(j,\alpha)$$

$$\overline{L}(\alpha) = \frac{A}{J\ N_1(\alpha)} = I\ \frac{N_0}{N_1(\alpha)}$$

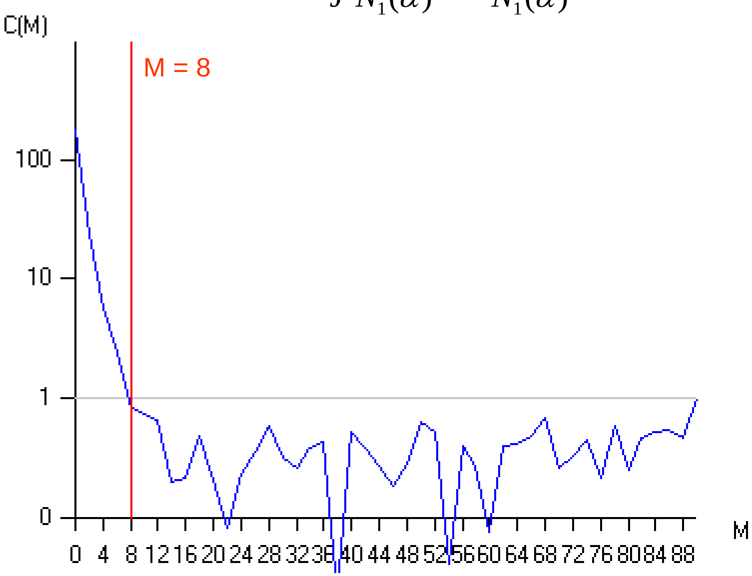

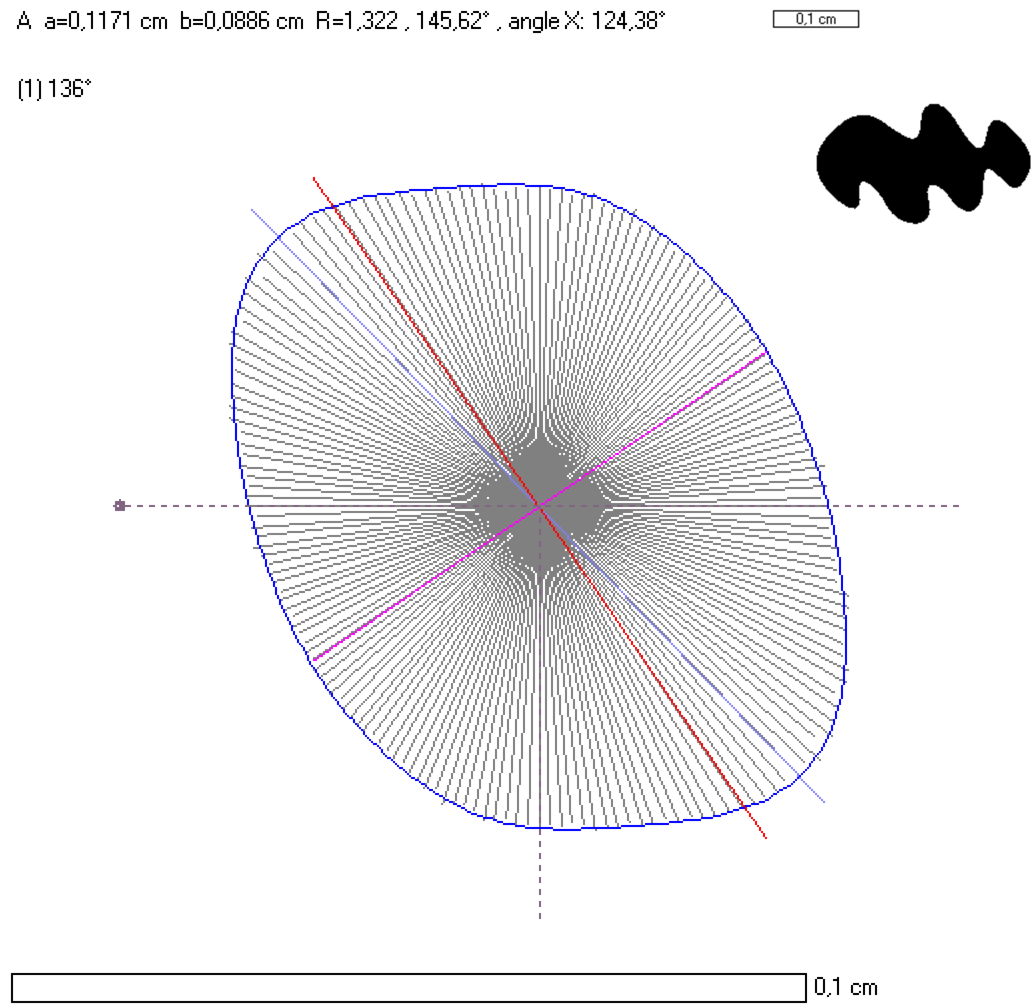

$$F_M\ (\alpha) = C_0 + \sum_{m=1}^{M/2} \left(A_{2m}\ \cos 2m\alpha + B_{2m}\ \sin 2m\alpha \right)$$

P. Launeau and P-Y. Robin (1996) "Fabric analysis using the intercept method". *Tectonophysics* 267, 91-119

Fourier series : rose of directions

For one rod :

$$D(\alpha) = L\,|\sin(\alpha - \psi)| = \frac{L}{\sqrt{2}}\sqrt{1 - \cos 2(\alpha - \psi)}$$

$D(\alpha) + D''(\alpha) = 0$ for $\alpha \neq \psi$ modulo π
∞ for $\alpha = \psi$ modulo π

Since the first derivative $D'(\alpha)$ changes from $-L$ to $+L$ on either side of the singularity, $D(\alpha) + D''(\alpha)$ for one rod is a Dirac 'function', $2L\,\delta(\alpha - \psi)$, i.e. with an integrated value of 2 L:
$D(\alpha) + D''(\alpha) = 2L\,\delta(\alpha - \psi)$

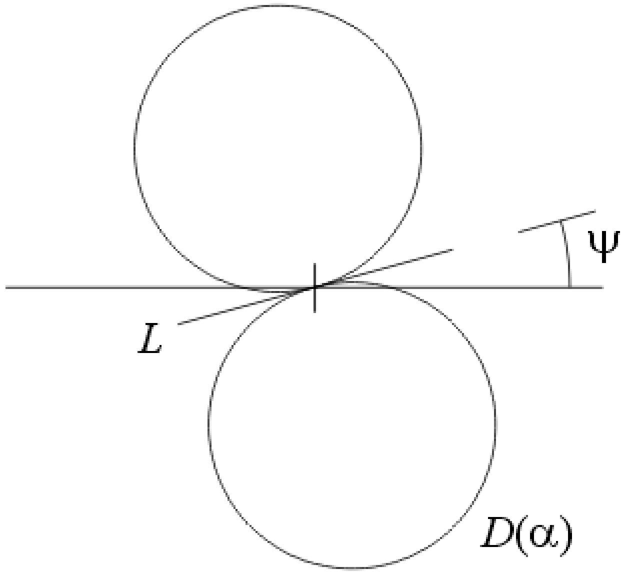

For a population of rods :

$$N_L(\alpha) = \frac{D(\alpha)}{A^w} = \frac{1}{A^w}\sum_{i=1}^{P} L^i\,\left|\sin(\alpha - \psi^i)\right|$$

$$N_L(\alpha) + N''_L(\alpha) = \frac{2}{A^w}\sum_{i=1}^{P} L^i\,\delta(\alpha - \psi^i)$$

Hilliard, J. E., 1962. Specification and measurement of microstructural anisotropy. Trans. of the Metallurgical Society of AIME, 224: 1201-1211.

P. Launeau and P-Y. Robin (1996) "Fabric analysis using the intercept method". *Tectonophysics* 267, 91-119

Fourier series : rose of directions

For a population of rods :

$$N_L(\alpha) = \frac{D(\alpha)}{A^w} = \frac{1}{A^w}\sum_{i=1}^{P} L^i \left|\sin(\alpha - \psi^i)\right|$$

$$N_L(\alpha) + N_L''(\alpha) = \frac{2}{A^w}\sum_{i=1}^{P} L^i\, \delta(\alpha - \psi^i)$$

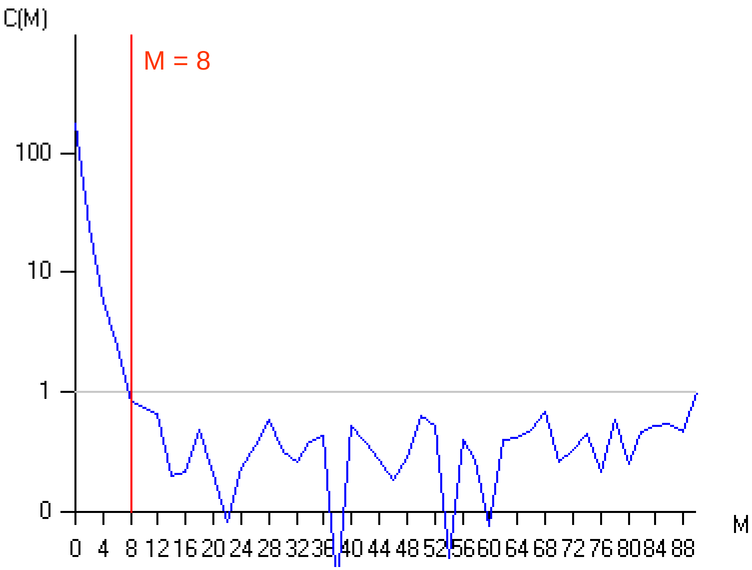

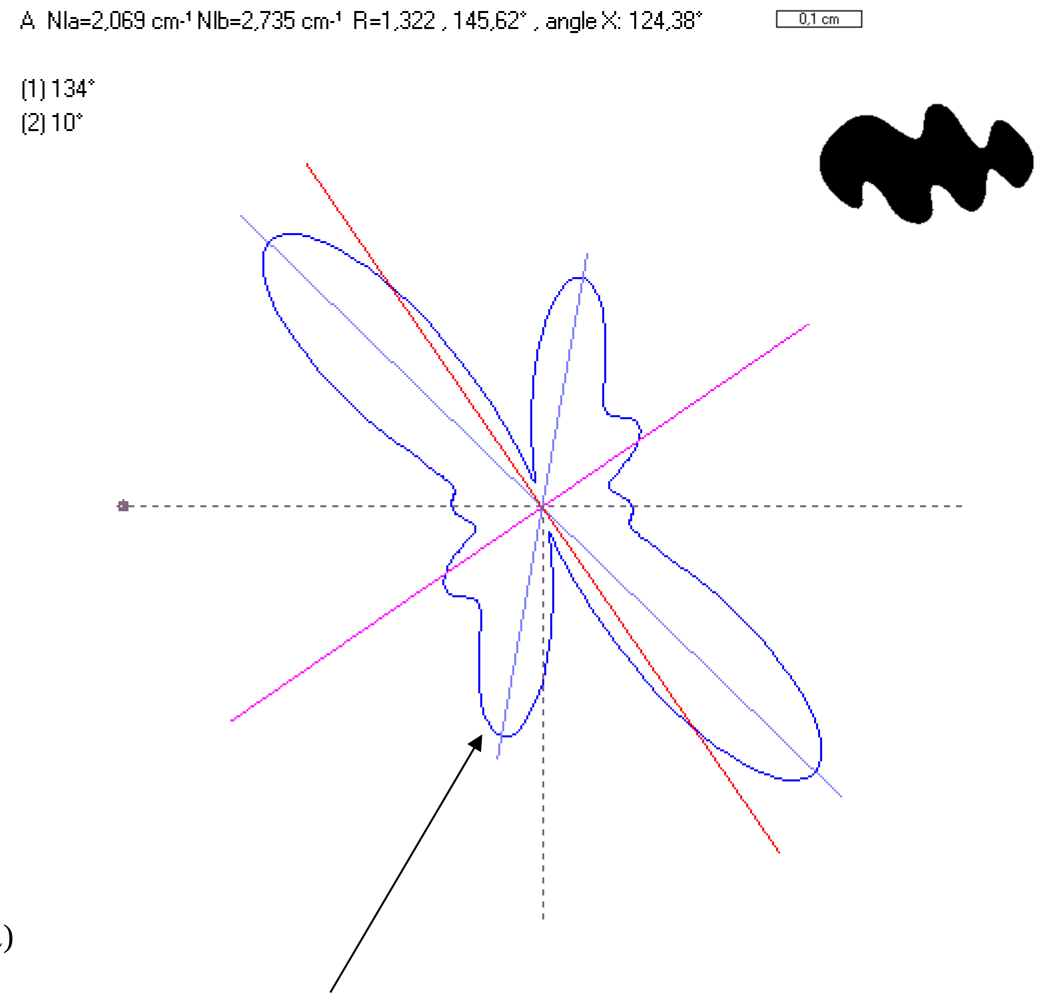

$$N_L''(\alpha) \approx F_M''(\alpha) = -\sum_{m=1}^{M/2}(2m)^2\,(A_{2m}\cos 2m\alpha + B_{2m}\sin 2m\alpha)$$

$$\frac{2\,l(\alpha)}{A^w} \approx F_M(\alpha) + F_M''(\alpha) = C_0 + \sum_{m=1}^{M/2}[1-(2m)^2]\;(A_{2m}\cos 2m\alpha + B_{2m}\sin 2m\alpha)$$

P. Launeau and P-Y. Robin (1996) "Fabric analysis using the intercept method". *Tectonophysics* 267, 91-119

Fourier series : characteristic shape

For a population of rods :

$$N_L(\alpha) = \frac{D(\alpha)}{A^w} = \frac{1}{A^w}\sum_{i=1}^{P} L^i \left|\sin(\alpha - \psi^i)\right|$$

$$N_L(\alpha) + N_L''(\alpha) = \frac{2}{A^w}\sum_{i=1}^{P} L^i\, \delta(\alpha - \psi^i)$$

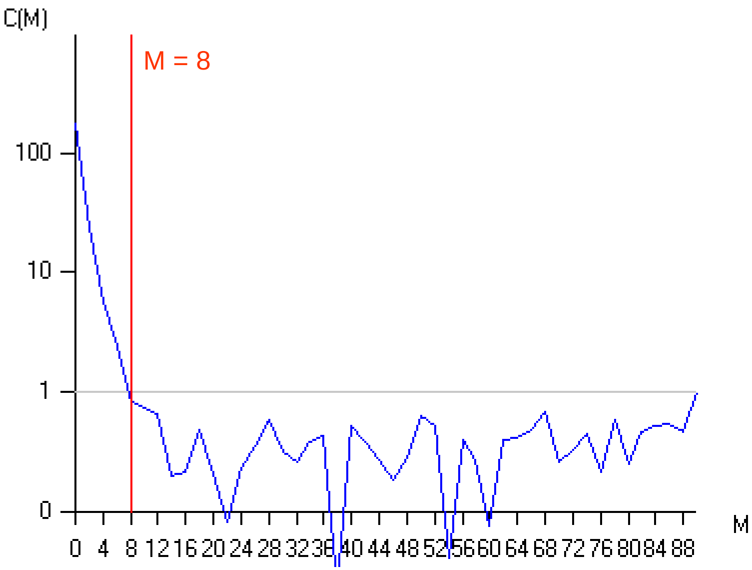

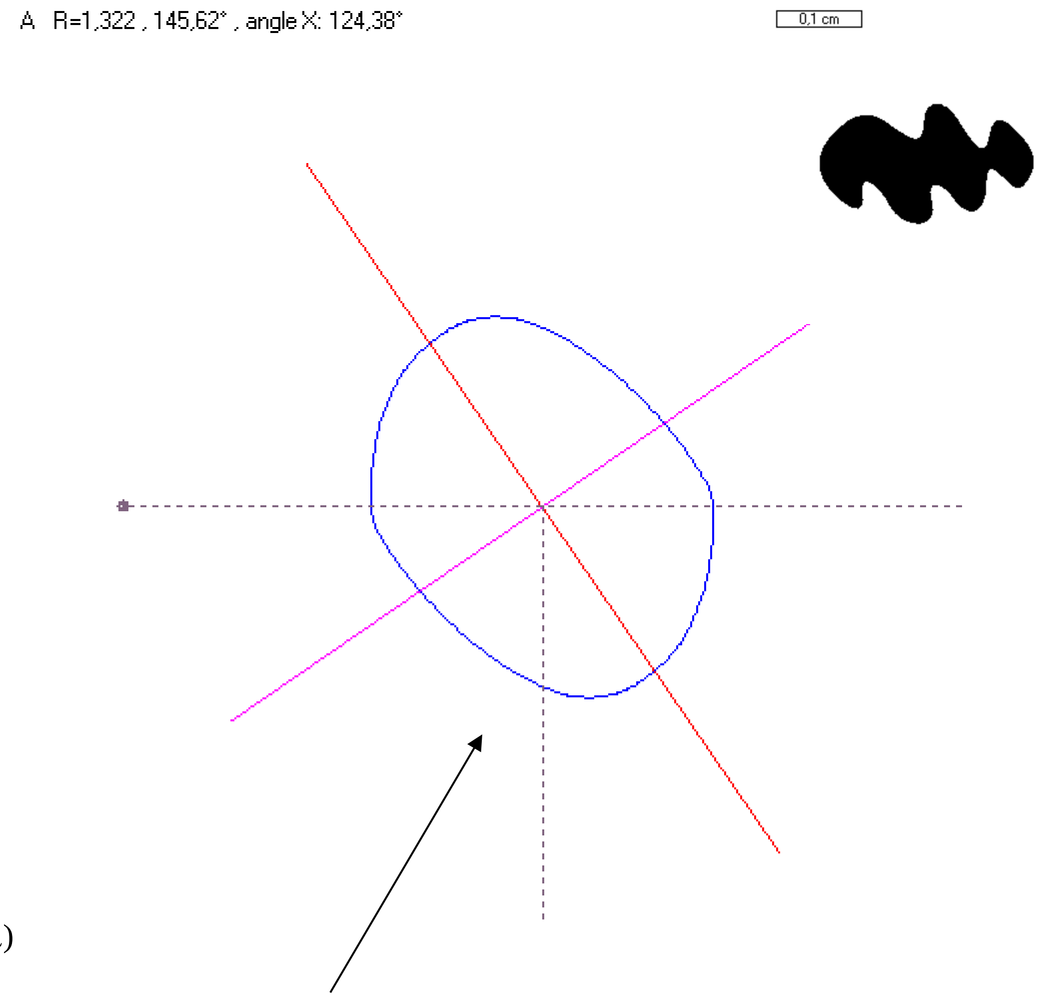

$$N_L''(\alpha) \approx F_M''(\alpha) = -\sum_{m=1}^{M/2}(2m)^2\,(A_{2m}\cos 2m\alpha + B_{2m}\sin 2m\alpha)$$

$$\frac{2\,l(\alpha)}{A^w} \approx F_M(\alpha) + F_M''(\alpha) = C_0 + \sum_{m=1}^{M/2}[1-(2m)^2]\;(A_{2m}\cos 2m\alpha + B_{2m}\sin 2m\alpha)$$

P. Launeau and P-Y. Robin (1996) "Fabric analysis using the intercept method". *Tectonophysics* 267, 91-119

Fourier series : noise

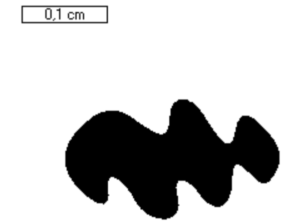

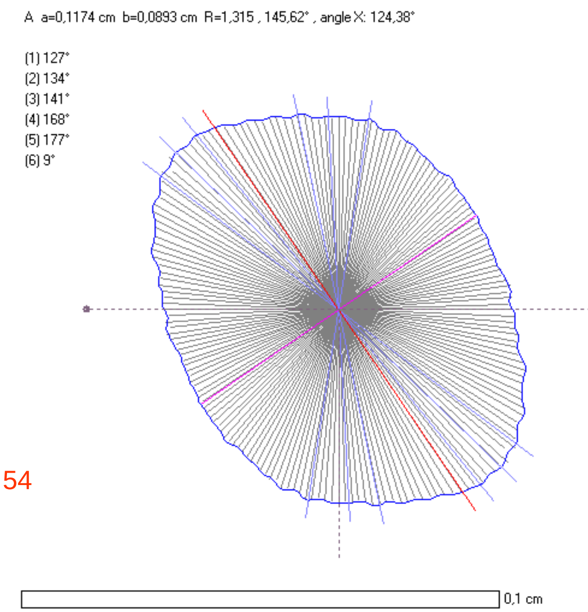

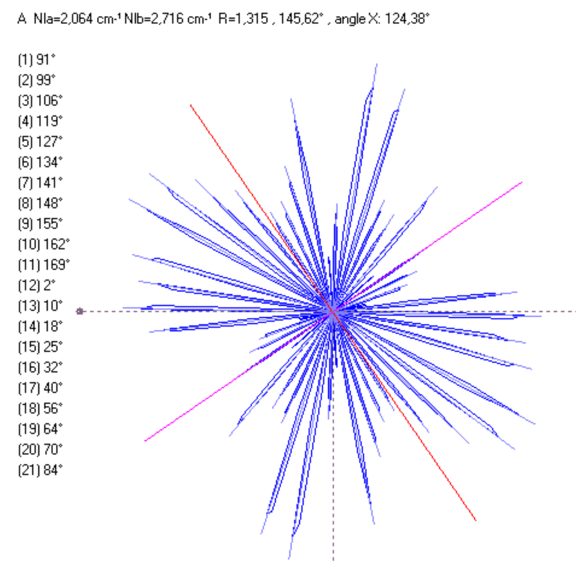

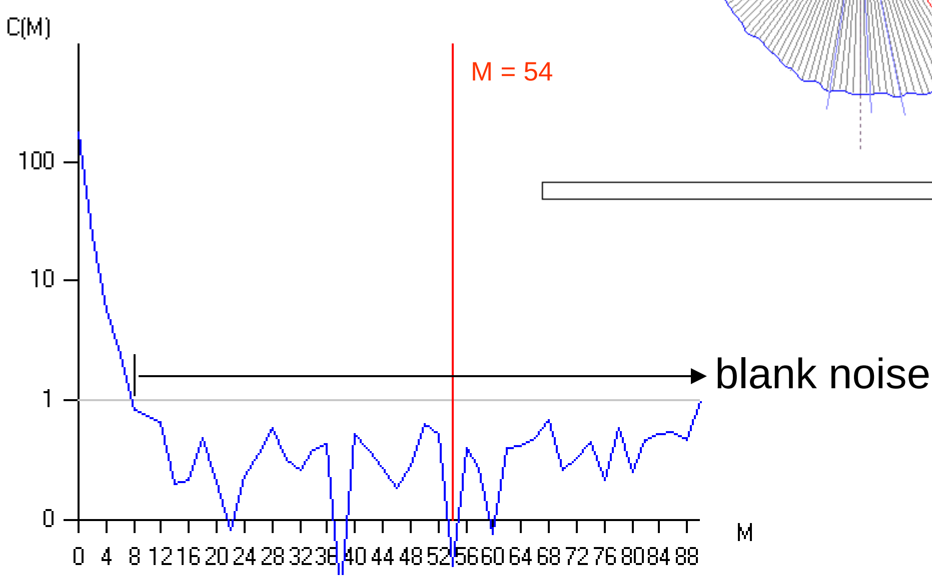

P. Launeau and P-Y. Robin (1996) "Fabric analysis using the intercept method". *Tectonophysics* 267, 91-119

Case of 1 object

Symmetry analysis with the Fourier power spectrum

C_2 = anisotropy
C_M = symmetry

Theoretical shapes of roses

Shapes | Intercept counts | Mean intercept lengths

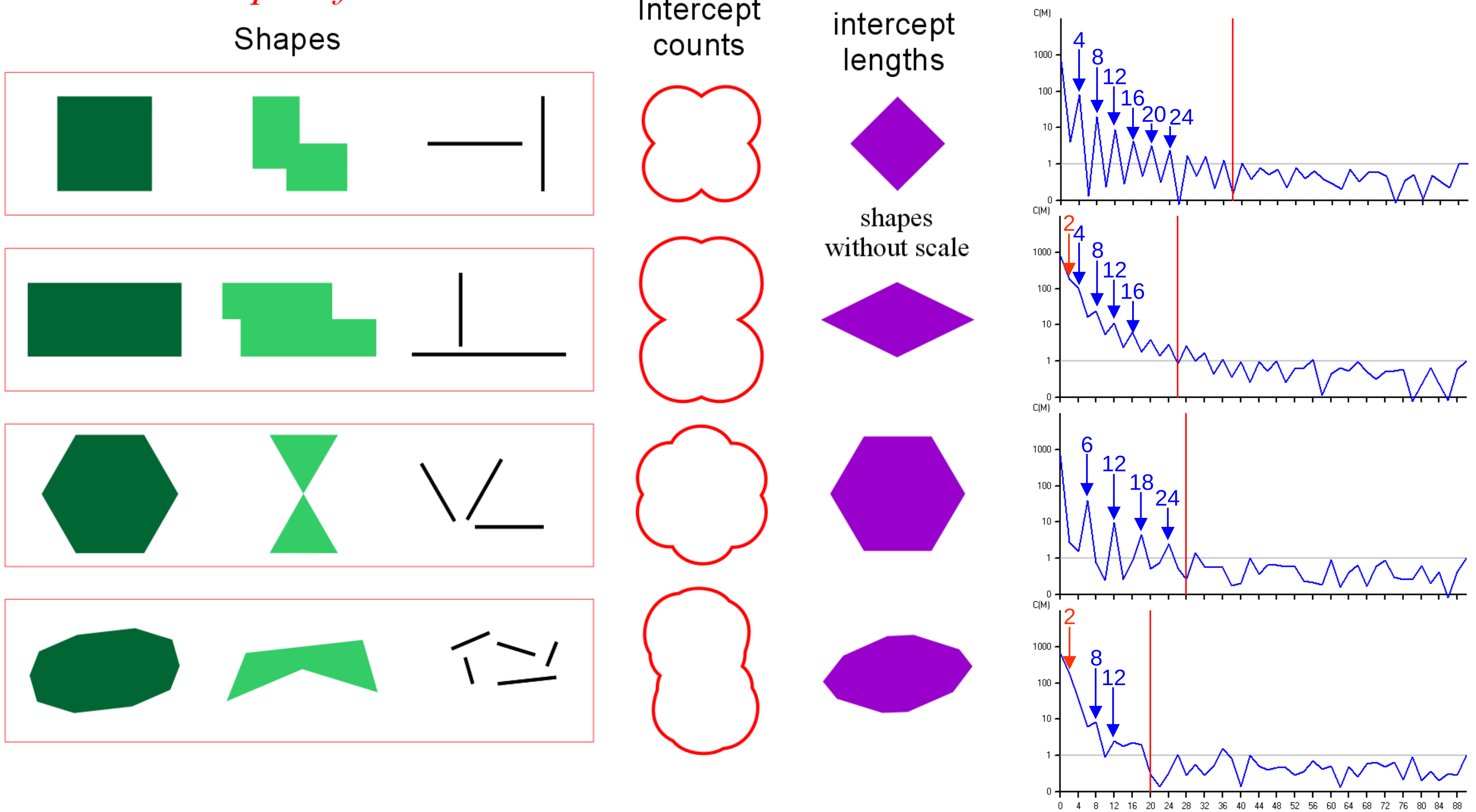

P. Launeau and P-Y. Robin (1996) "Fabric analysis using the intercept method". *Tectonophysics* 267, 91-119

Case of 1 object

Symmetry analysis with the Fourier power spectrum

C_2 = anisotropy
C_M = symmetry

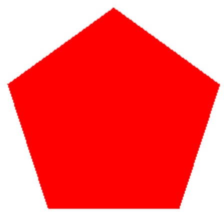

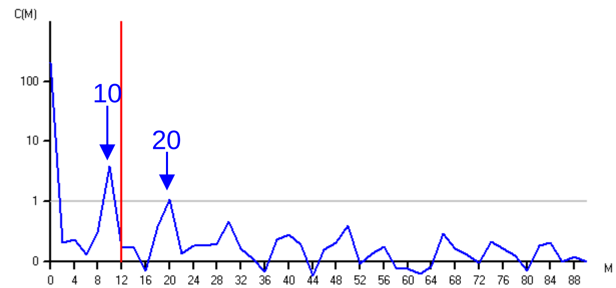

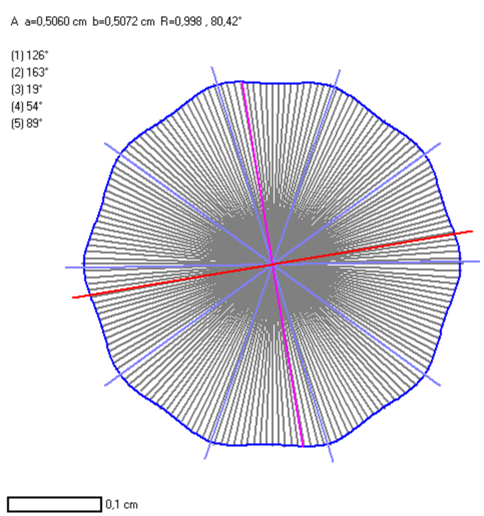

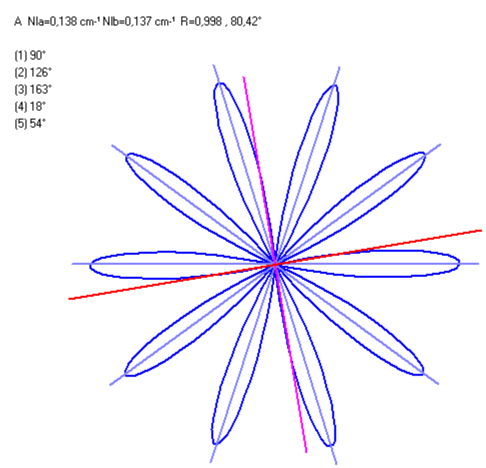

P. Launeau and P-Y. Robin (1996) "Fabric analysis using the intercept method". *Tectonophysics* 267, 91-119

Shape analysis with boundary directions

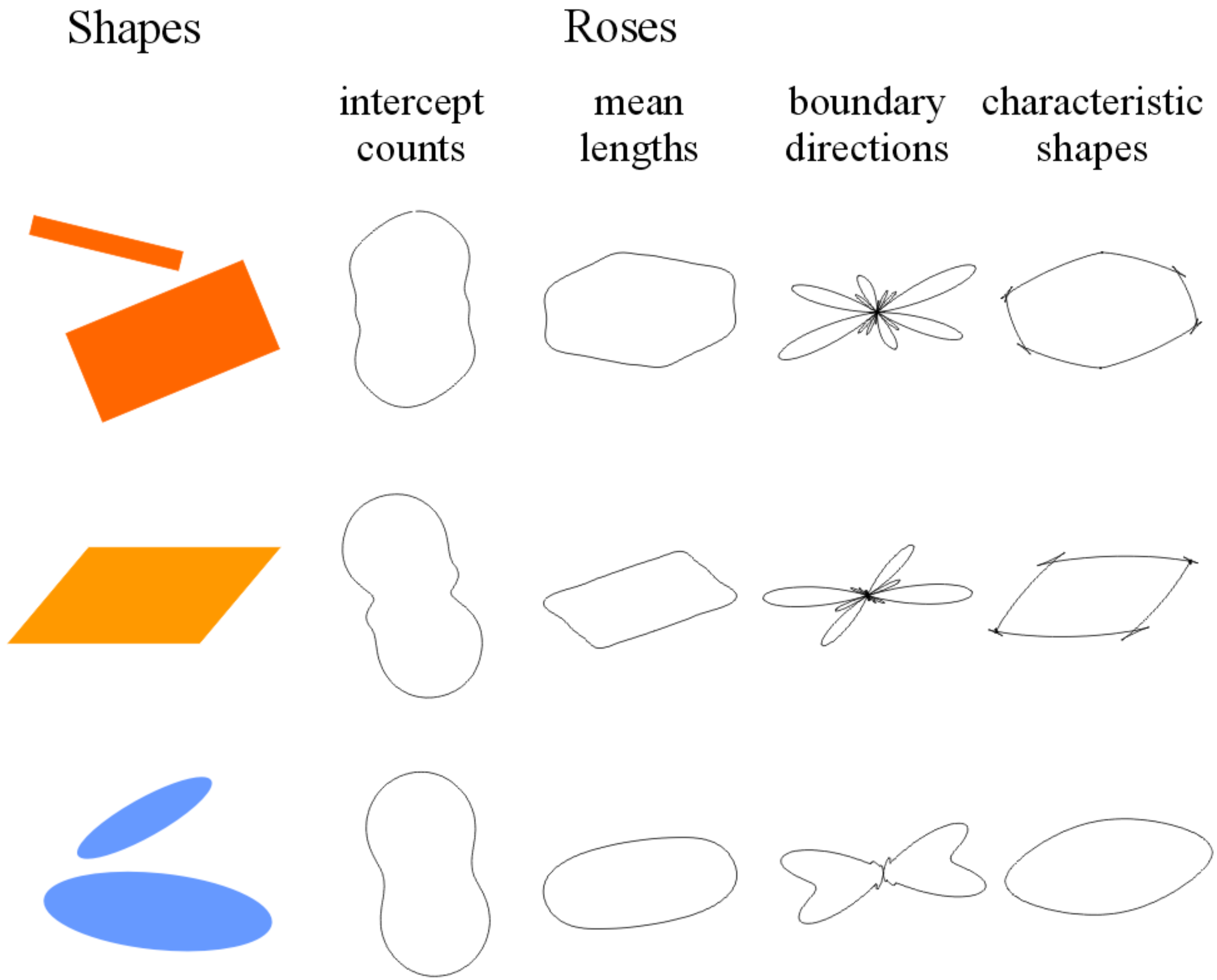

P. Launeau and P-Y. Robin (1996) "Fabric analysis using the intercept method". *Tectonophysics* 267, 91-119

$4/\pi$ size correction

This is the ratio between the mean intercept length and the long axis of an ellipse

Therefore the correction is :

- valid only for ellipses and population of objects giving an elliptical mean shape

- not valid on rectangles parallel to each other

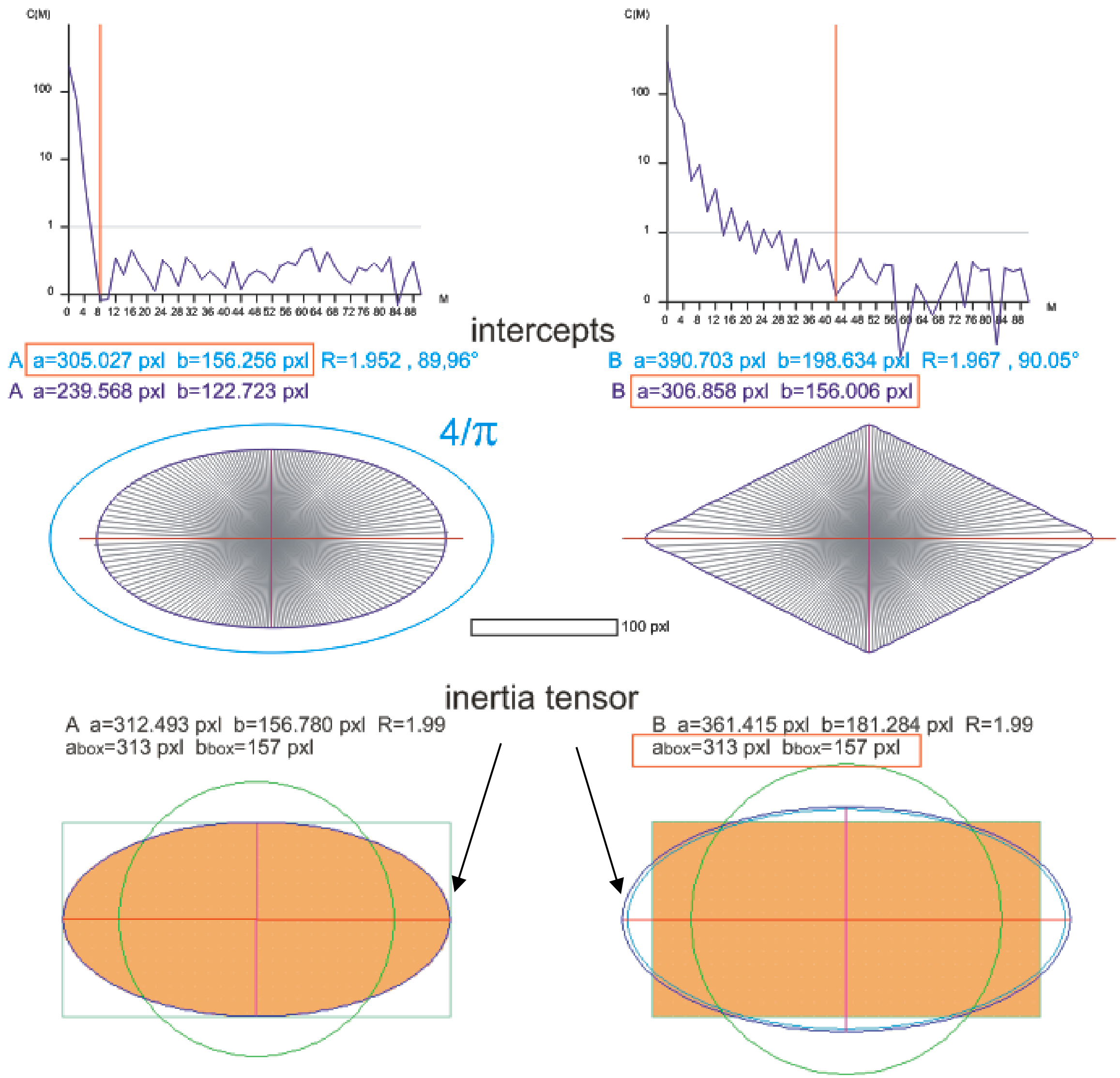

P. Launeau (2004) "Mise en évidence des écoulements magmatiques par analyse d'images 2-D des distributions 3-D d'Orientations Préférentielles de Formes". *Bull. Soc. Géol. Fr* , 175, 331-350

Quantitative Image Analysis of Minerals and Rocks

http://www.sciences.univ-nantes.fr/lpgnantes/SPO

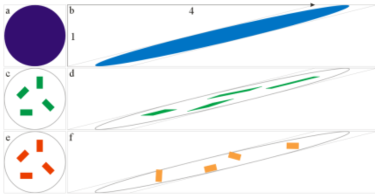

Passive / active deformation of object population

1 passive object

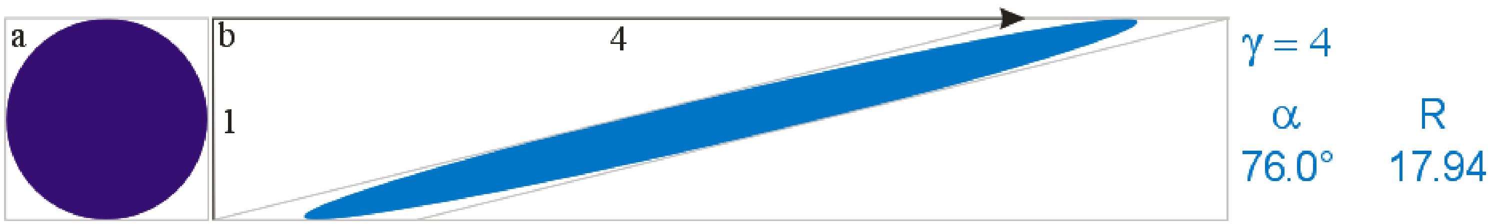

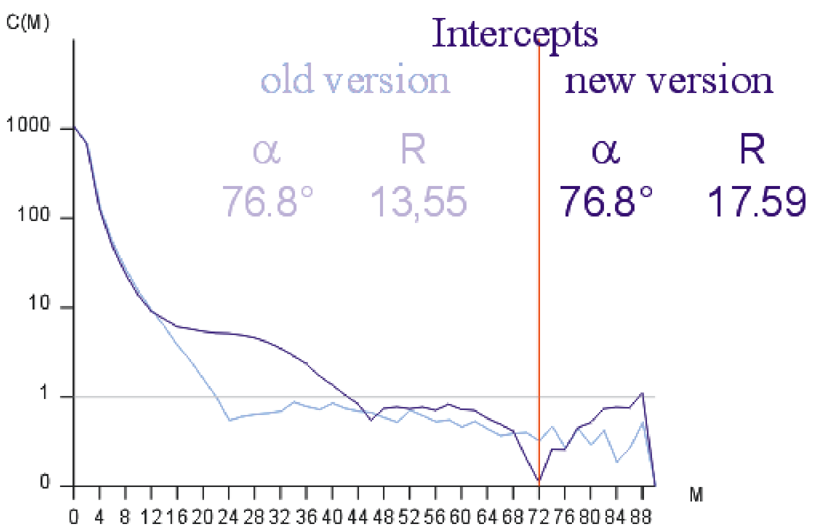

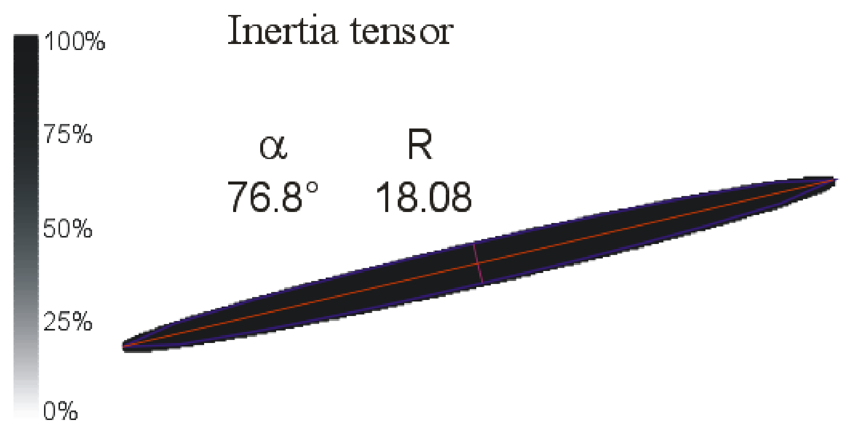

Launeau P., Archanjo C. J., Picard D., Arbaret L., Robin P.Y. (2010). Two- and three-dimensional shape fabric analysis by the intercept method in grey levels. Tectonophysics, Volume 492, Issues 1-4, 20 September 2010, Pages 230-239

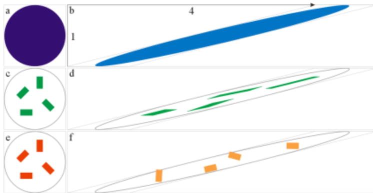

Passive / active deformation of object population

4 passive rectangles

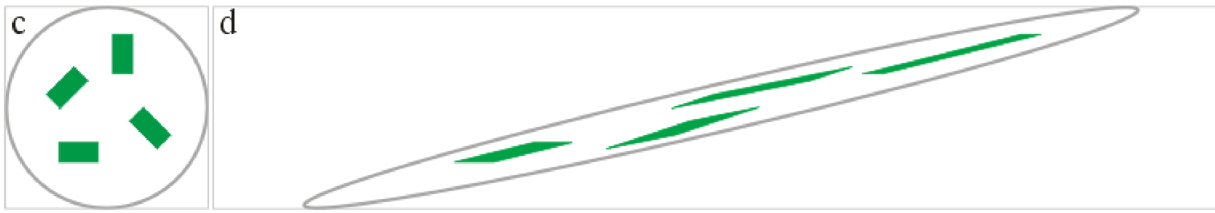

$\gamma = 4$

α	R
77.4°	17.94

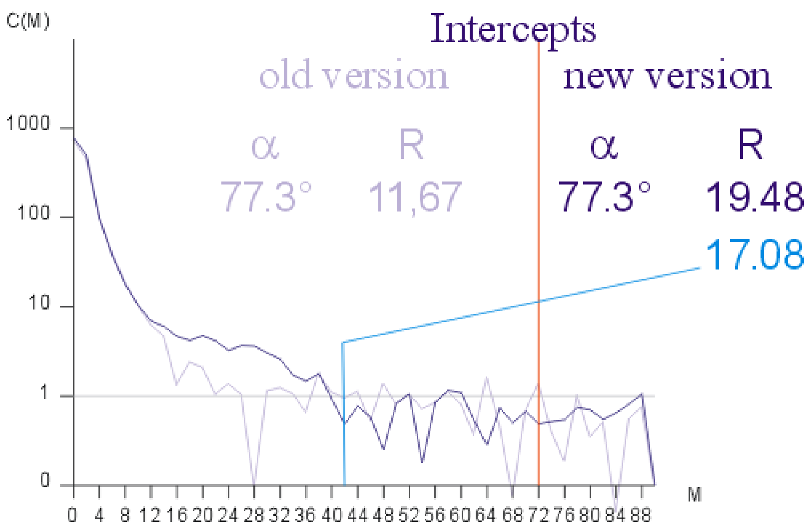

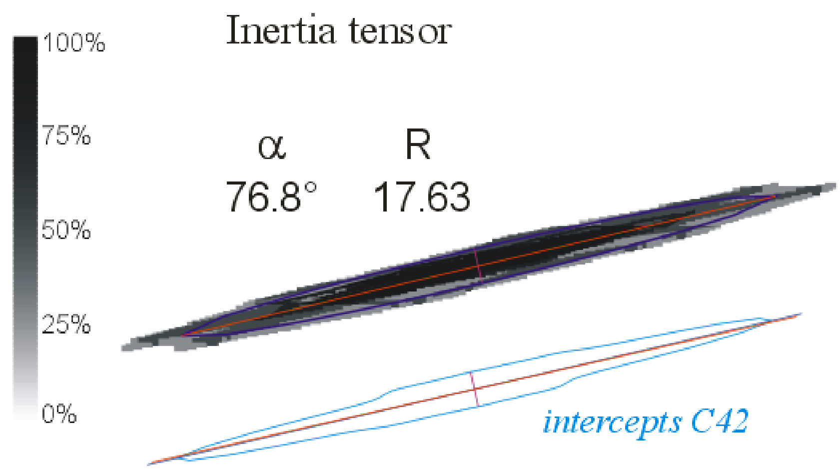

Launeau P., Archanjo C. J., Picard D., Arbaret L., Robin P.Y. (2010). Two- and three-dimensional shape fabric analysis by the intercept method in grey levels. Tectonophysics, Volume 492, Issues 1-4, 20 September 2010, Pages 230-239

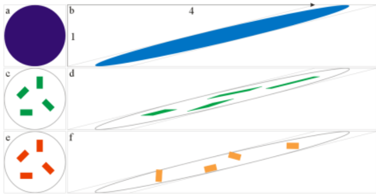

Passive / active deformation of object population

4 active rectangles

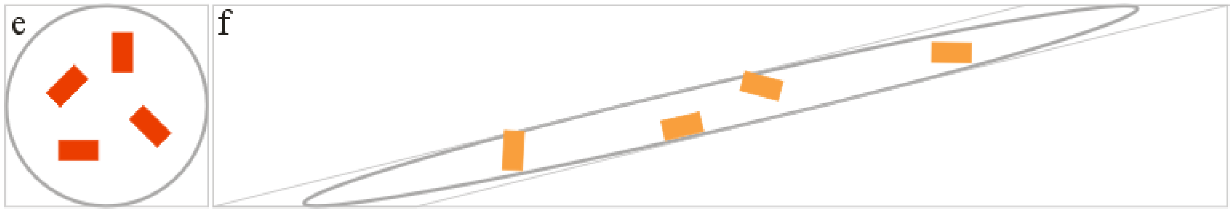

$\gamma = 4$

α	R
90.6°	1.609

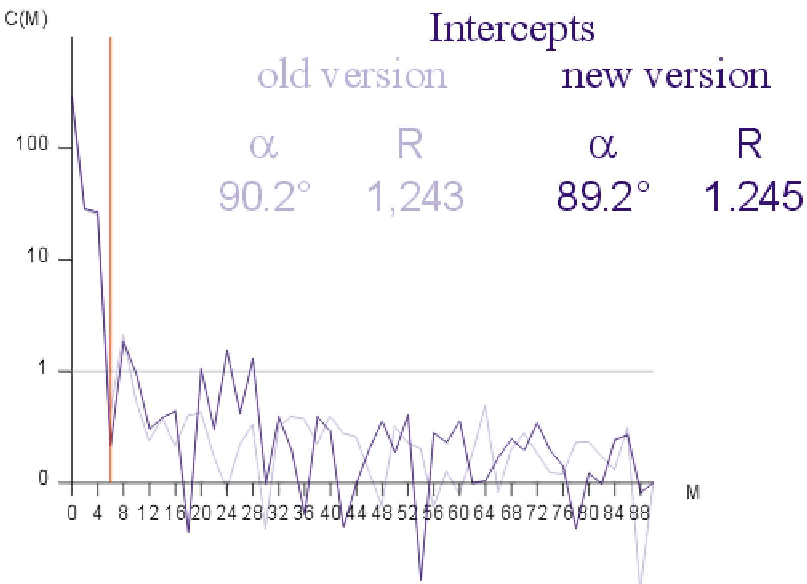

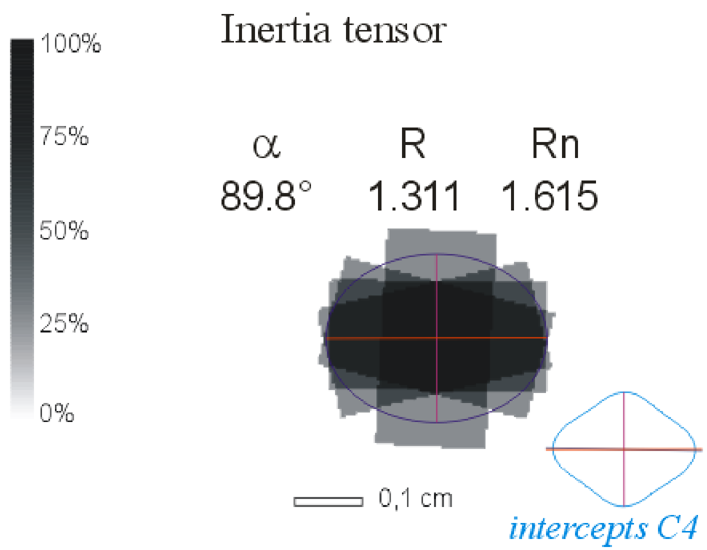

Launeau P., Archanjo C. J., Picard D., Arbaret L., Robin P.Y. (2010). Two- and three-dimensional shape fabric analysis by the intercept method in grey levels. Tectonophysics, Volume 492, Issues 1-4, 20 September 2010, Pages 230-239

Passive deformation of Spirifers

A a=2,4855 cm b=1,5591 cm R=1,594 , 40,07°

(1) 39°

1.59

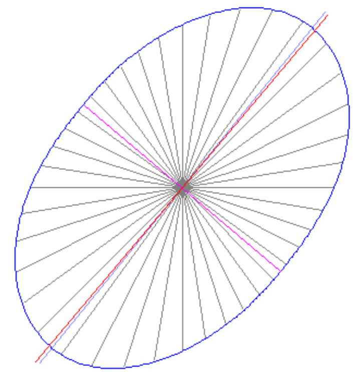

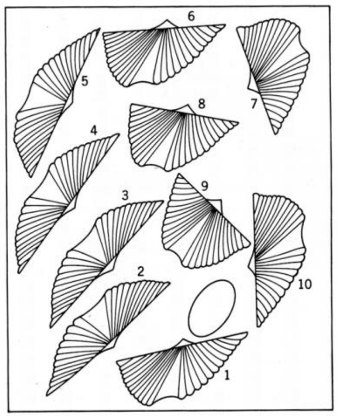

Fig. 5.6. Slab of deformed fossil shells.

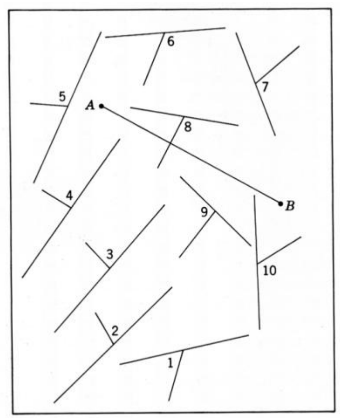

Fig. 5.8. Preliminary steps in construction of strain ellipse by Wellman's method.

1.62

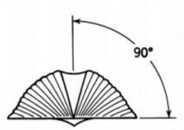

Fig. 5.7. Form of individual shell in undeformed state.

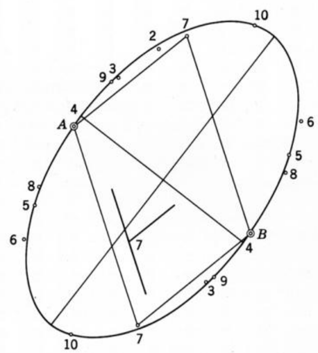

Fig. 5.9. Strain ellipse.

A n=10 a=3,9526 cm b=2,3792 cm R=1,661 [2,105]n [2,120]b , 39,73° , angle X : 129,73°
K=0,468, Kn=0,632 {0,741}, Kbn=0,636 {0,736}

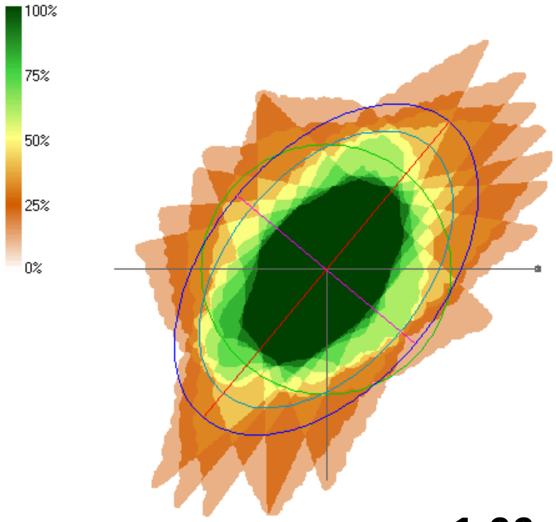

1.66

0,1 cm

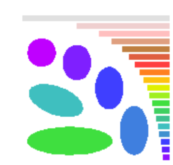

Quantitative Image Analysis of Minerals and Rocks

http://www.sciences.univ-nantes.fr/lpgnantes/SPO

UMR 6112
PLANÉTOLOGIE & GÉODYNAMIQUE

Launeau P., Archanjo C. J., Picard D., Arbaret L., Robin P.Y. (2010). Two- and three-dimensional shape fabric analysis by the intercept method in grey levels. Tectonophysics, Volume 492, Issues 1-4, 20 September 2010, Pages 230-239

Window of measurement

with mask

Means no intercept detection along grey levels of the mask

R=2

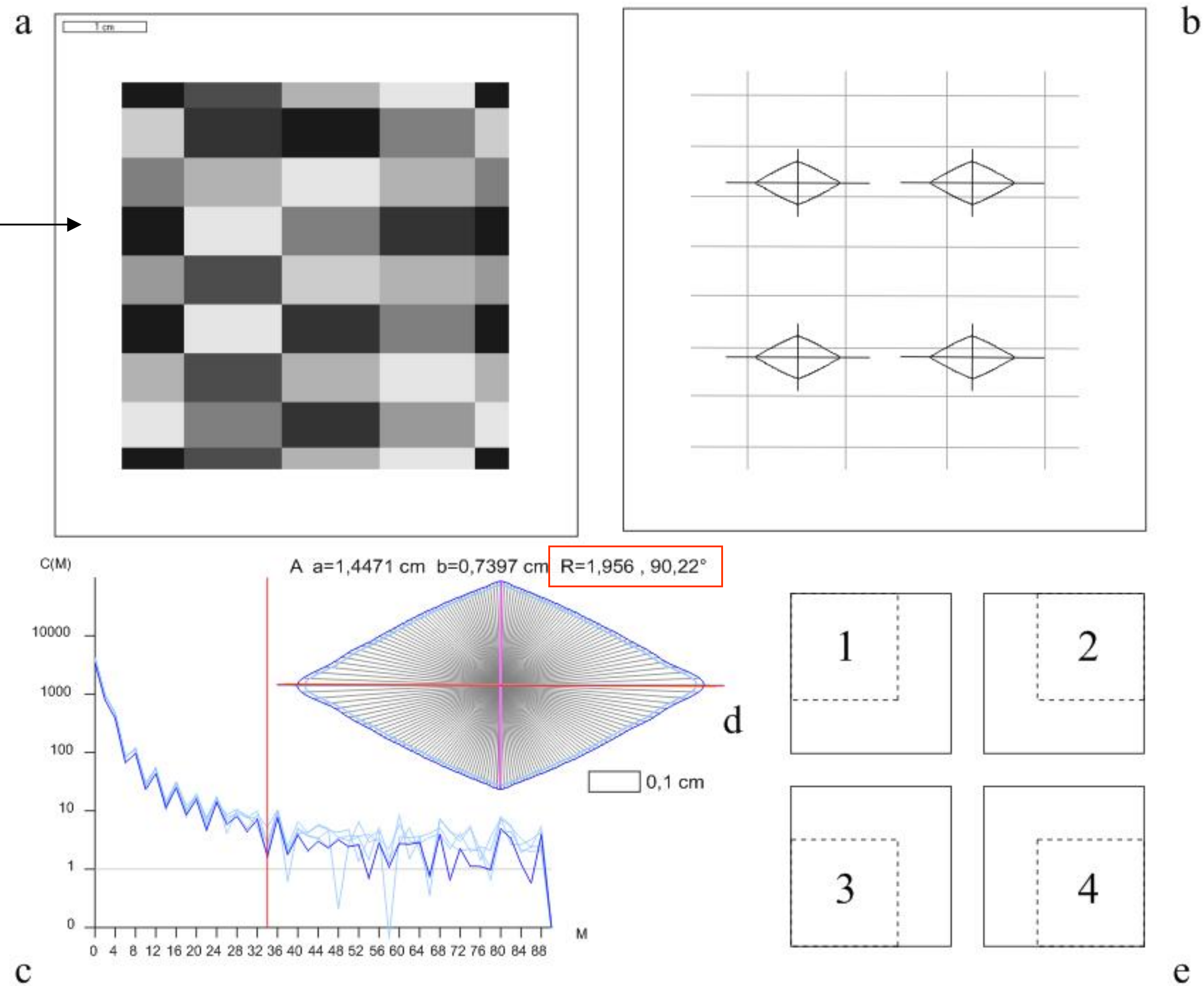

a=1.137 cm b=0.581 cm (without 4/π correction)

a_{box}=1,18cm b_{box}=0,69cm

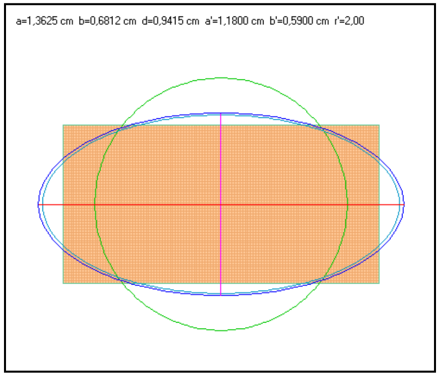

Inertia tensor of one rectangle

UMR 6112
PLANÉTOLOGIE & GÉODYNAMIQUE

Quantitative Image Analysis of Minerals and Rocks

http://www.sciences.univ-nantes.fr/lpgnantes/SPO

Window of measurement

with mask

Means no intercept detection along grey levels of the mask

Standard grey levels

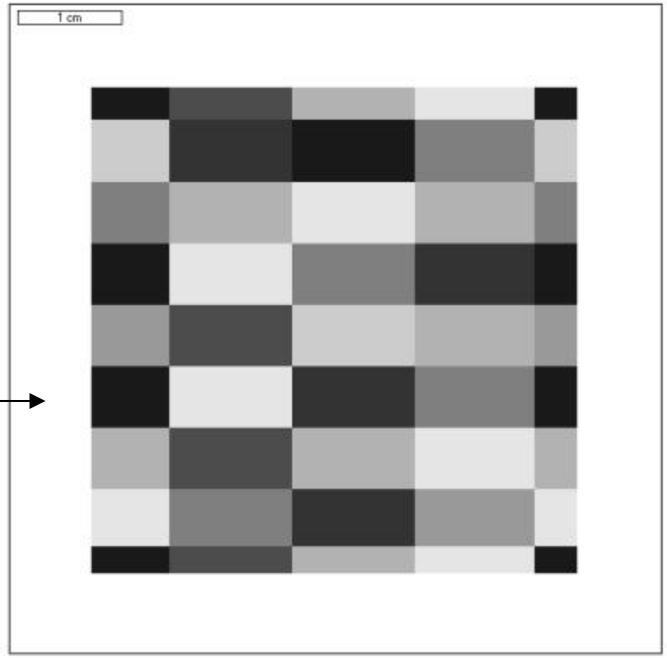

On grey phase with dark edges

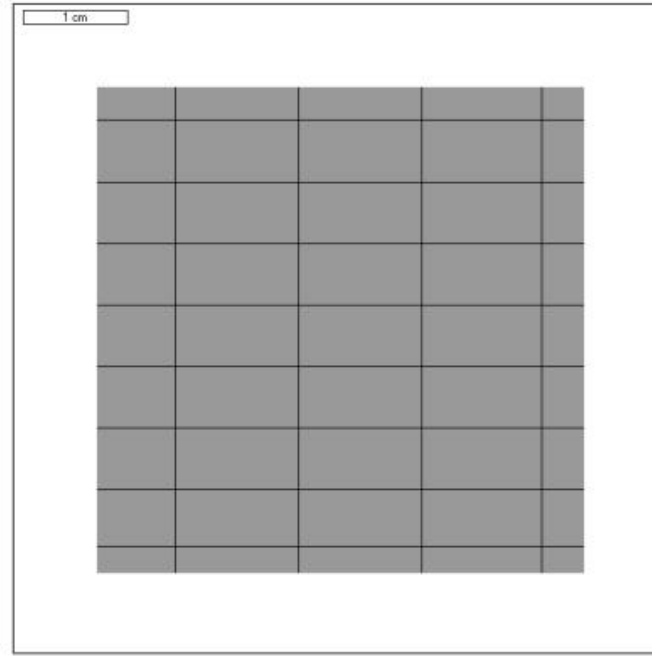

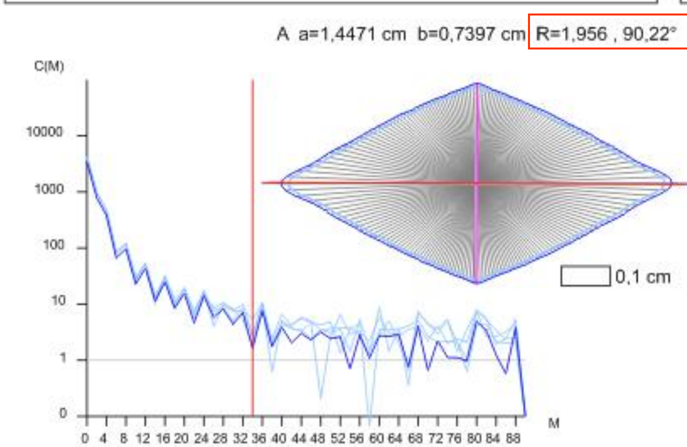

abs [-1 1]

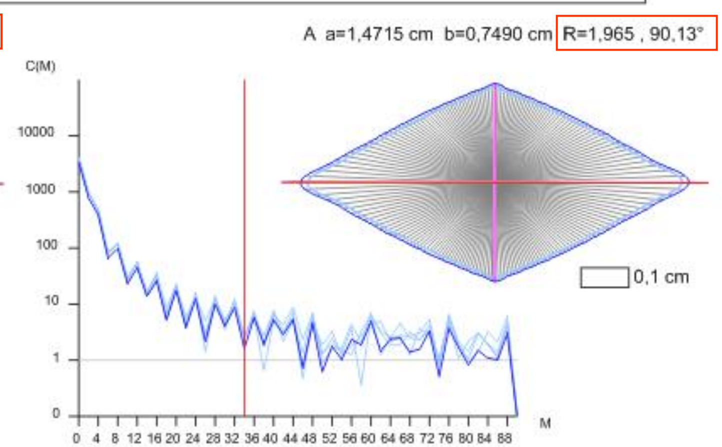

if [-1 1] > 0 then display [-1 1]

Launeau P., Archanjo C. J., Picard D., Arbaret L., Robin P.Y. (2010). Two- and three-dimensional shape fabric analysis by the intercept method in grey levels. Tectonophysics, Volume 492, Issues 1-4, 20 September 2010, Pages 230-239

Direct analysis versus drawing

Launeau P., Archanjo C. J., Picard D., Arbaret L., Robin P.Y. (2010). Two- and three-dimensional shape fabric analysis by the intercept method in grey levels. Tectonophysics, Volume 492, Issues 1-4, 20 September 2010, Pages 230-239

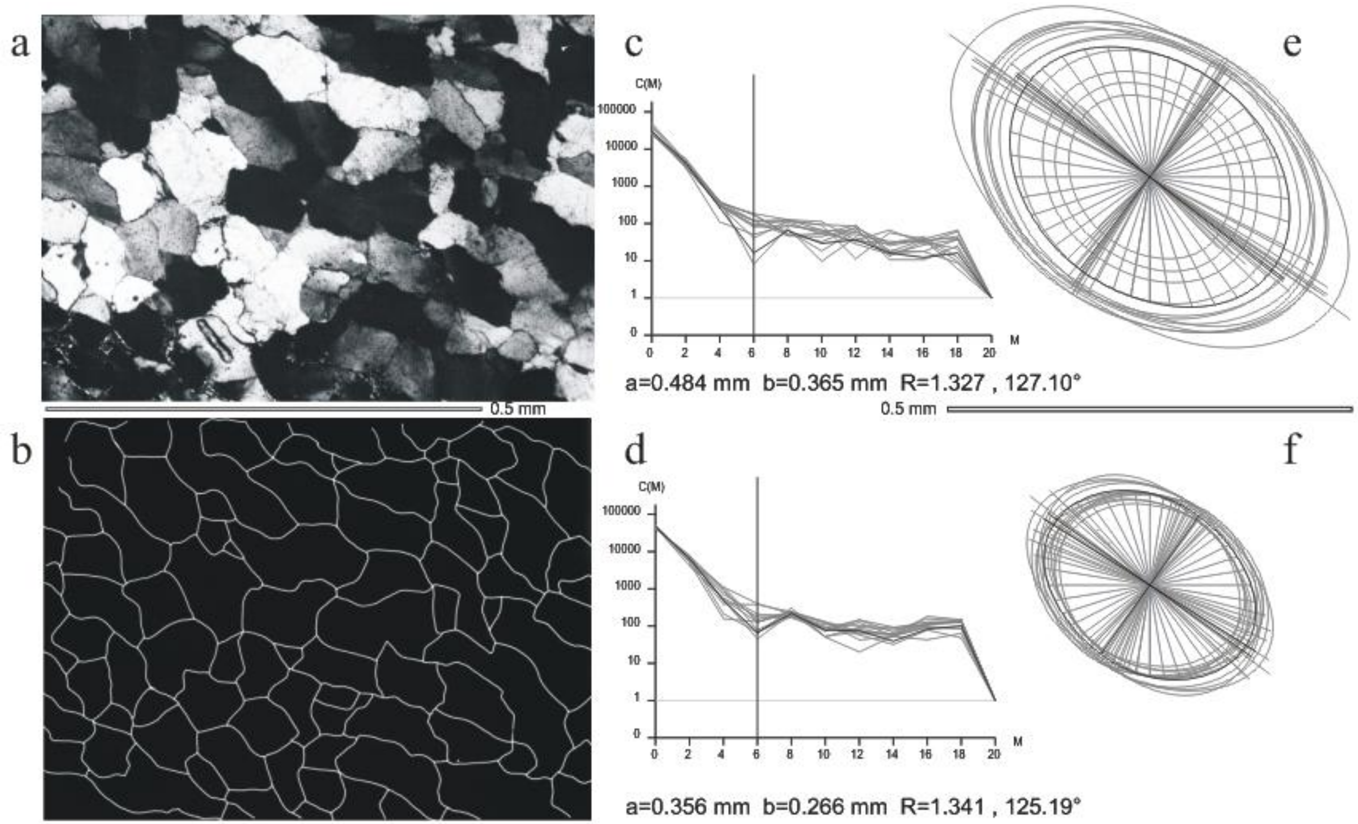

abs [-1 1]

Standard grey levels

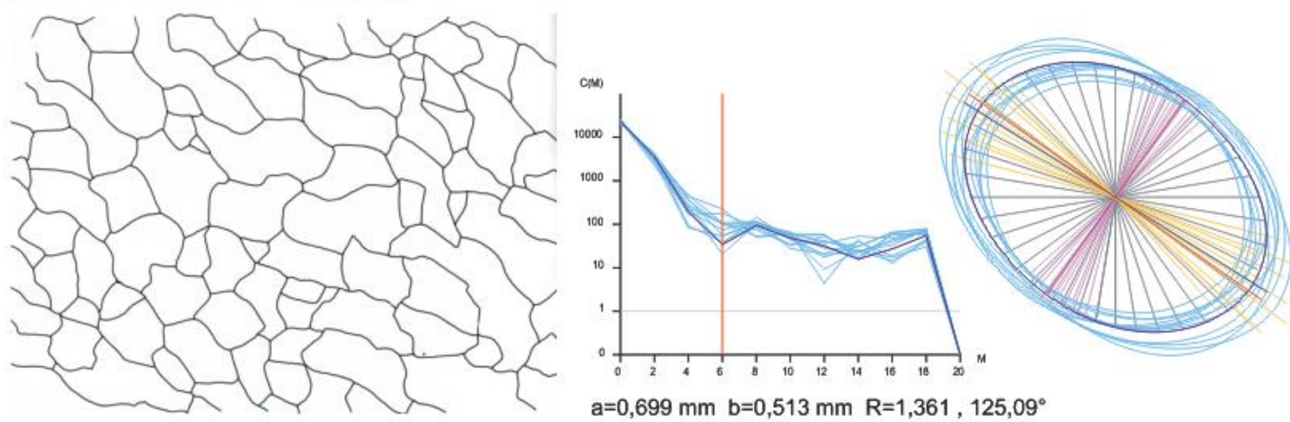

if [-1 1] > 0 then display [-1 1]

One grey phase with dark edges

UMR 6112
PLANÉTOLOGIE &
GÉODYNAMIQUE

Quantitative Image Analysis of Minerals and Rocks

http://www.sciences.univ-nantes.fr/lpgnantes/SPO

Direct analysis versus drawing with inertia tensor

mask →

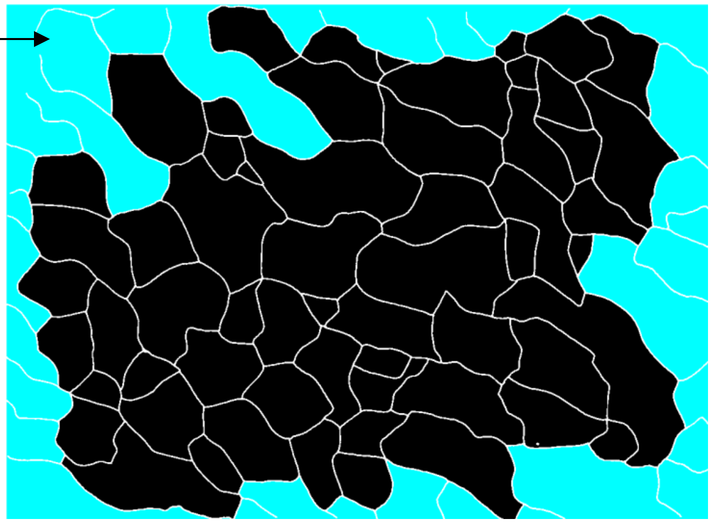

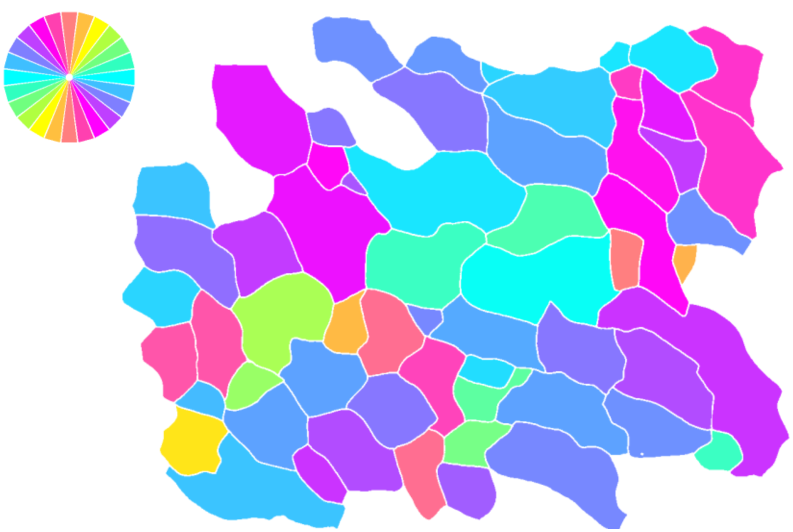

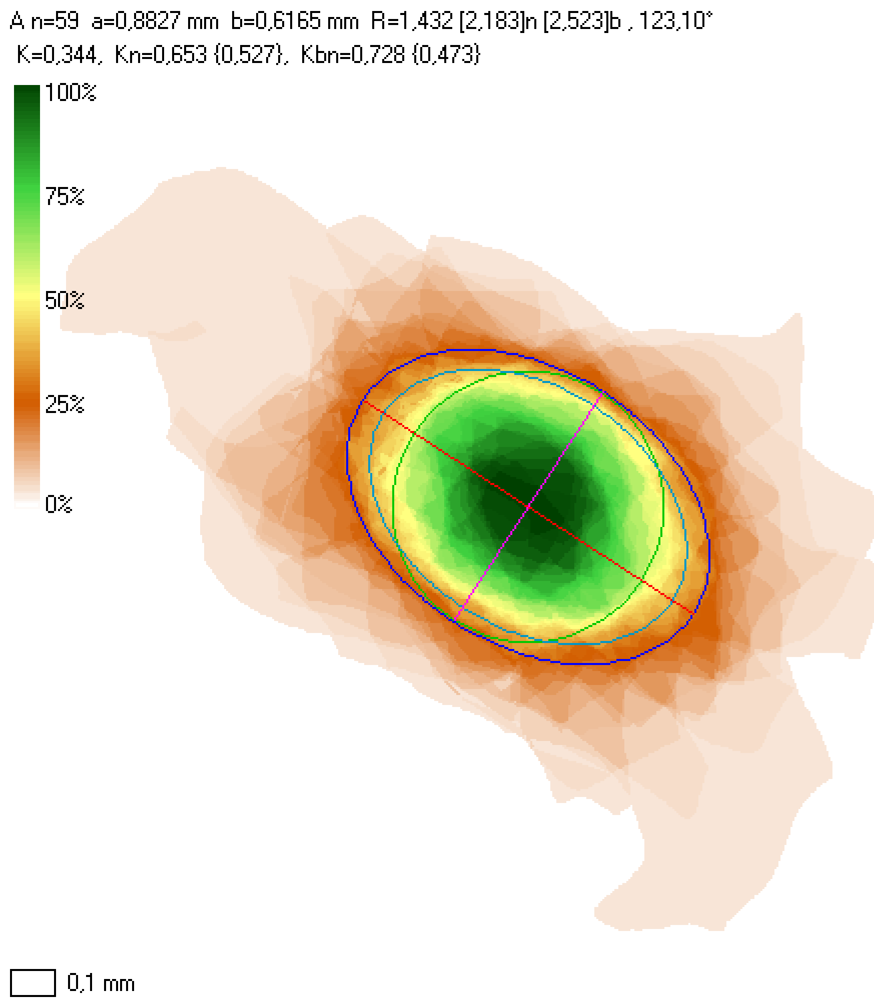

P. Launeau and P-Y. Robin (1996) "Fabric analysis using the intercept method". *Tectonophysics* 267, 91-119

Application to the BSE image of a synthetic magma

Plagioclase-bearing suspension composed of 52% of crystals was synthesized and then deformed using a Paterson HP-HT apparatus at a confining pressure of 300 MPa, a temperature of 850 C and a shear strain γ = 3.5

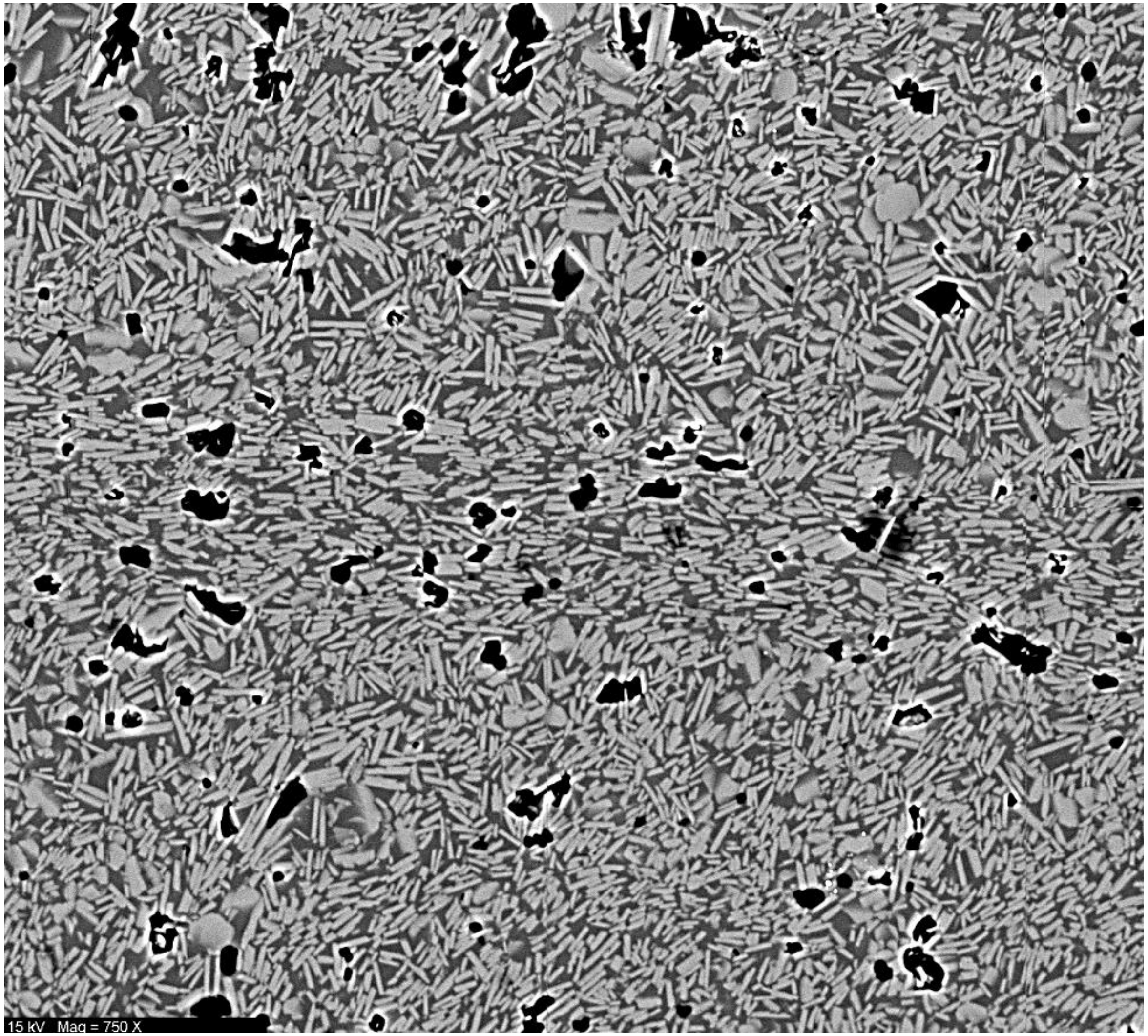

D. Picard, L. Arbaret, M. Pichavant, R. Champallier and P. Launeau, 2011, *Rheology and microstructures of experimentally deformed plagioclase suspensions*, Geology, doi 10.1130/G32217.1

Application to the BSE image of a synthetic magma

Threshold at grey level 140

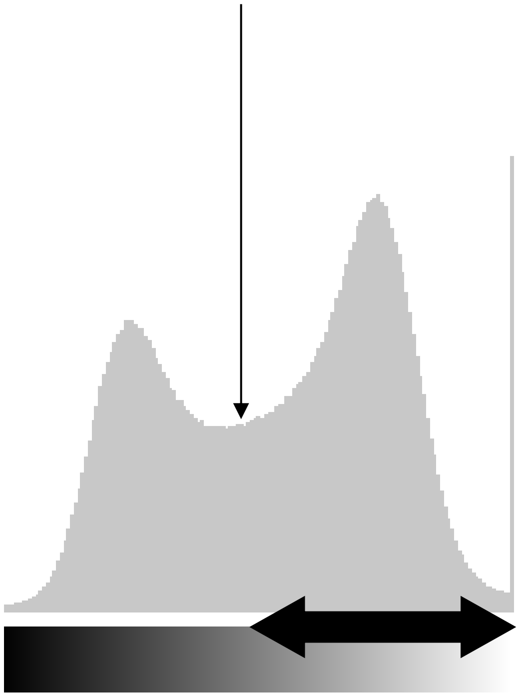

+ drawing a lot of missing boundaries

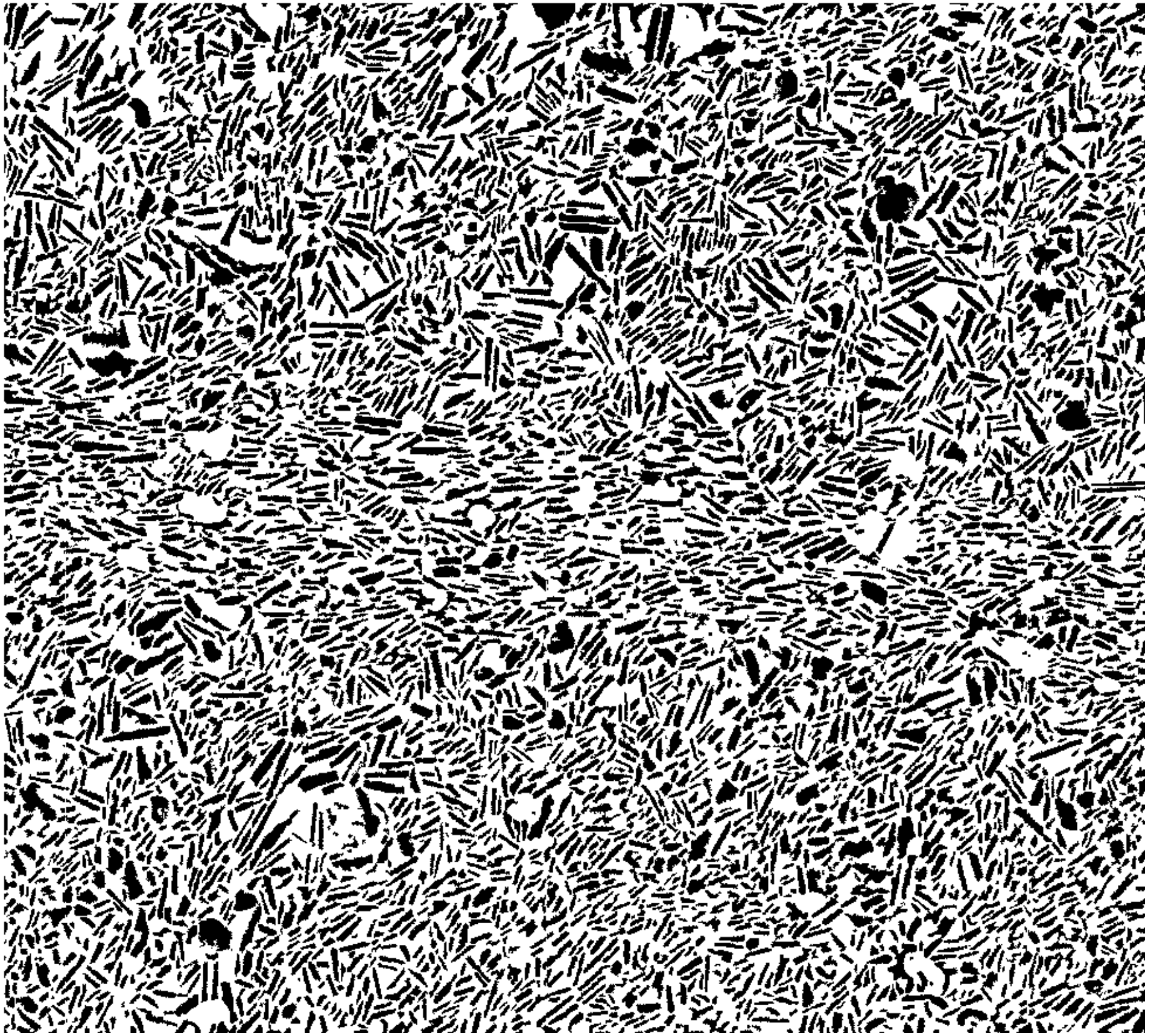

Launeau P., Archanjo C. J., Picard D., Arbaret L., Robin P.Y. (2010). Two- and three-dimensional shape fabric analysis by the intercept method in grey levels. Tectonophysics, Volume 492, Issues 1-4, 20 September 2010, Pages 230-239

Application to the BSE image of a synthetic magma

Inertia tensor : R

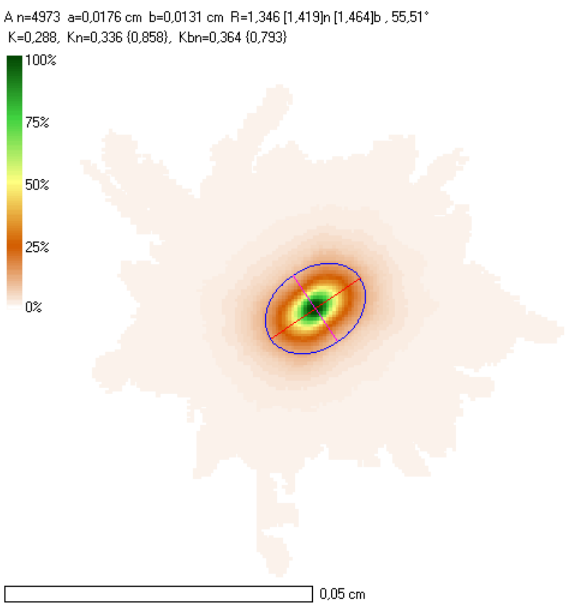

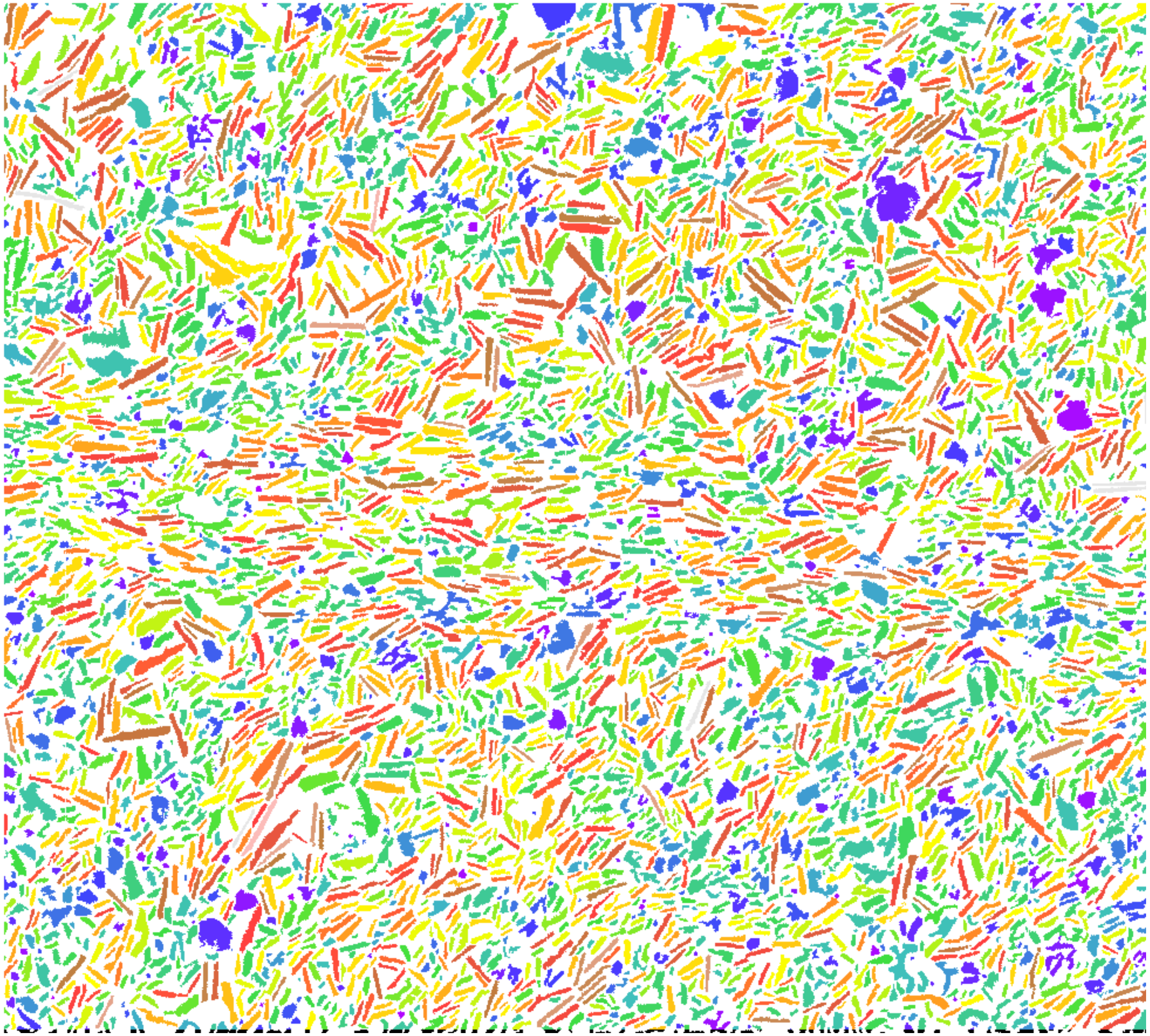

Launeau P., Archanjo C. J., Picard D., Arbaret L., Robin P.Y. (2010). Two- and three-dimensional shape fabric analysis by the intercept method in grey levels. Tectonophysics, Volume 492, Issues 1-4, 20 September 2010, Pages 230-239

Application to the BSE image of a synthetic magma

Inertia tensor : α

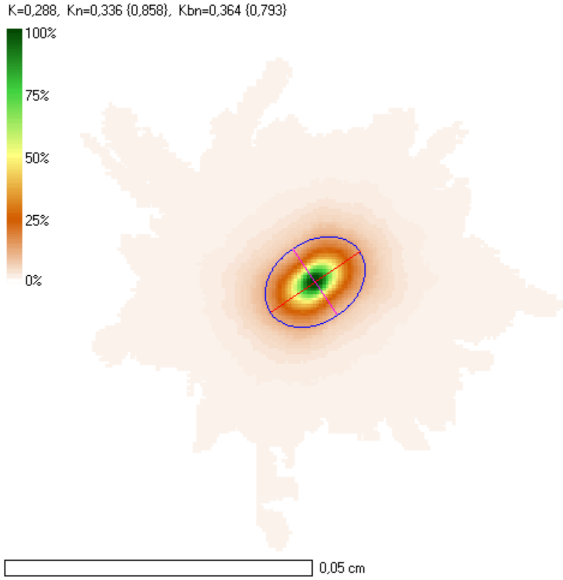

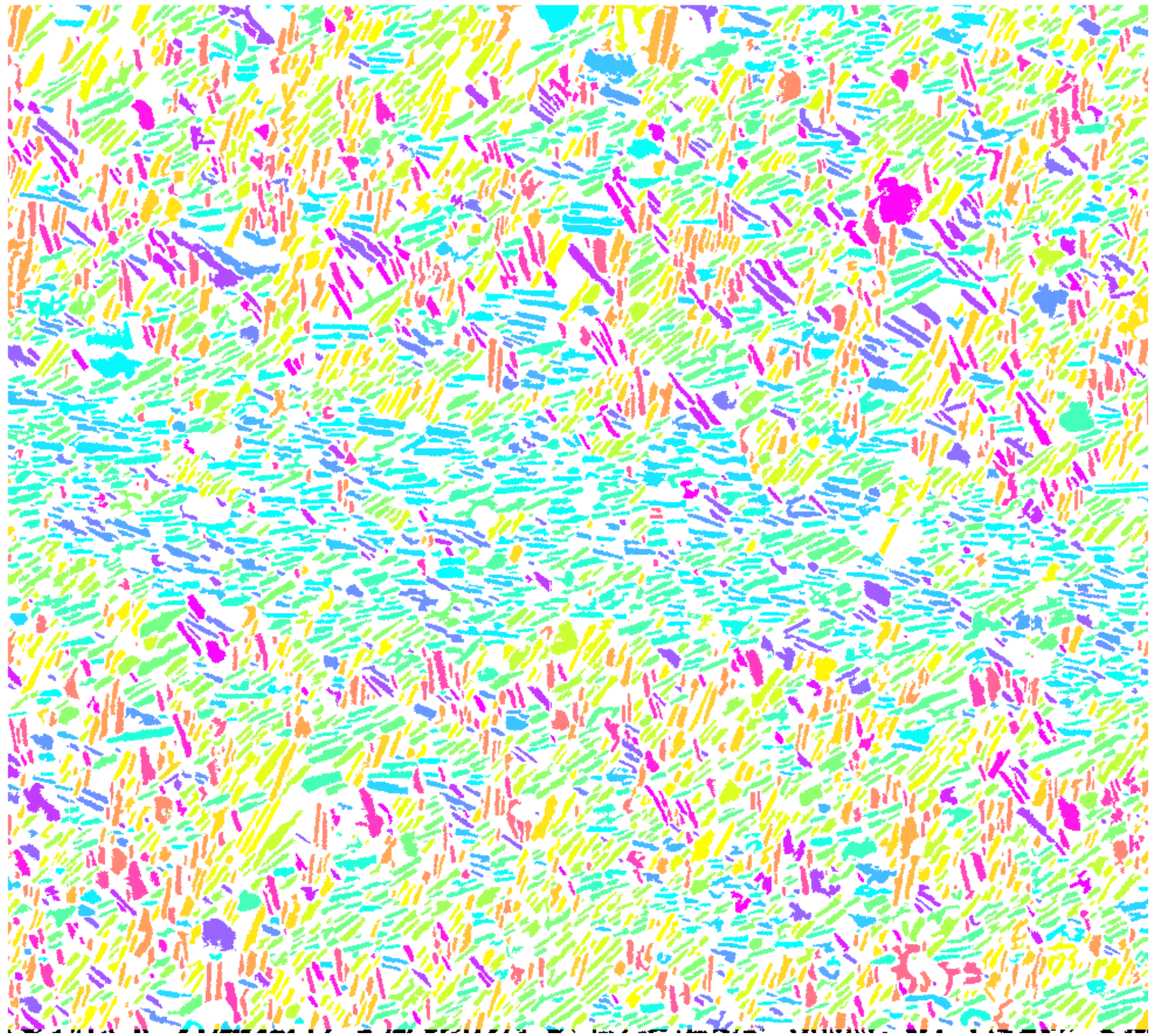

Launeau P., Archanjo C. J., Picard D., Arbaret L., Robin P.Y. (2010). Two- and three-dimensional shape fabric analysis by the intercept method in grey levels. Tectonophysics, Volume 492, Issues 1-4, 20 September 2010, Pages 230-239

Application to the BSE image of a synthetic magma

Inertia tensor : R, α

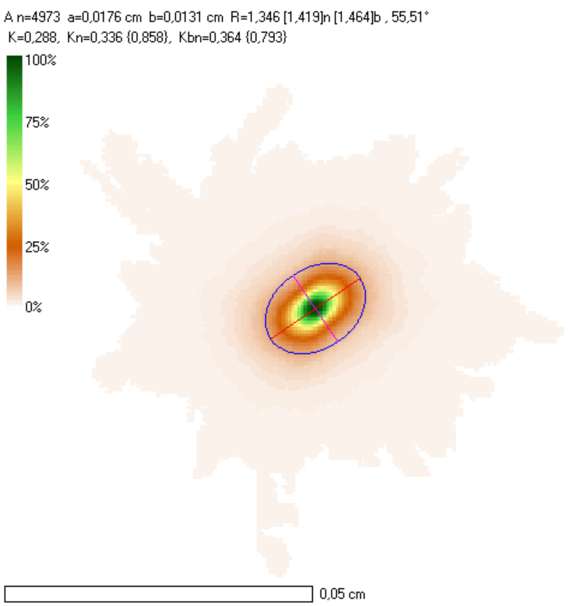

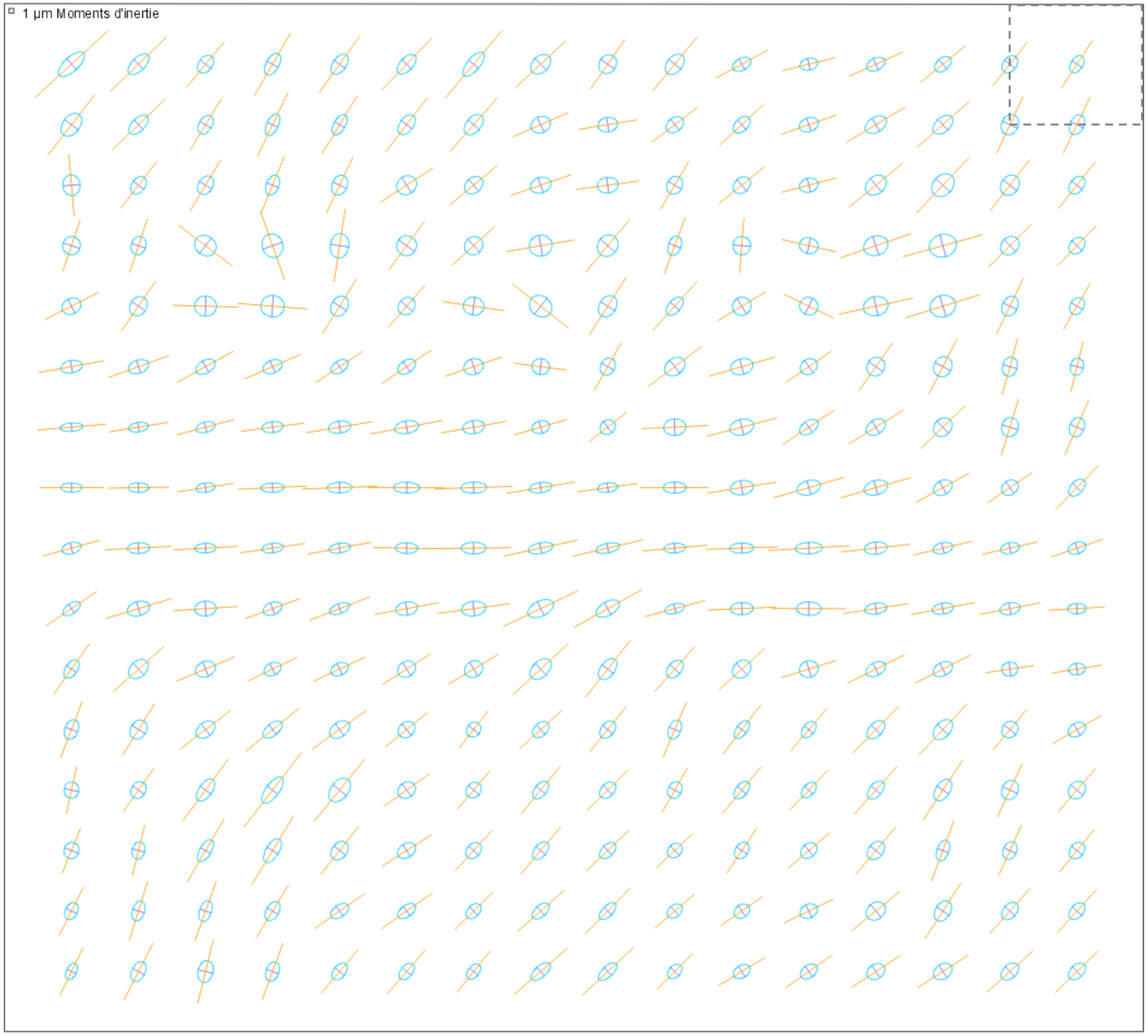

Launeau P., Archanjo C. J., Picard D., Arbaret L., Robin P.Y. (2010). Two- and three-dimensional shape fabric analysis by the intercept method in grey levels. Tectonophysics, Volume 492, Issues 1-4, 20 September 2010, Pages 230-239

Application to the BSE image of a synthetic magma

Analysis by intercept in grey level

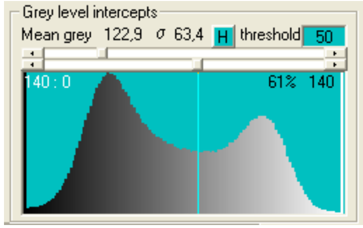

boundary = ⟷

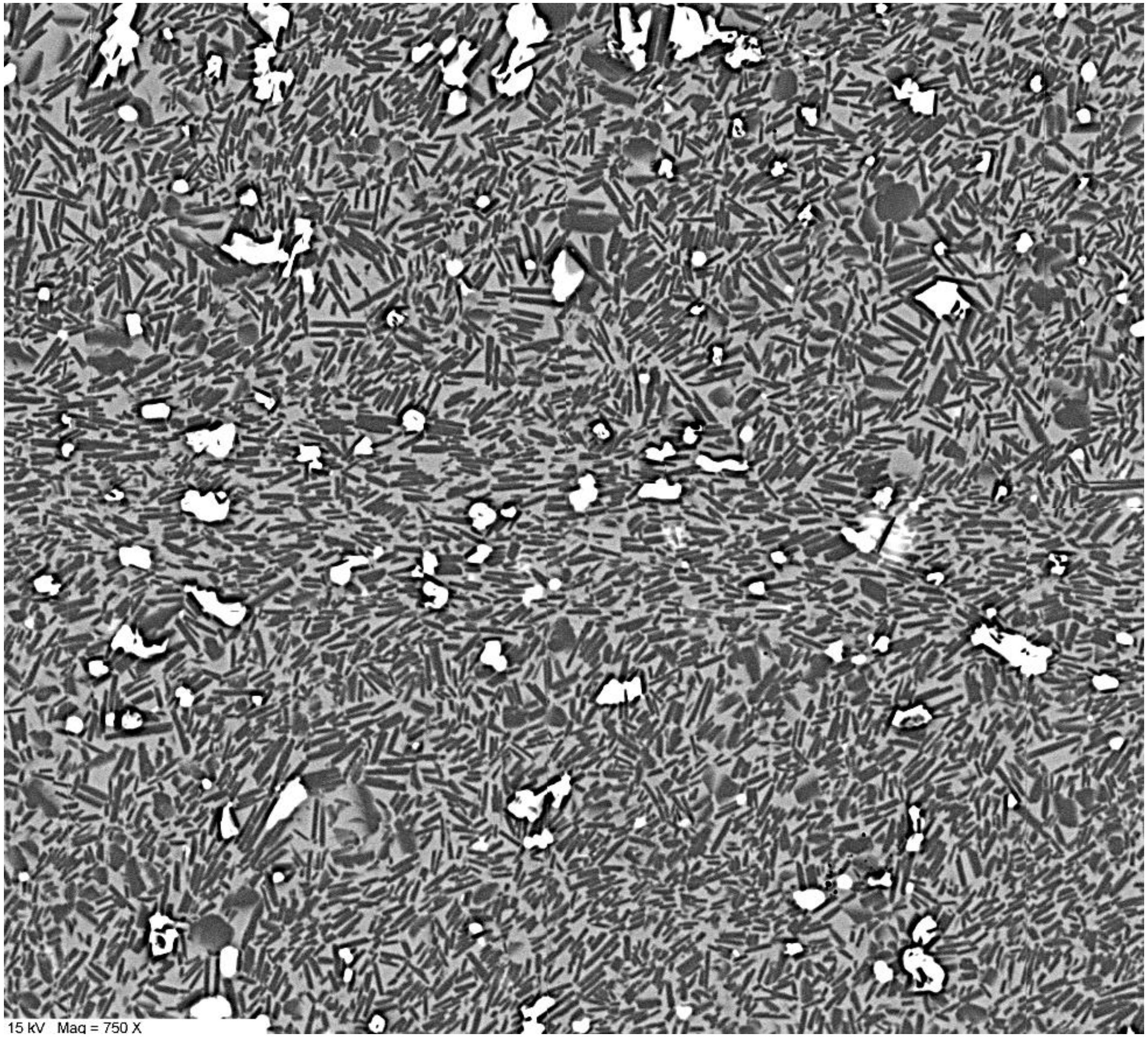

Launeau P., Archanjo C. J., Picard D., Arbaret L., Robin P.Y. (2010). Two- and three-dimensional shape fabric analysis by the intercept method in grey levels. Tectonophysics, Volume 492, Issues 1-4, 20 September 2010, Pages 230-239

Application to the BSE image of a synthetic magma

Analysis by intercept in grey level

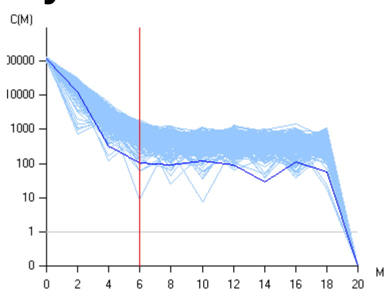

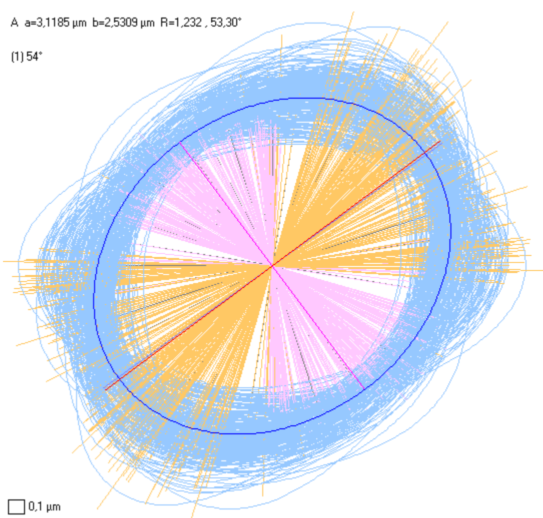

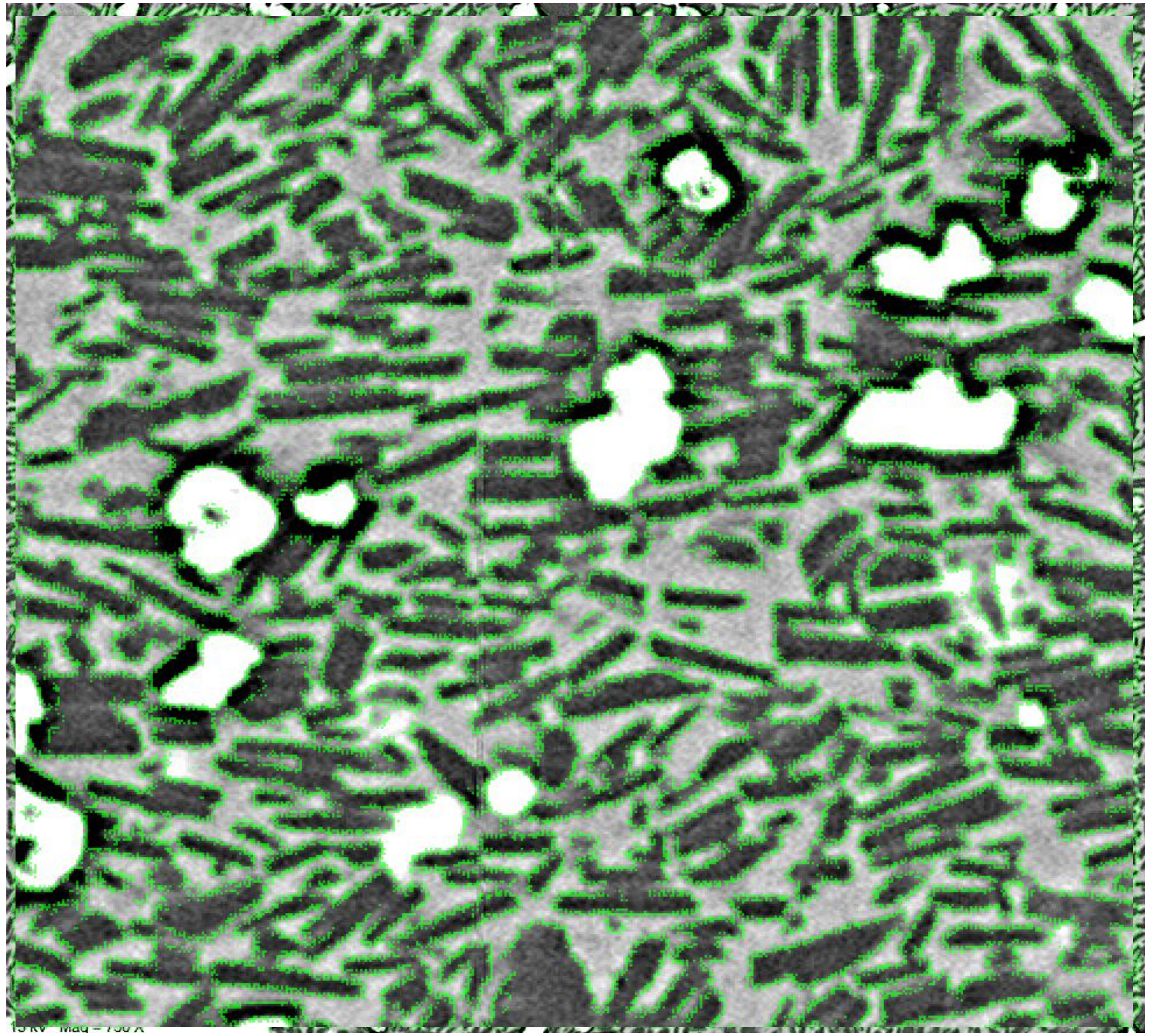

Launeau P., Archanjo C. J., Picard D., Arbaret L., Robin P.Y. (2010). Two- and three-dimensional shape fabric analysis by the intercept method in grey levels. Tectonophysics, Volume 492, Issues 1-4, 20 September 2010, Pages 230-239

Application to the BSE image of a synthetic magma

Analysis by intercept in grey level

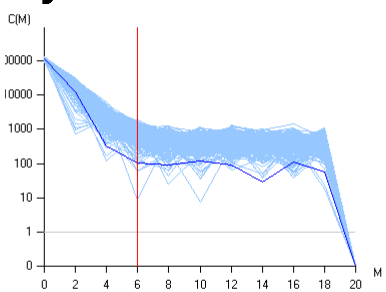

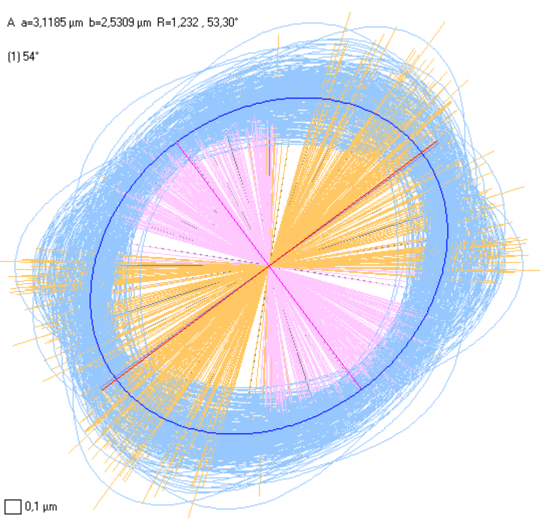

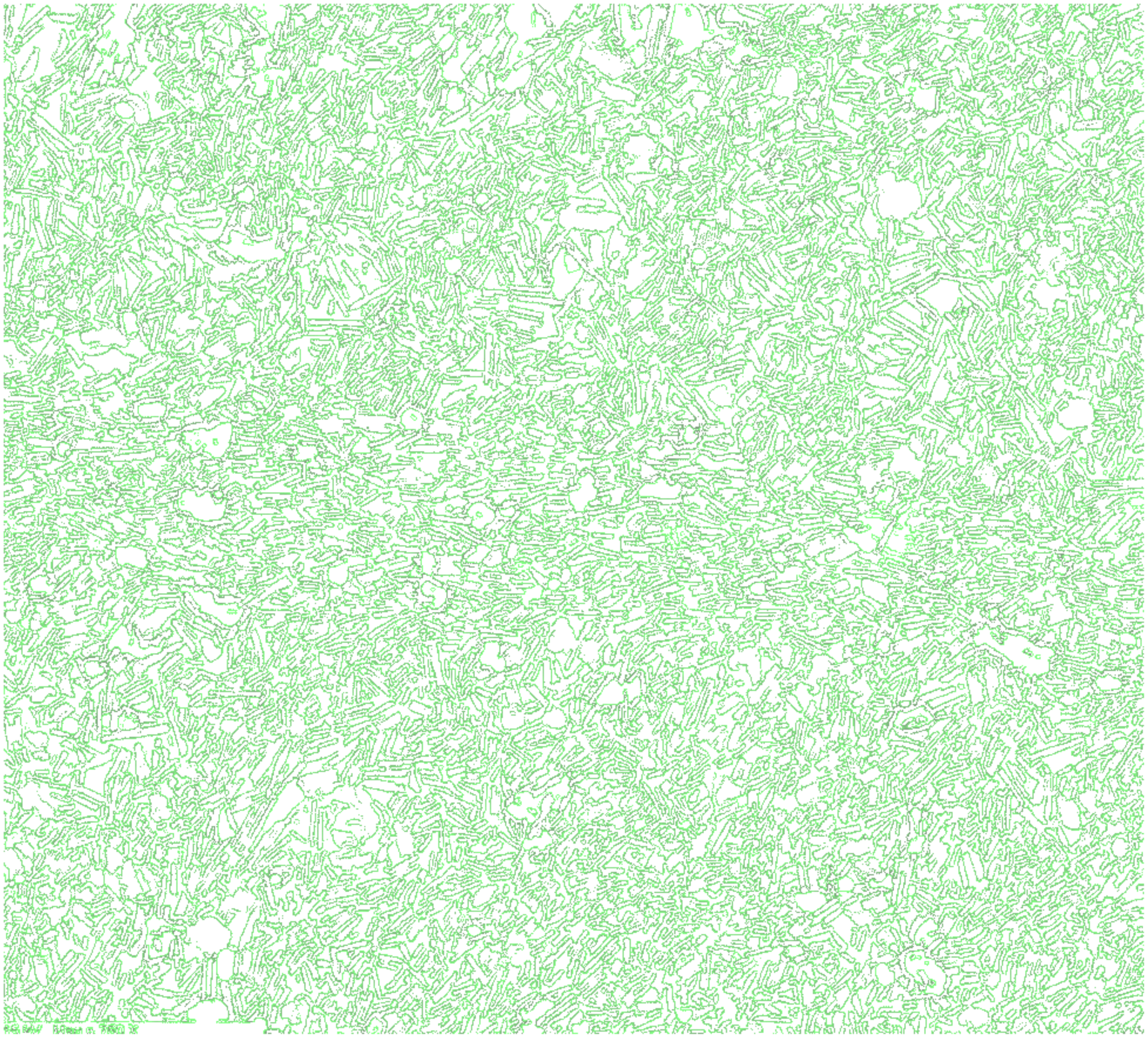

Launeau P., Archanjo C. J., Picard D., Arbaret L., Robin P.Y. (2010). Two- and three-dimensional shape fabric analysis by the intercept method in grey levels. Tectonophysics, Volume 492, Issues 1-4, 20 September 2010, Pages 230-239

Quantitative Image Analysis of Minerals and Rocks

http://www.sciences.univ-nantes.fr/lpgnantes/SPO

Application to the BSE image of a synthetic magma

Analysis by intercept in grey level

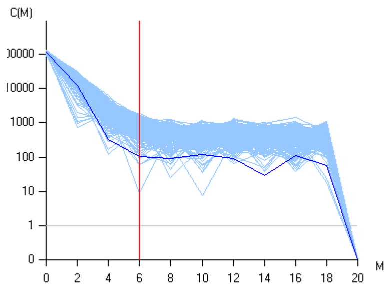

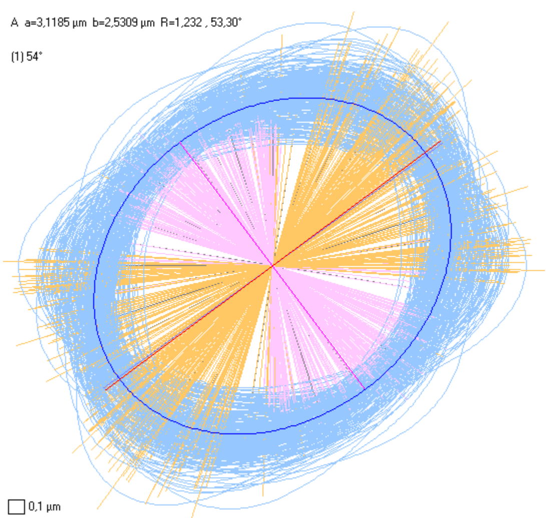

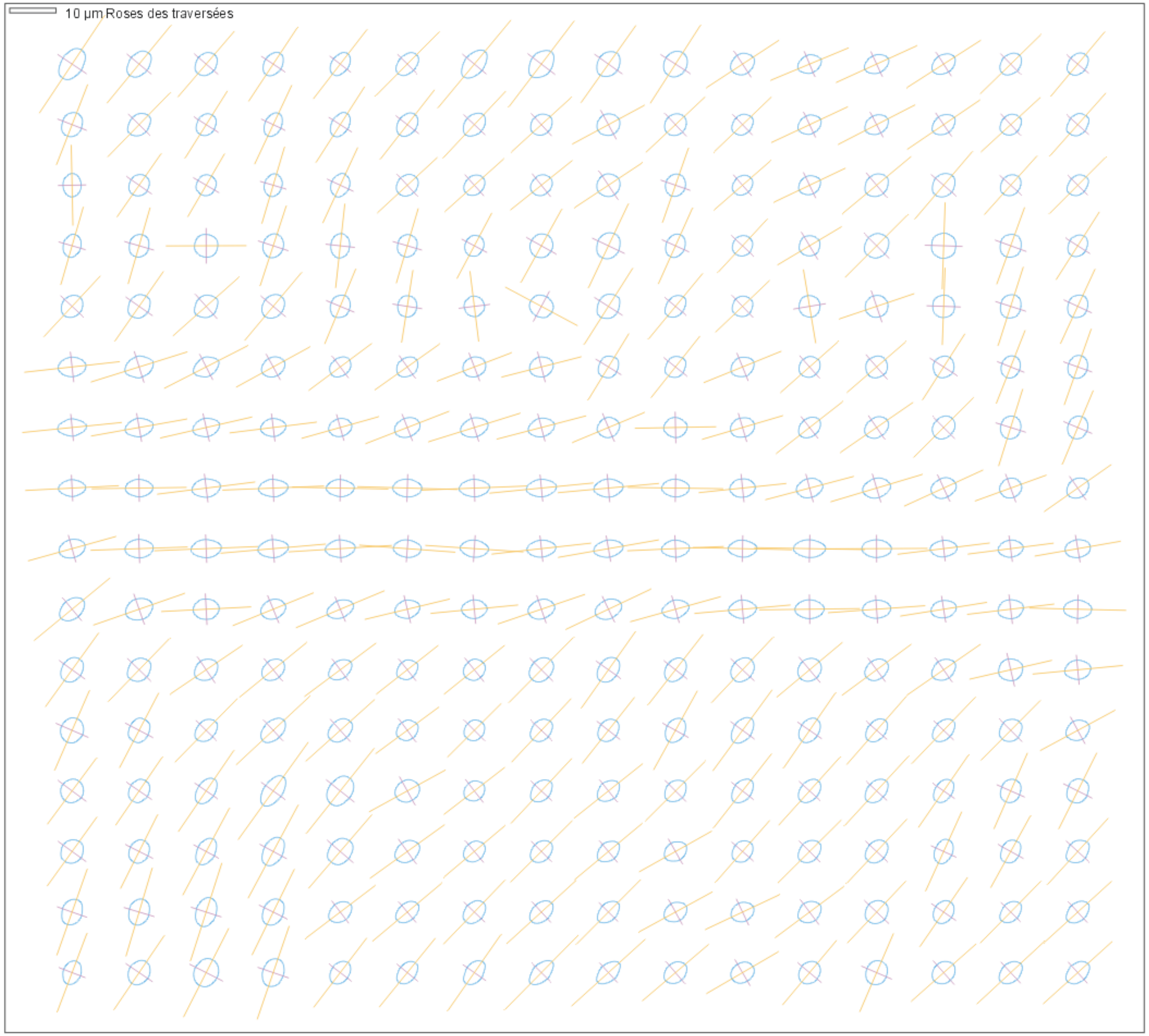

Launeau P., Archanjo C. J., Picard D., Arbaret L., Robin P.Y. (2010). Two- and three-dimensional shape fabric analysis by the intercept method in grey levels. Tectonophysics, Volume 492, Issues 1-4, 20 September 2010, Pages 230-239

Application to the BSE image of a synthetic magma

Analysis by intercept in grey level

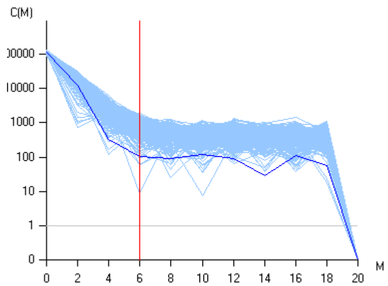

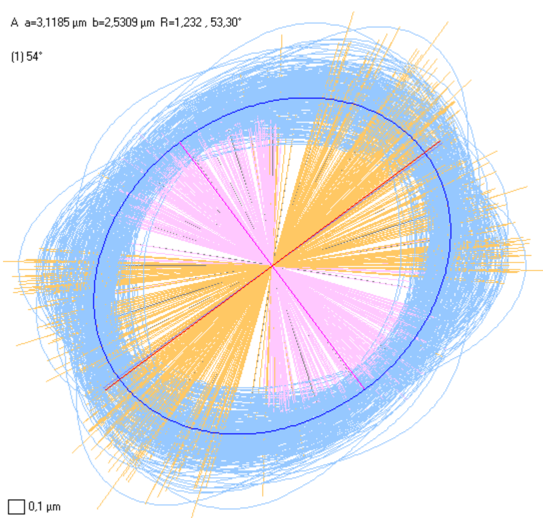

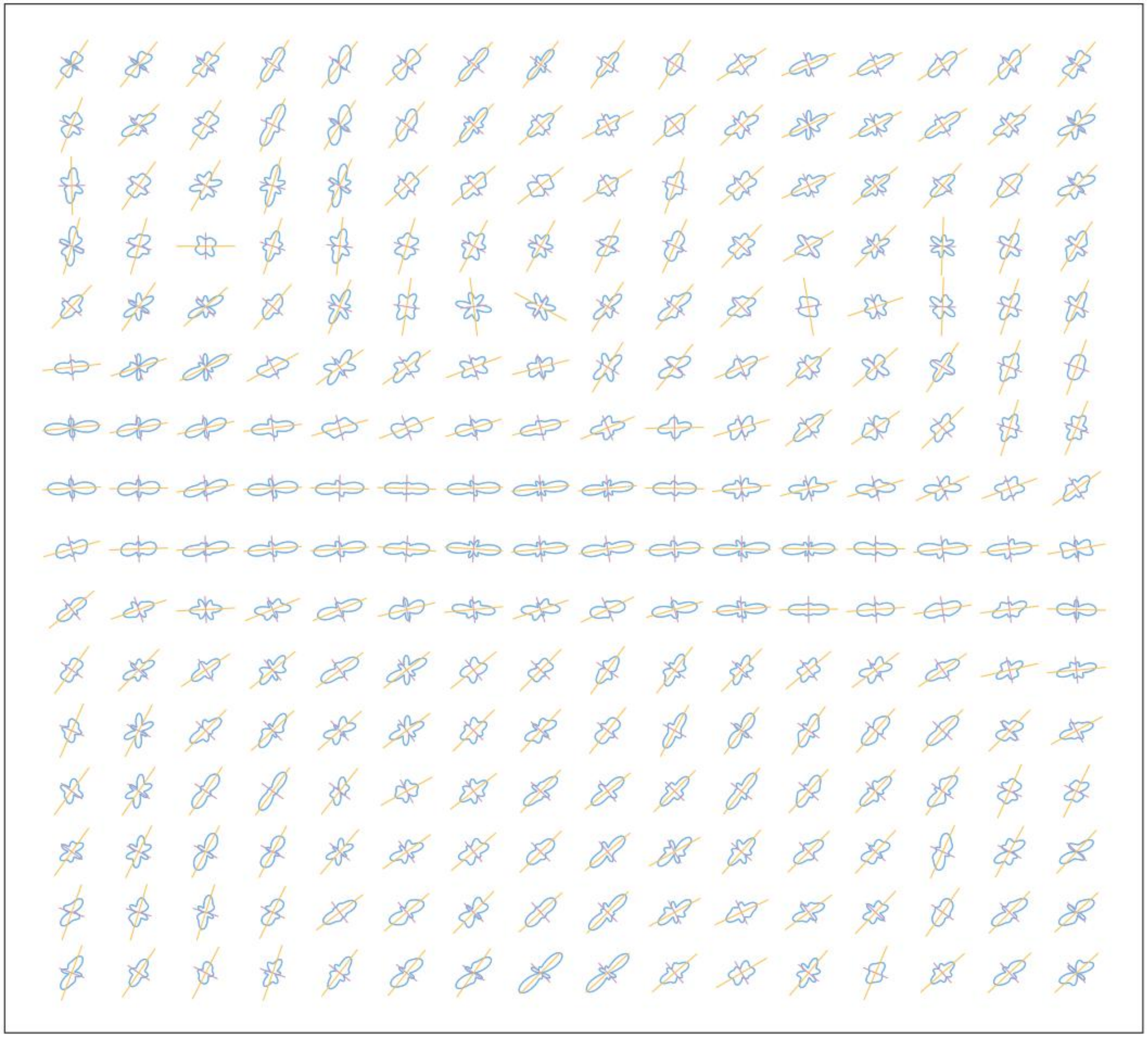

Launeau P., Archanjo C. J., Picard D., Arbaret L., Robin P.Y. (2010). Two- and three-dimensional shape fabric analysis by the intercept method in grey levels. Tectonophysics, Volume 492, Issues 1-4, 20 September 2010, Pages 230-239

Application to the BSE image of a synthetic magma

Analysis by intercept in grey level

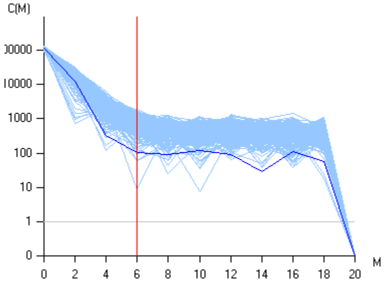

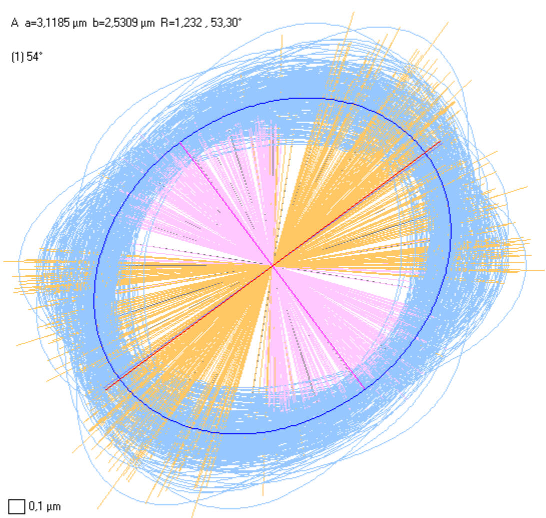

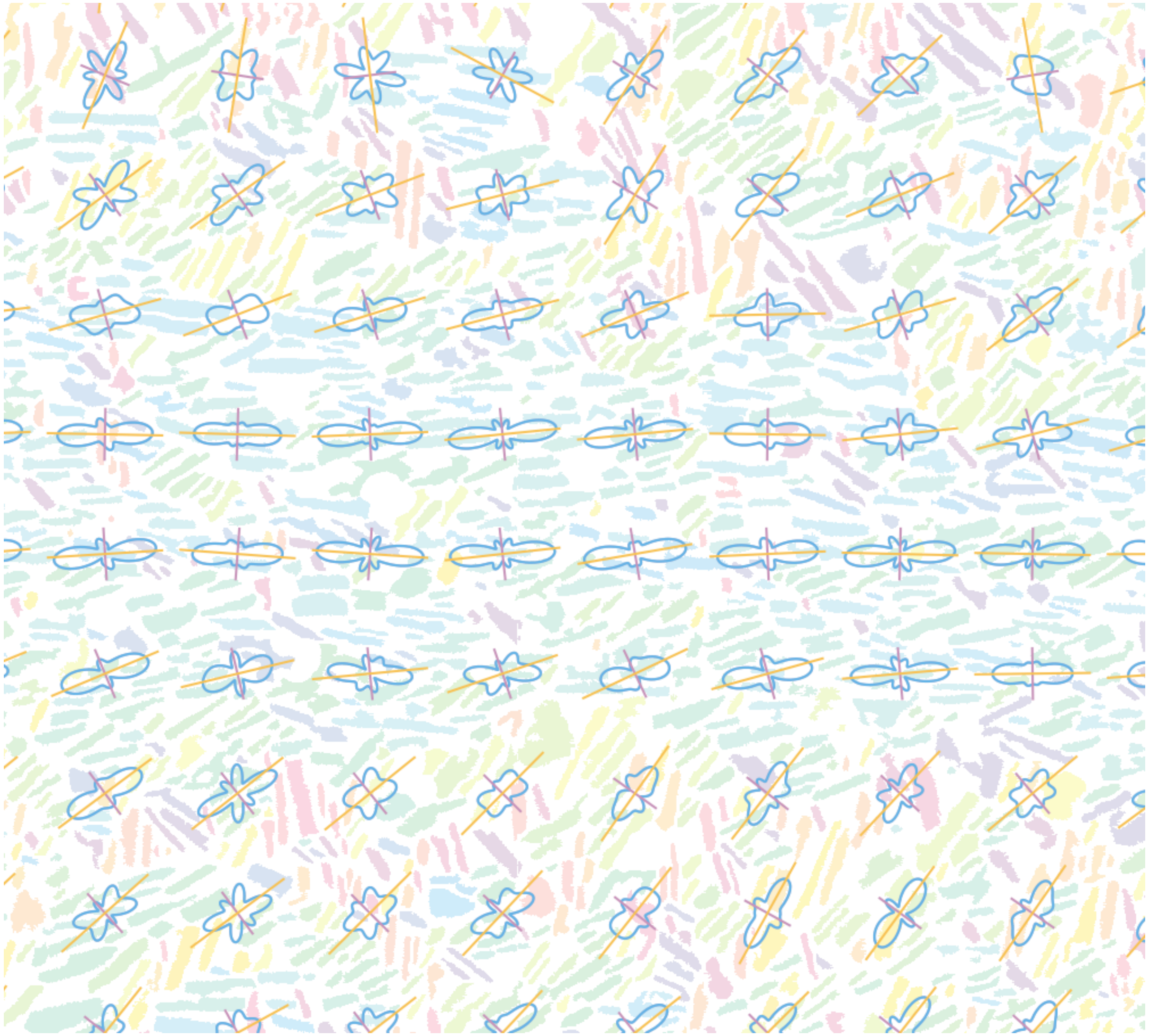

Launeau P., Archanjo C. J., Picard D., Arbaret L., Robin P.Y. (2010). Two- and three-dimensional shape fabric analysis by the intercept method in grey levels. Tectonophysics, Volume 492, Issues 1-4, 20 September 2010, Pages 230-239

Application to lineaments (Kaapvaal dikes - South Africa)

Analysis by intercept in grey level

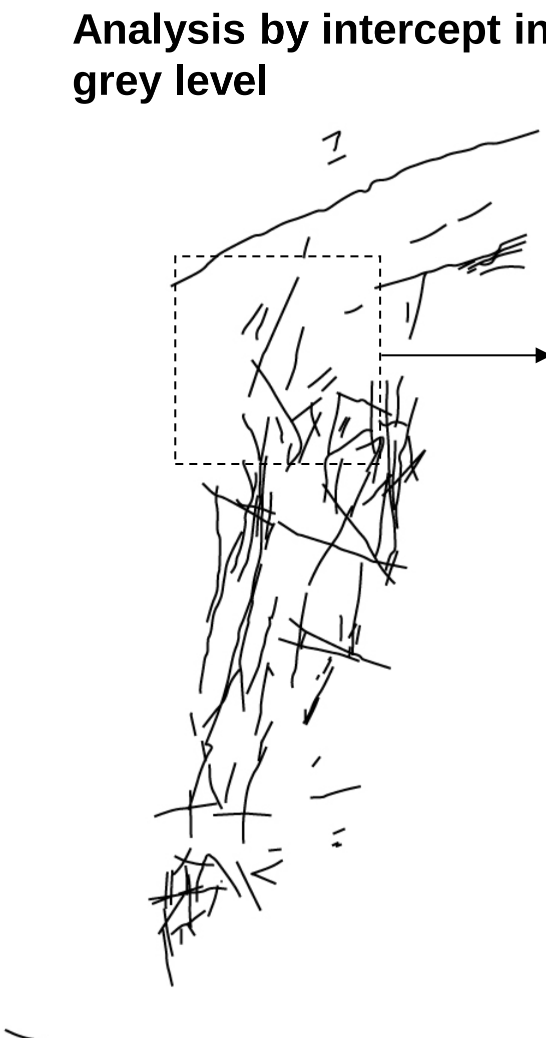

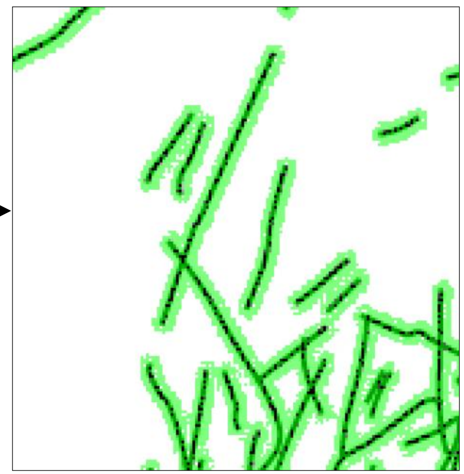

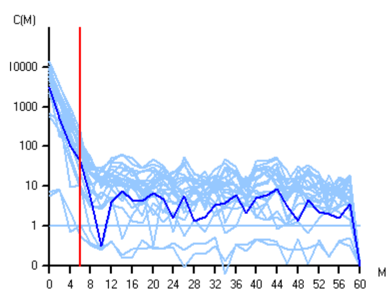

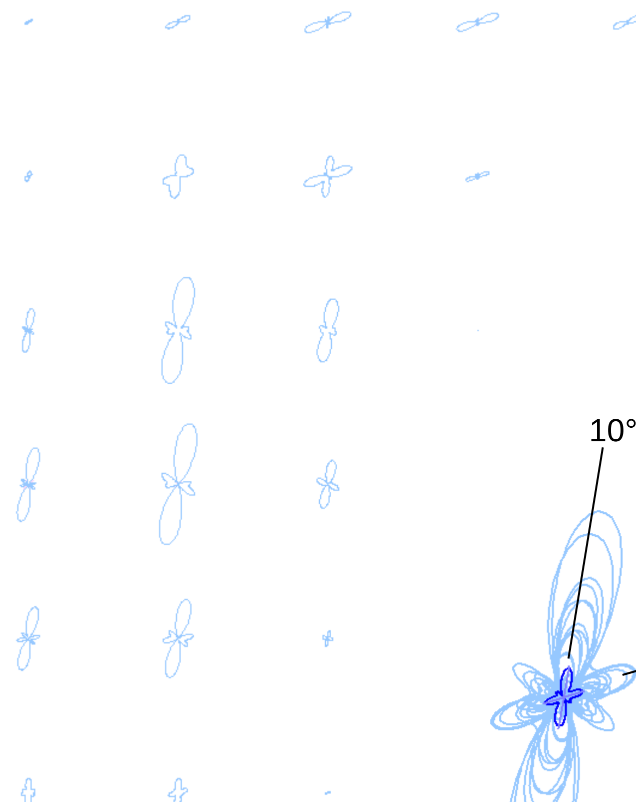

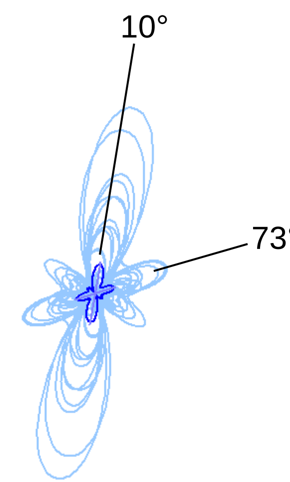

P. Launeau and P-Y. Robin (1996) "Fabric analysis using the intercept method". *Tectonophysics* 267, 91-119

Patrick Launeau

Quantitative Image Analysis off Minerals and Rocks

Fabric analysis

- Shape preferred orientation (SPO) vs. strain quantification.
- Intercepts in digital images : a tool to analyze interconnection of grains in rocks vs. inertia tensor of individualized grains
- SPO vs Spatial distribution (Fry)
- Ellipsoid of SPO and strain by combining 3 ⊥ images.

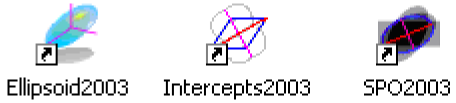

Inertia tensor = Fry diagram

Centre to centre method = Spatial distribution

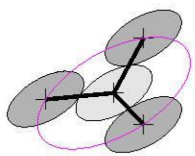

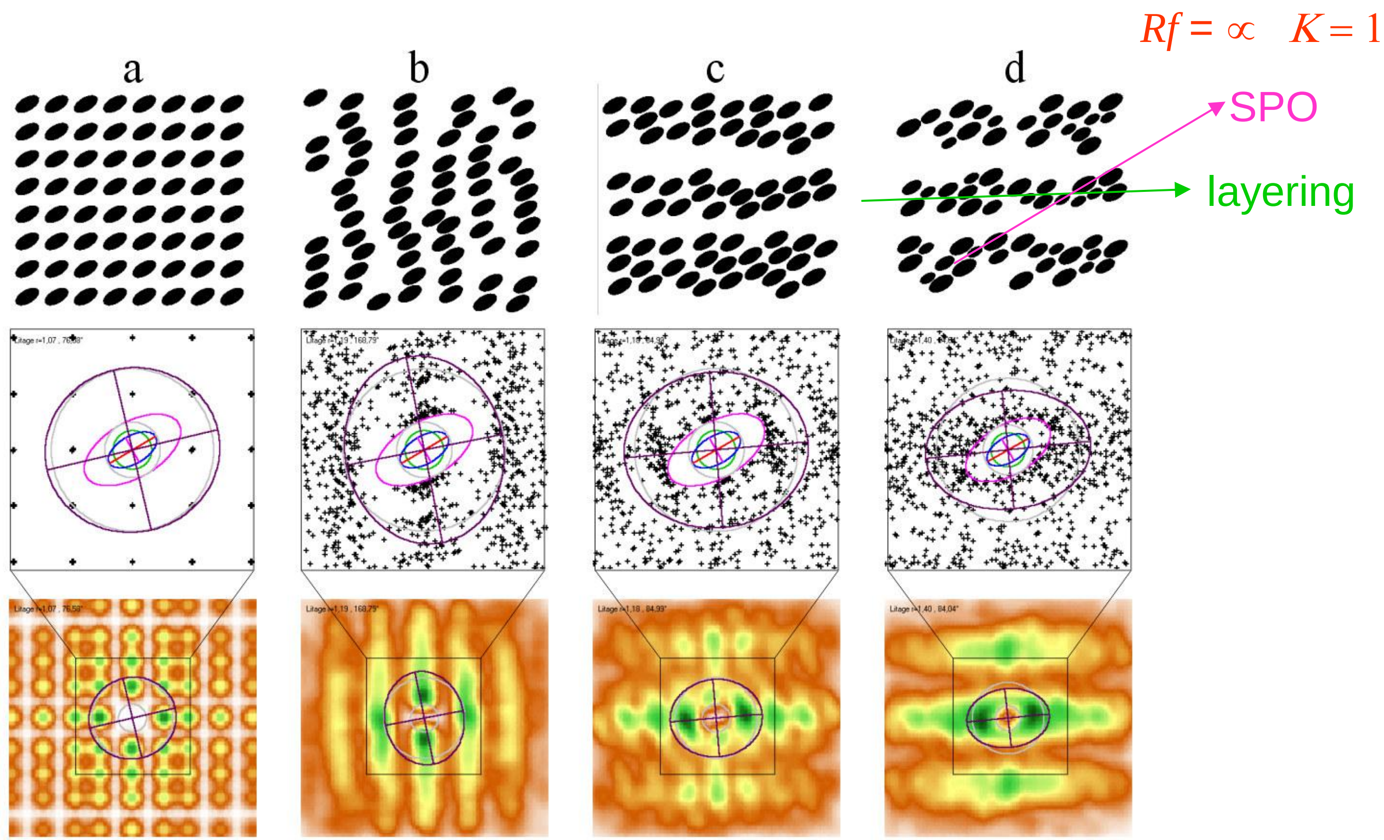

Quantitative Image Analysis of Minerals and Rocks

http://www.sciences.univ-nantes.fr/lpgnantes/SPO

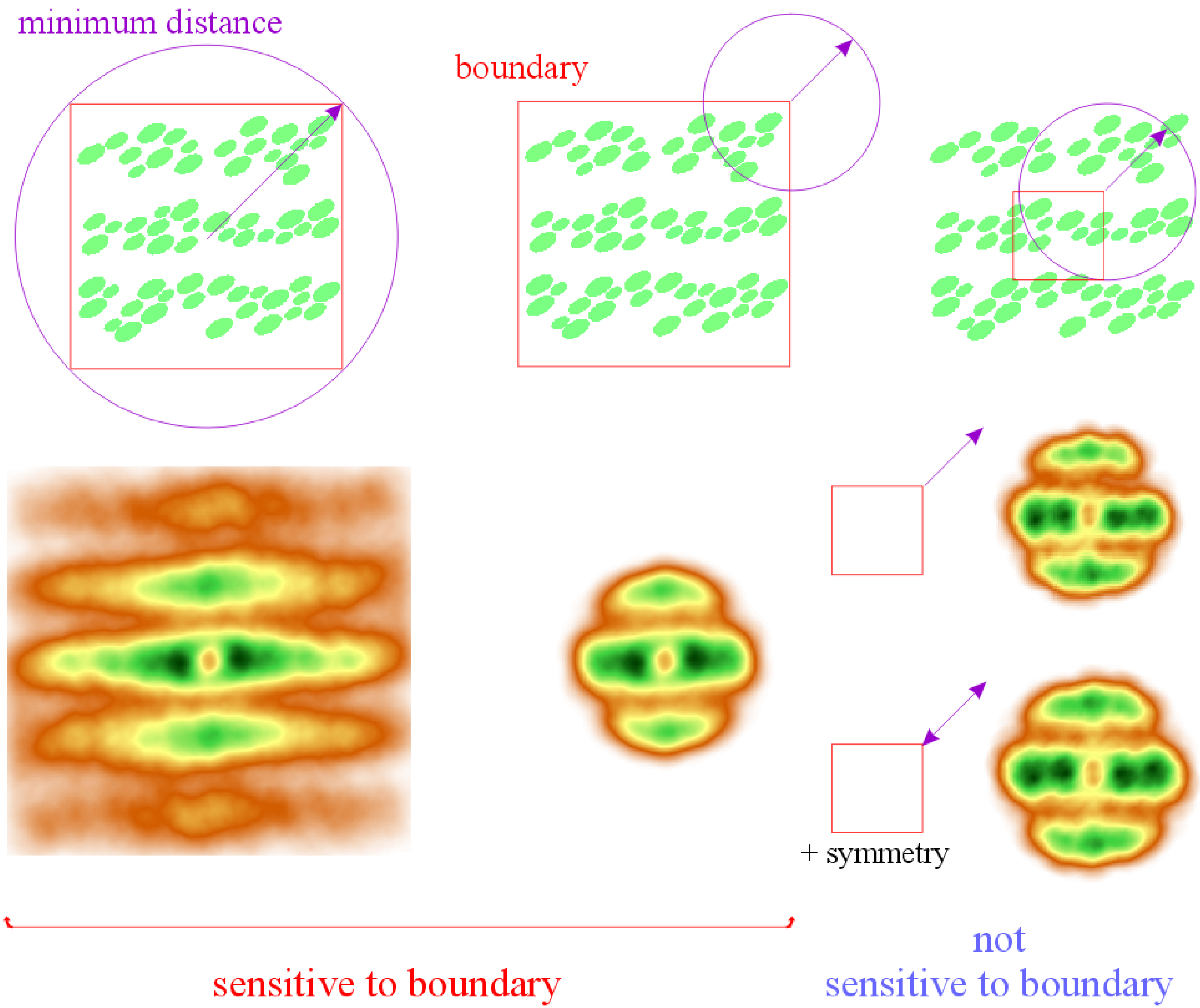

Fry

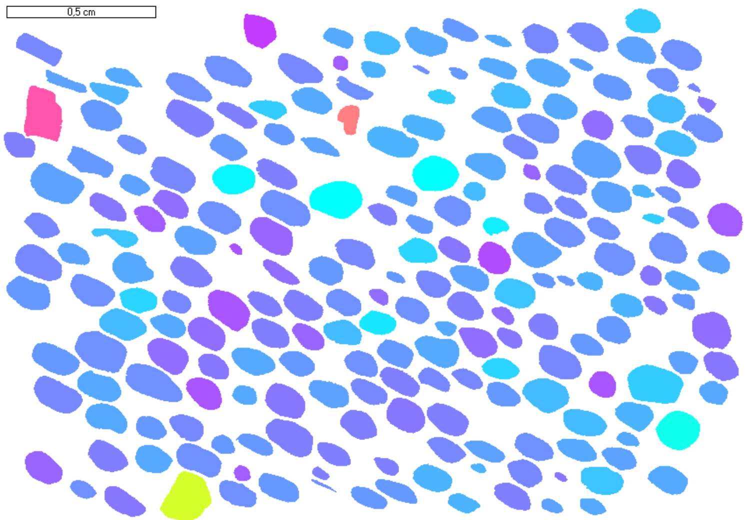

Mean intercept length

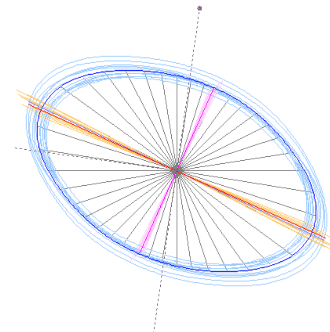

R= 1.630 @ 114,3°

1mm

R= 1.645 @ 114,1°

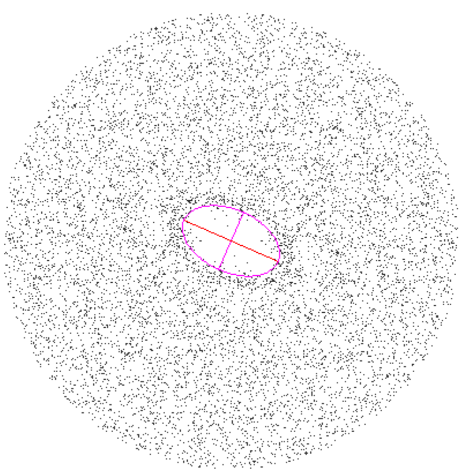

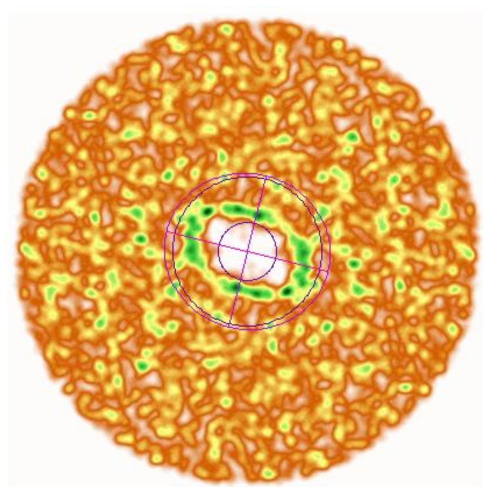

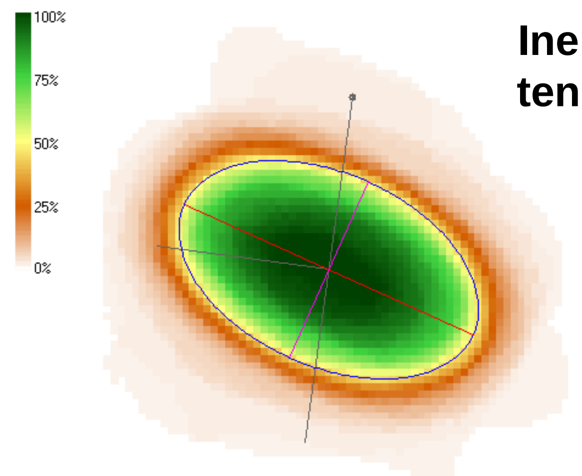

Inertia tensor

Spatial distribution and Compaction

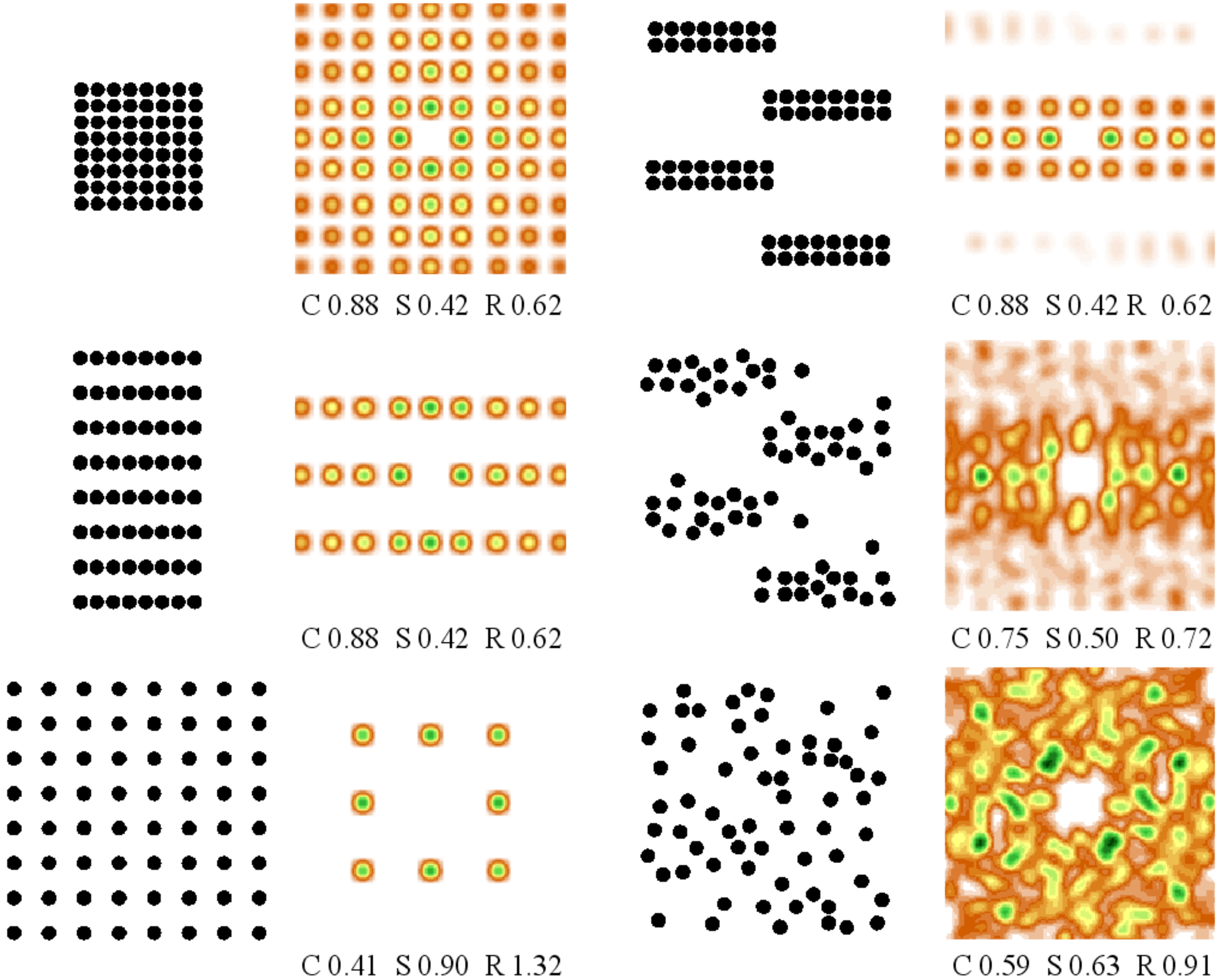

Autocorrelation / intercepts

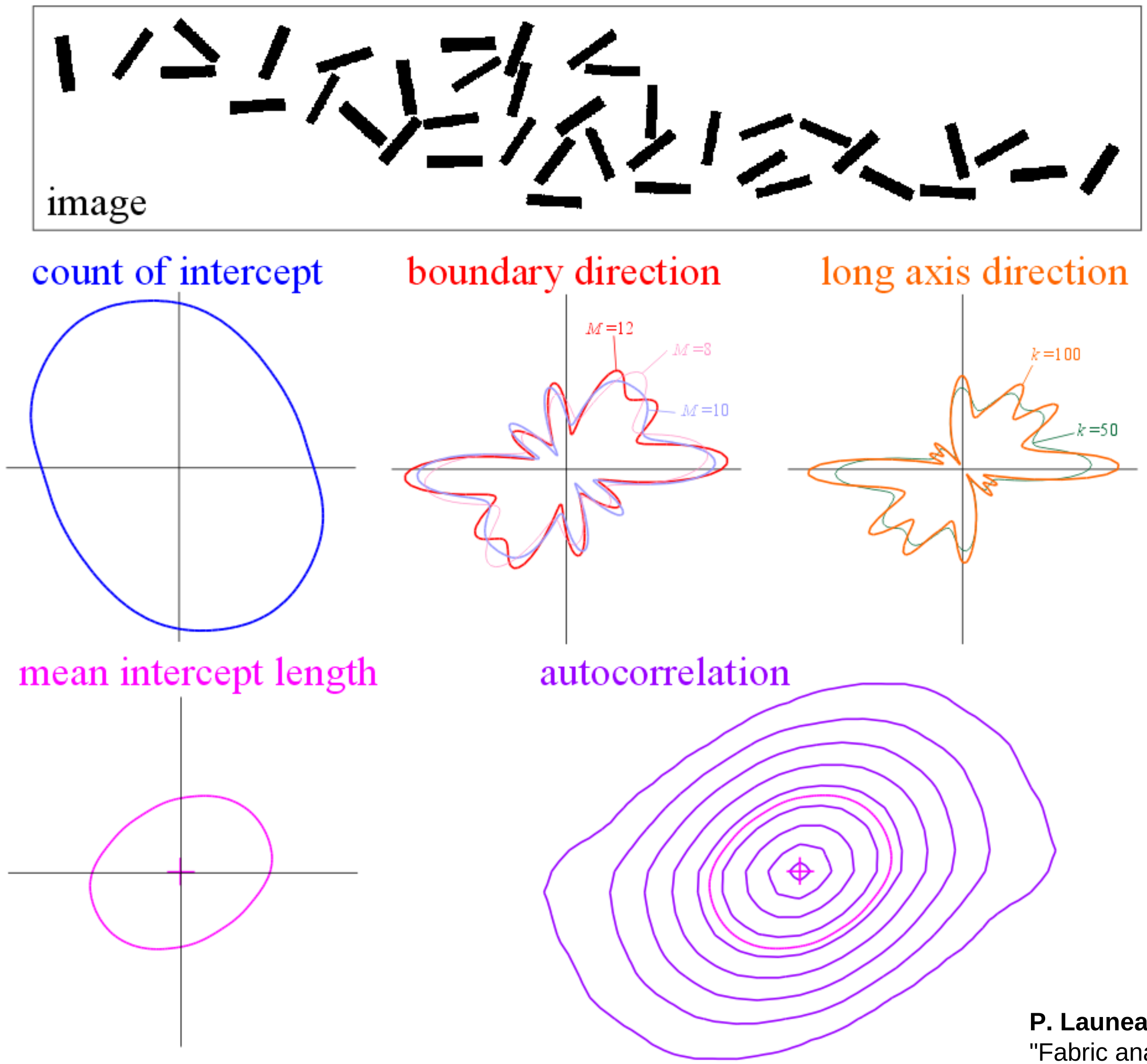

P. Launeau and P-Y. Robin (1996)
"Fabric analysis using the intercept method". *Tectonophysics* 267, 91-119

CSD

ln(n) with n=number of object / surface area / class length

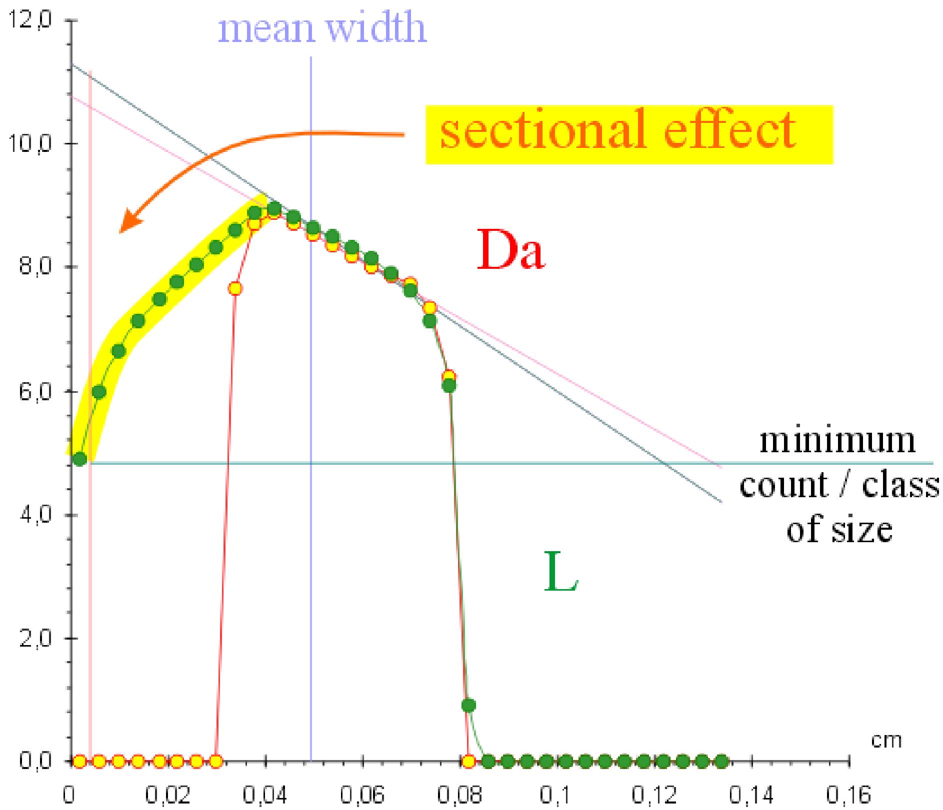

Ideal CSD of 222 circles

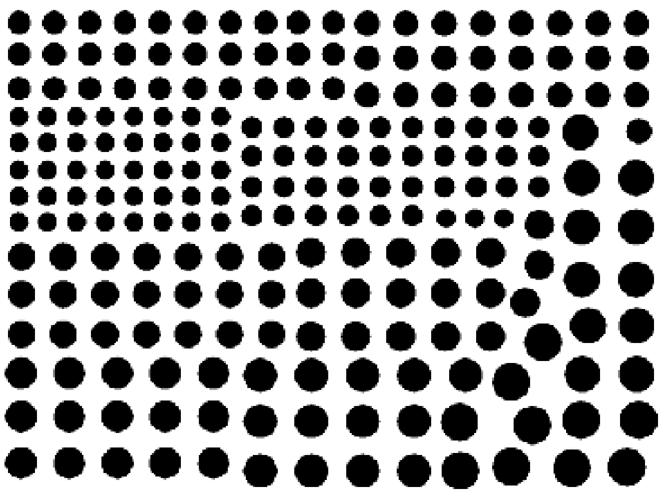

CSD

ln(n) with n=number of object / surface area / class length

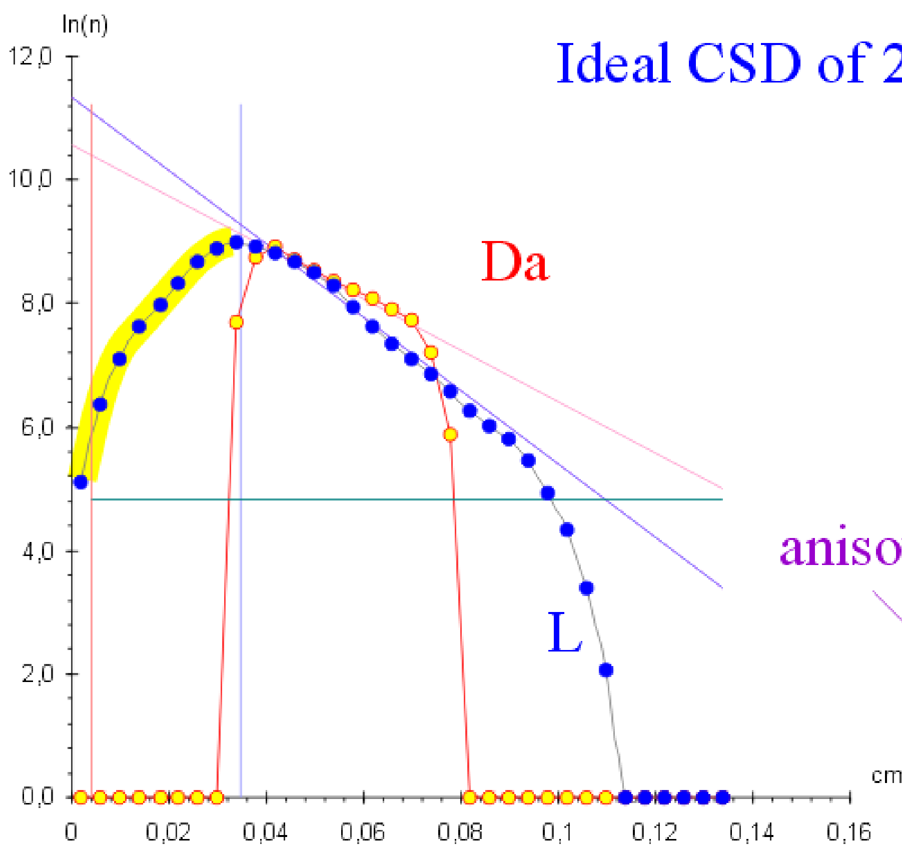

Ideal CSD of 222 ellipses with shape ratio = 2

anisotropy

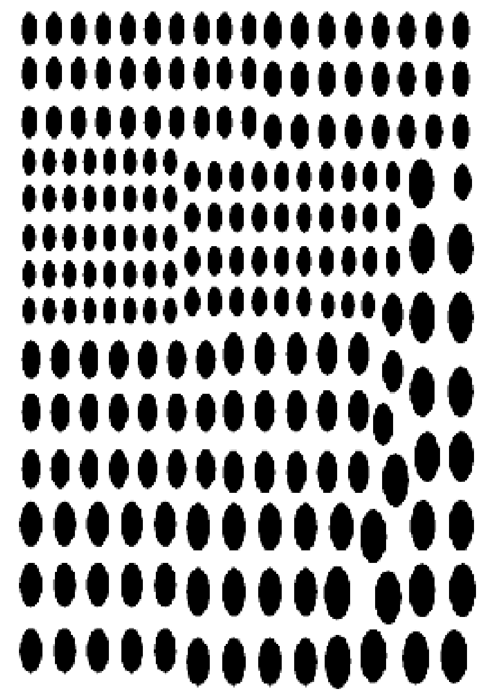

CSD

ln(n) with n=number of object / surface area / class length

Ideal CSD of 222 rectangles with shape ratio = 2

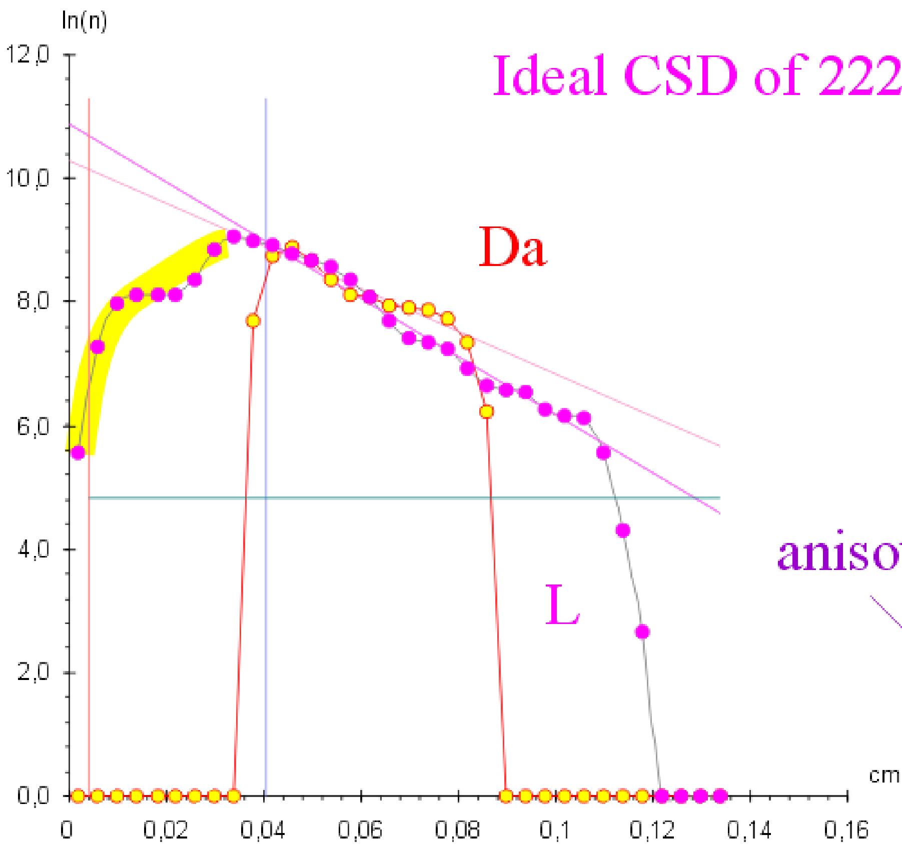

anisotropy

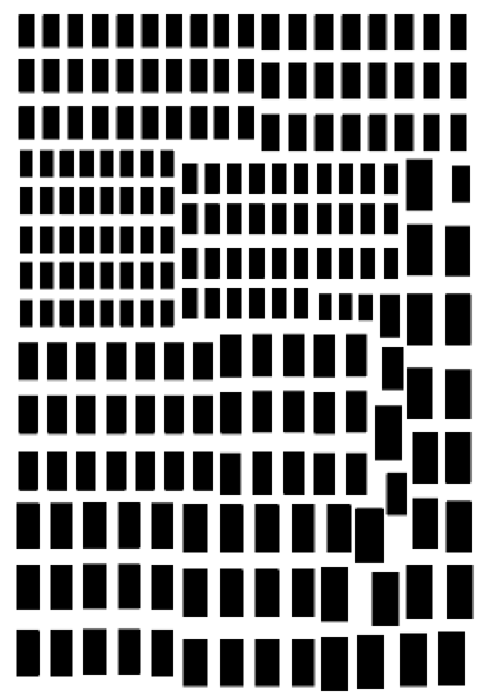

CSD

Histogram of segments cut by a set of lines between 0 and 180°

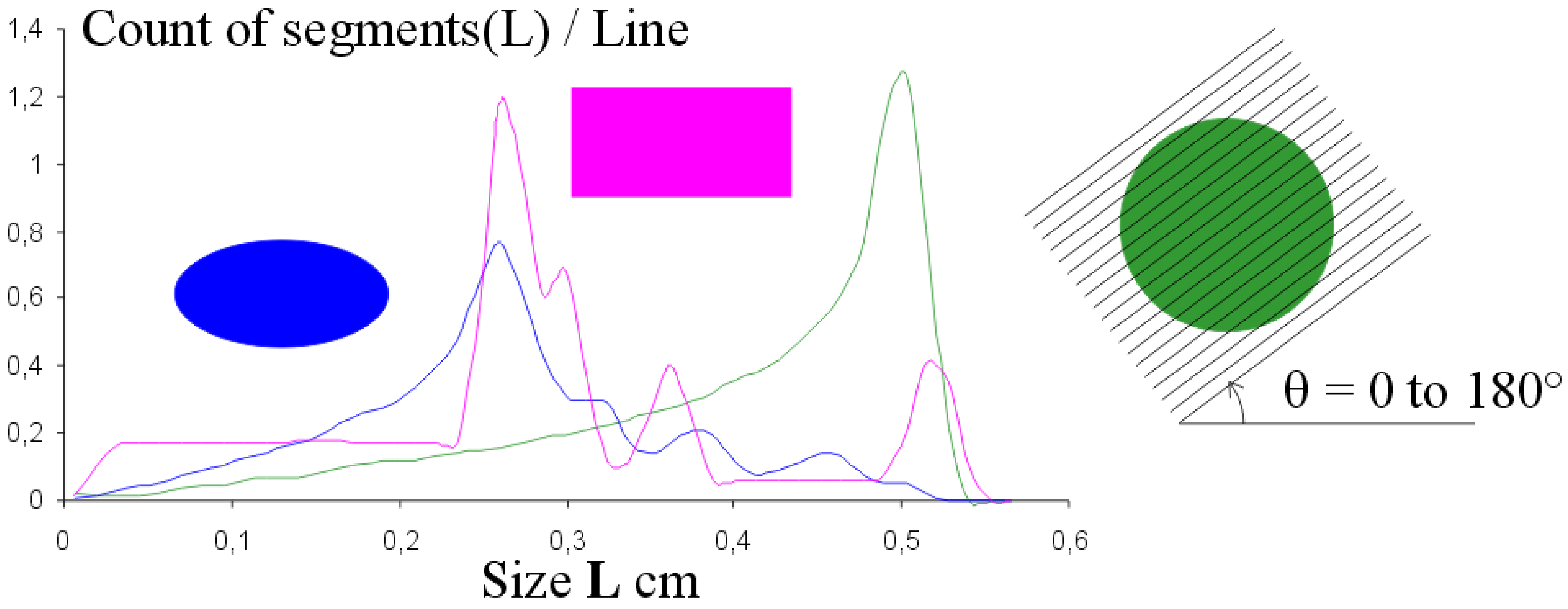

Patrick Launeau

Quantitative Image Analysis off Minerals and Rocks

Fabric analysis

- Shape preferred orientation (SPO) vs. strain quantification.
- Intercepts in digital images : a tool to analyze interconnection of grains in rocks vs. inertia tensor of individualized grains
- SPO vs Spatial distribution (Fry)
- Ellipsoid of SPO and strain by combining 3 ⊥ images.

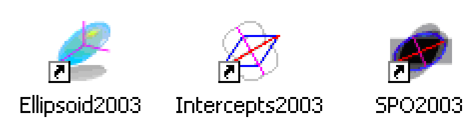

From 2D image analysis to 3D ellipsoid construction

$$\mathbf{R}_L = \begin{bmatrix} \cos\alpha\cos\varphi - \sin\alpha\cos\theta\sin\varphi \\ \sin\alpha\cos\varphi + \cos\alpha\cos\theta\sin\varphi \\ \sin\theta\sin\varphi \end{bmatrix}$$

North,East,Down convention

Euler angles : strike α , dip θ, pitch or rake φ

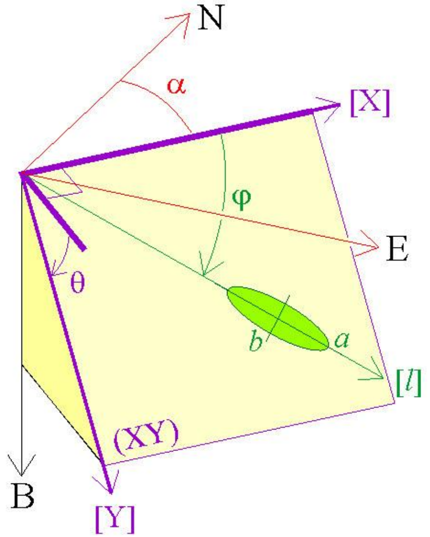

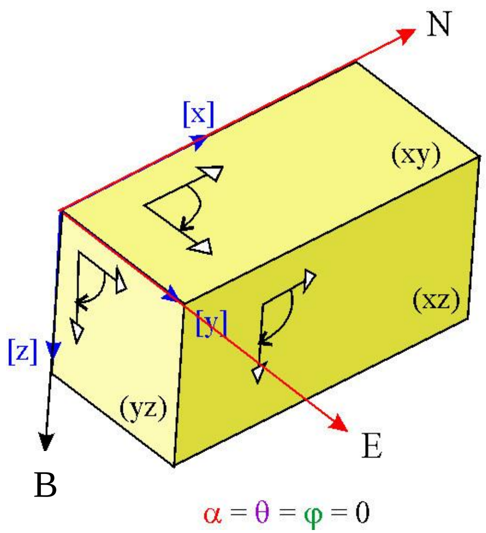

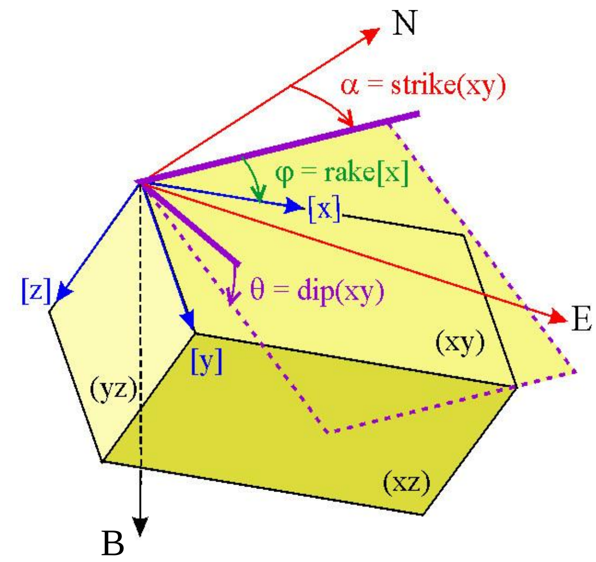

P. Launeau, P.-Y. F. Robin (2005) "Determination of fabric and strain ellipsoids from measured sectional ellipses—implementation and applications". *Journal of Structural Geology,* 27, 2223-2233

$$\mathbf{R}_V = \begin{bmatrix} \cos\alpha\cos\varphi - \sin\alpha\cos\theta\sin\varphi & -\cos\alpha\sin\varphi - \sin\alpha\cos\theta\cos\varphi & \sin\alpha\sin\theta \\ \sin\alpha\cos\varphi + \cos\alpha\cos\theta\sin\varphi & -\sin\alpha\sin\varphi + \cos\alpha\cos\theta\cos\varphi & -\cos\alpha\sin\theta \\ \sin\theta\sin\varphi & \sin\theta\cos\varphi & \cos\theta \end{bmatrix}$$

From 2D ellipse to 3D ellipsoid

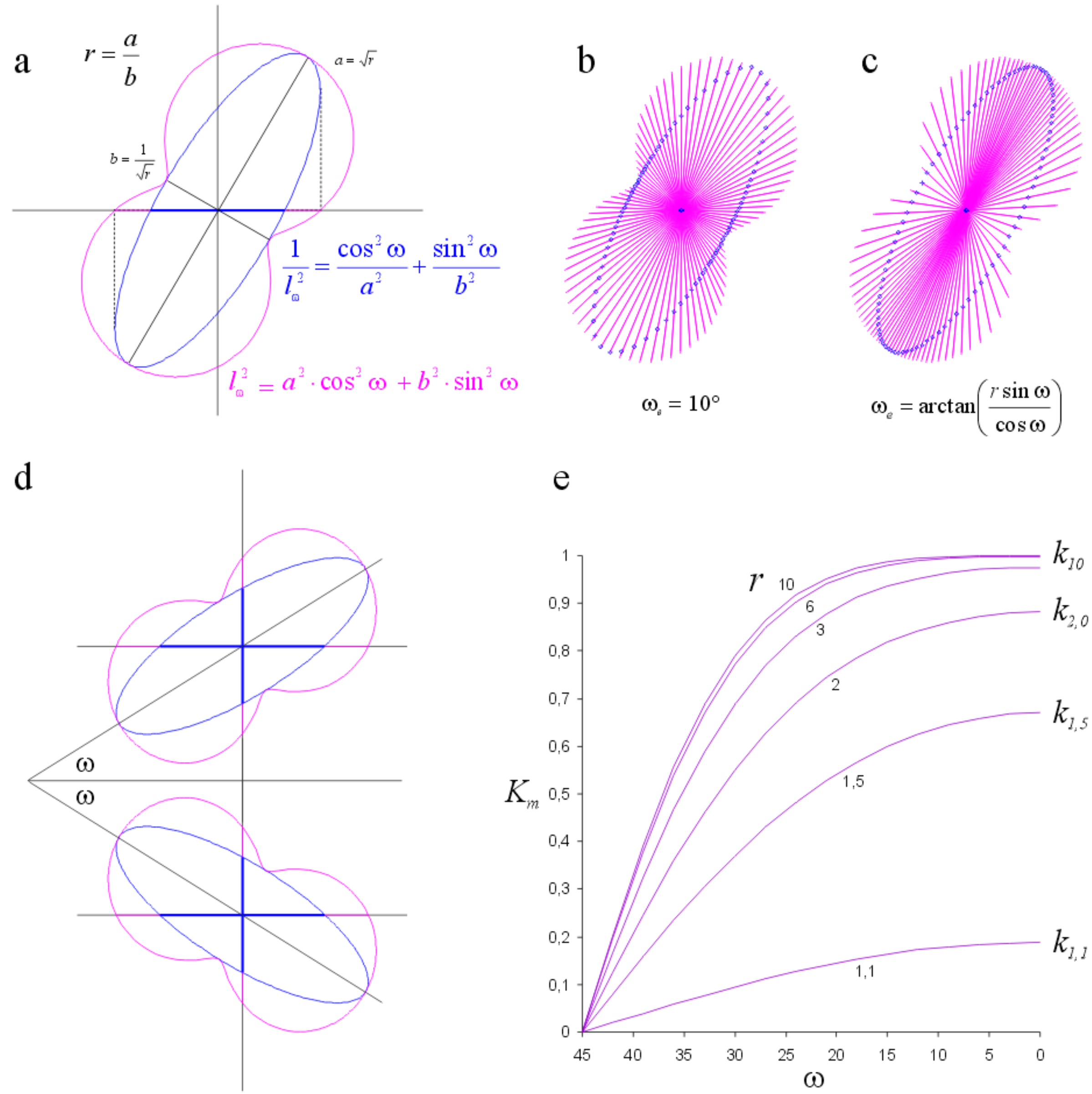

P. Launeau (2004) "Mise en évidence des écoulements magmatiques par analyse d'images 2-D des distributions 3-D d'Orientations Préférentielles de Formes". *Bull. Soc. Géol. Fr* , 175, 331-350

Quantitative Image Analysis of Minerals and Rocks

http://www.sciences.univ-nantes.fr/lpgnantes/SPO

UMR 6112 PLANÉTOLOGIE & GÉODYNAMIQUE

2D ellipses & 3D ellipsoids

$$\frac{1}{l(\omega)^2} = \frac{\cos^2\omega}{a^2} + \frac{\sin^2\omega}{b^2}$$

$$\mathbf{B}_{12} = \begin{bmatrix} b_{11} & b_{12} \\ b_{12} & b_{22} \end{bmatrix} = \begin{bmatrix} \cos\varphi & \sin\varphi \\ -\sin\varphi & \cos\varphi \end{bmatrix} \cdot \begin{bmatrix} 1/a^2 & 0 \\ 0 & 1/b^2 \end{bmatrix} \cdot \begin{bmatrix} \cos\varphi & -\sin\varphi \\ \sin\varphi & \cos\varphi \end{bmatrix}$$

$$\frac{1}{l(x,y,z)^2} = \frac{x^2}{a^2} + \frac{y^2}{b^2} + \frac{z^2}{c^2}$$

$$\mathbf{B}_{123} = \begin{bmatrix} b_{11} & b_{12} & b_{13} \\ b_{12} & b_{22} & b_{23} \\ b_{13} & b_{23} & b_{33} \end{bmatrix} = \mathbf{R}_V^T \cdot \begin{bmatrix} 1/a^2 & 0 & 0 \\ 0 & 1/b^2 & 0 \\ 0 & 0 & 1/c^2 \end{bmatrix} \cdot \mathbf{R}_V$$

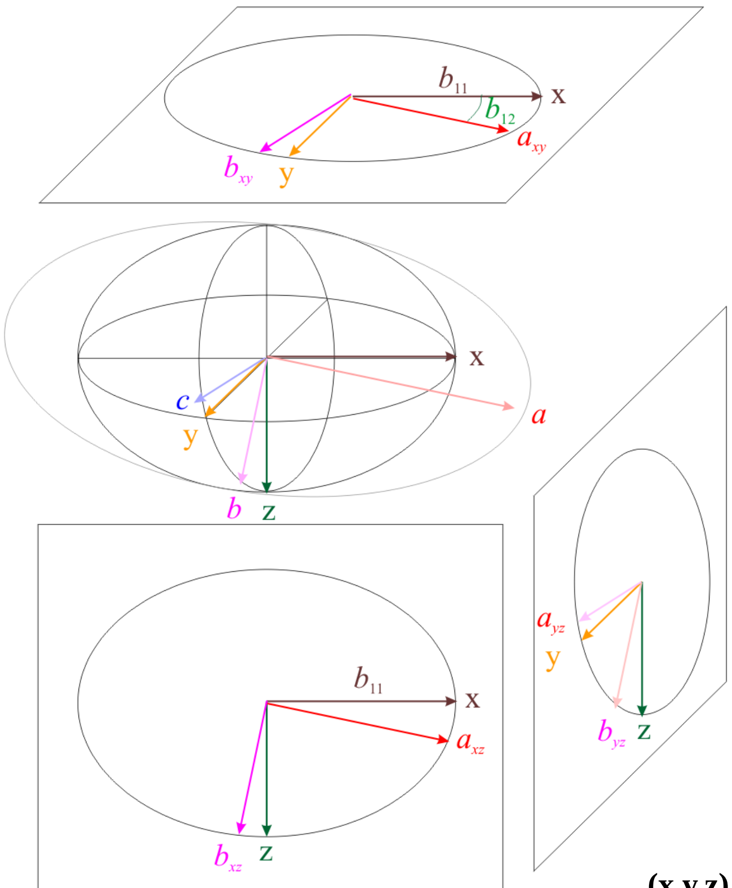

$$\mathbf{B}_{12} = \begin{bmatrix} b_{11} & b_{12} \\ b_{12} & b_{22} \end{bmatrix} = \begin{bmatrix} \cos\varphi_{12} & \sin\varphi_{12} \\ -\sin\varphi_{12} & \cos\varphi_{12} \end{bmatrix} \cdot \begin{bmatrix} 1/a_{12}^2 & 0 \\ 0 & 1/b_{12}^2 \end{bmatrix} \cdot \begin{bmatrix} \cos\varphi_{12} & -\sin\varphi_{12} \\ \sin\varphi_{12} & \cos\varphi_{12} \end{bmatrix}$$

$$\mathbf{B}_{13} = \begin{bmatrix} b_{11} & b_{13} \\ b_{13} & b_{33} \end{bmatrix} = \begin{bmatrix} \cos\varphi_{13} & \sin\varphi_{13} \\ -\sin\varphi_{13} & \cos\varphi_{13} \end{bmatrix} \cdot \begin{bmatrix} 1/a_{13}^2 & 0 \\ 0 & 1/b_{13}^2 \end{bmatrix} \cdot \begin{bmatrix} \cos\varphi_{13} & -\sin\varphi_{13} \\ \sin\varphi_{13} & \cos\varphi_{13} \end{bmatrix}$$

$$\mathbf{B}_{23} = \begin{bmatrix} b_{22} & b_{23} \\ b_{23} & b_{33} \end{bmatrix} = \begin{bmatrix} \cos\varphi_{23} & \sin\varphi_{23} \\ -\sin\varphi_{23} & \cos\varphi_{23} \end{bmatrix} \cdot \begin{bmatrix} 1/a_{23}^2 & 0 \\ 0 & 1/b_{23}^2 \end{bmatrix} \cdot \begin{bmatrix} \cos\varphi_{23} & -\sin\varphi_{23} \\ \sin\varphi_{23} & \cos\varphi_{23} \end{bmatrix}$$

$$\mathbf{B} = \begin{bmatrix} \bar{b}_{11} & b_{12} & b_{13} \\ b_{12} & \bar{b}_{22} & b_{23} \\ b_{13} & b_{23} & \bar{b}_{33} \end{bmatrix}$$

(x,y,z) (1,2,3)

Launeau, P. and Cruden, A.R. (1998). – Magmatic fabric acquisition mechanism in a syenite: Results of a combined anisotropy of magnetic susceptibility and image analysis study. J. Geophys. Res. 103, 5067-5089.

2D ellipses & 3D ellipsoids

***I* = 1 to 4**

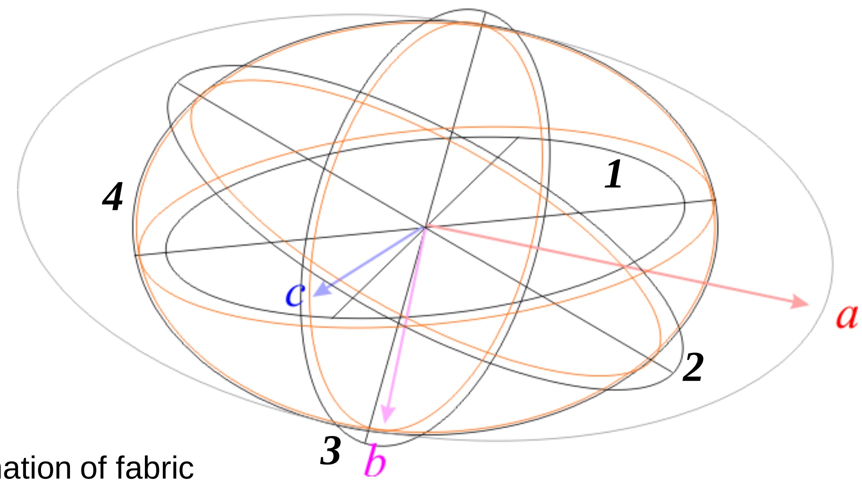

Robin, P.-Y.F. (2002). – Determination of fabric and strain ellipsoids from measured sectional ellipses – Theory. *Journal of Structural Geology*, 24, 531-544.

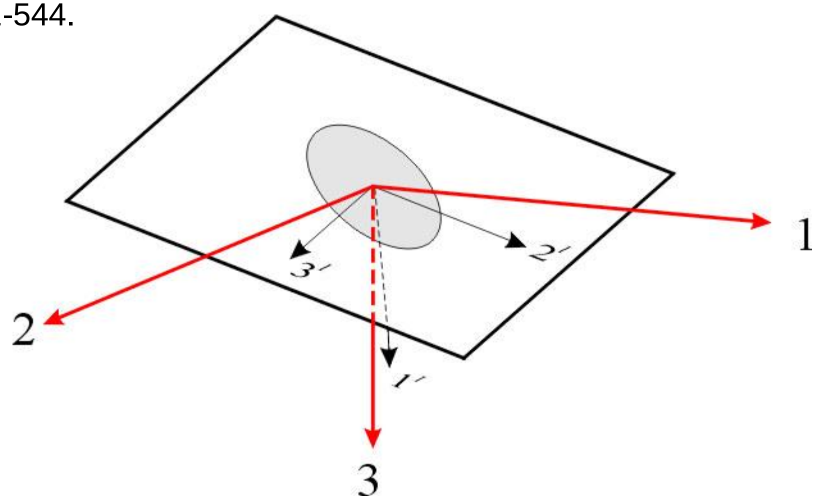

$$\mathbf{B}_{23}^{I} = \mathbf{L}_{23}^{IT} \cdot \mathbf{B}_{123} \cdot \mathbf{L}_{23}^{I} + \mathbf{X}^{I}$$

with

$$\mathbf{X}^{I} = \begin{bmatrix} \chi_{22}^{I} & \chi_{23}^{I} \\ \chi_{23}^{I} & \chi_{33}^{I} \end{bmatrix}$$

deviations to measurements

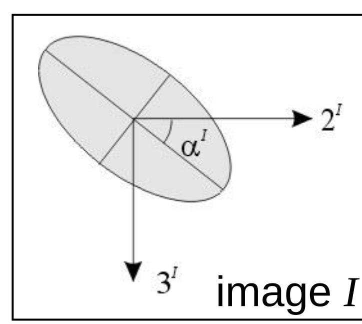

$$\mathbf{B}_{23}^{I} = \begin{bmatrix} b_{22}^{I} & b_{23}^{I} \\ b_{23}^{I} & b_{33}^{I} \end{bmatrix}$$

of the section

$$\mathbf{L}_{23}^{I} = \begin{bmatrix} l_{21}^{I} & l_{31}^{I} \\ l_{22}^{I} & l_{32}^{I} \\ l_{23}^{I} & l_{33}^{I} \end{bmatrix}$$

of ellipsoid $\mathbf{B}_{123}$

Scale factors of the Robin 2002 method

Scale factor available

$$\mathbf{B}_{23}^{I} = \begin{bmatrix} \cos\varphi & \sin\varphi \\ -\sin\varphi & \cos\varphi \end{bmatrix} \cdot \begin{bmatrix} 1/a^2 & 0 \\ 0 & 1/b^2 \end{bmatrix} \cdot \begin{bmatrix} \cos\varphi & -\sin\varphi \\ \sin\varphi & \cos\varphi \end{bmatrix}$$

length a et b

$$\frac{1}{\bar{a}^I} \cdot \begin{bmatrix} 1/\rho & 0 \\ 0 & \rho \end{bmatrix}$$

mean surface area $\bar{a}^I = A^I / j^I$

with $\rho = \frac{a}{b}$ the shape ratio

$$\bar{n}^I \cdot \begin{bmatrix} 1/\rho & 0 \\ 0 & \rho \end{bmatrix}$$

mean density $\bar{n}^I = j^I / A^I$

$$\mathbf{B}_{23}^{I} = f^I \cdot \begin{bmatrix} \cos\varphi & \sin\varphi \\ -\sin\varphi & \cos\varphi \end{bmatrix} \cdot \begin{bmatrix} 1/\rho & 0 \\ 0 & \rho \end{bmatrix} \cdot \begin{bmatrix} \cos\varphi & -\sin\varphi \\ \sin\varphi & \cos\varphi \end{bmatrix}$$

No scale factor available

$\sqrt{F_{\min}^{I}}$ Compatibility index of section I

In case of 3 perpendicular sections

$$\begin{bmatrix} b_{11} & b_{12} & b_{13} \\ b_{21} & b_{22} & b_{23} \\ b_{31} & b_{23} & b_{33} \end{bmatrix} = \begin{bmatrix} (b_{33}^2 + b_{22}^3)/2 & b_{23}^3 & b_{23}^2 \\ b_{23}^3 & (b_{22}^1 + b_{33}^3)/2 & b_{23}^1 \\ b_{23}^2 & b_{23}^1 & (b_{33}^1 + b_{22}^2)/2 \end{bmatrix}$$

Compatibility index of all sections

$$\tilde{F} = \frac{1}{6} \frac{(b_{33}^2 - b_{22}^3)^2 + (b_{22}^1 - b_{33}^3)^2 + (b_{33}^1 - b_{22}^2)^2}{(b_1)^2 + (b_2)^2 + (b_3)^2}$$

Robin, P.-Y.F. (2002). – Determination of fabric and strain ellipsoids from measured sectional ellipses – Theory. *Journal of Structural Geology*, 24, 531-544.

Convergence of the Robin 2002 method

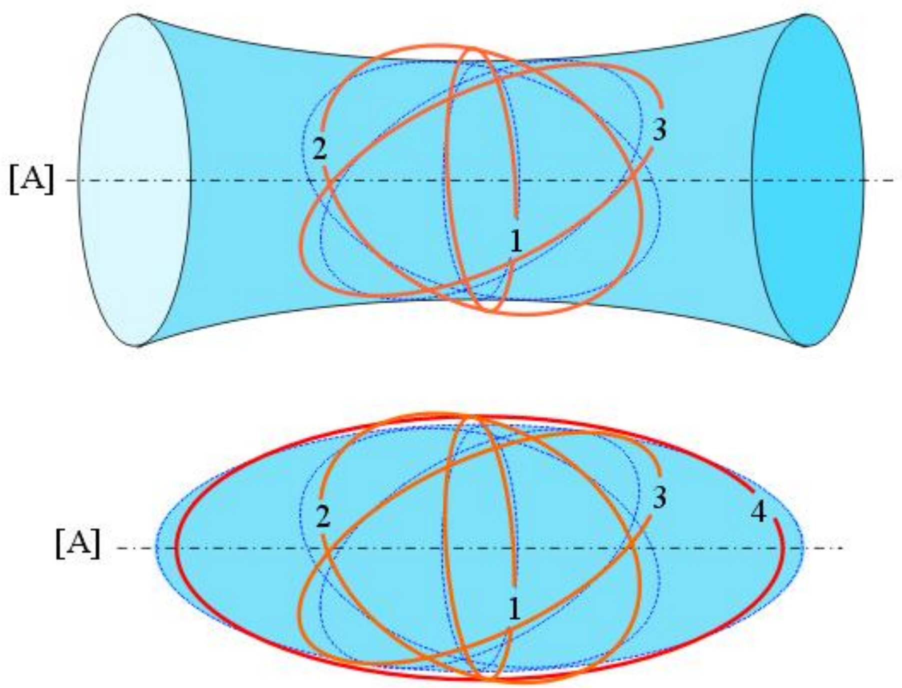

Robin, P.-Y.F. (2002). – Determination of fabric and strain ellipsoids from measured sectional ellipses – Theory. *Journal of Structural Geology*, 24, 531-544.

Quantitative Image Analysis of Minerals and Rocks

http://www.sciences.univ-nantes.fr/lpgnantes/SPO

Application to gabbronorites of the Bushveld complex

Orthopyroxene

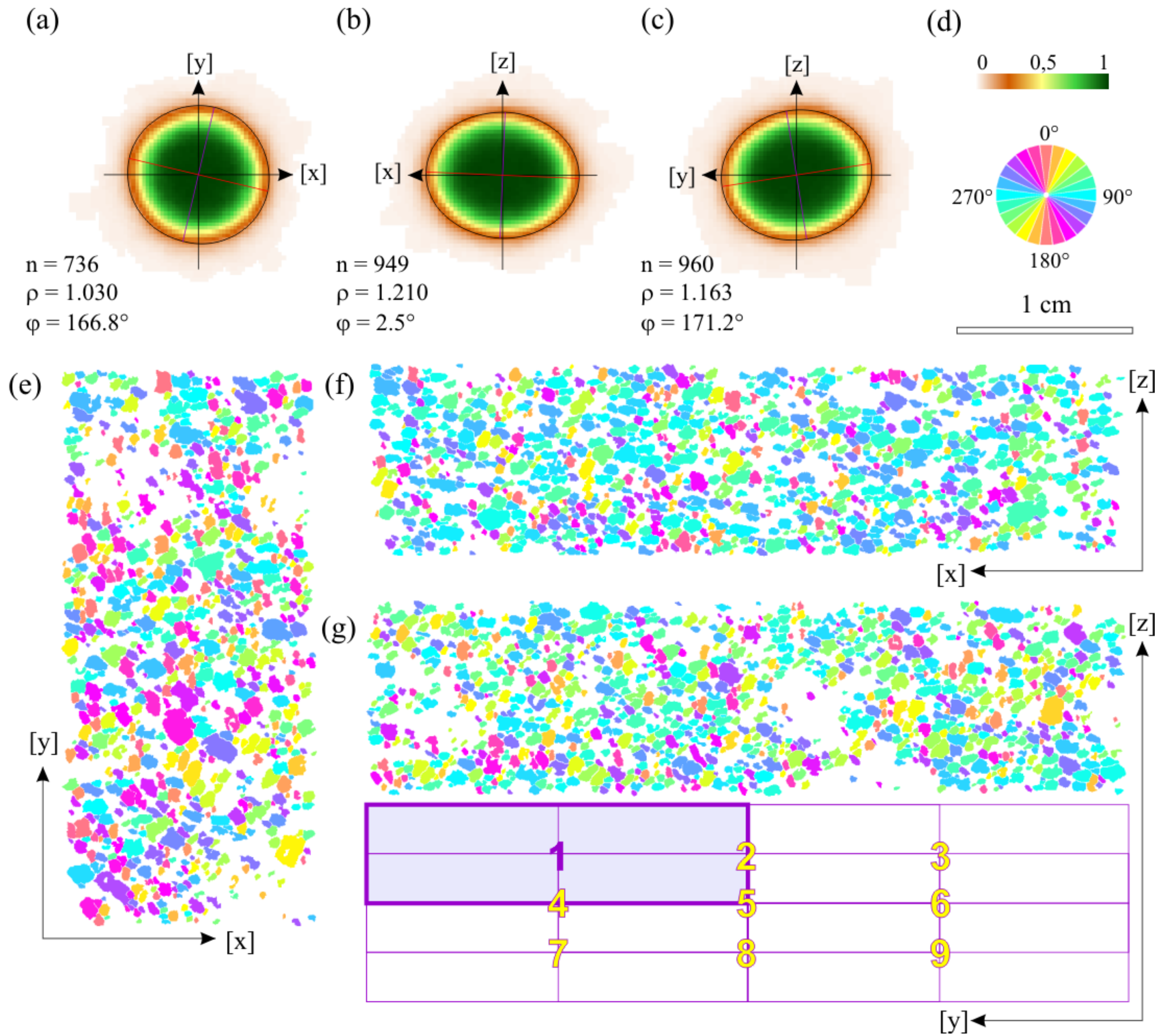

P. Launeau, P.-Y. F. Robin (2005) "Determination of fabric and strain ellipsoids from measured sectional ellipses—implementation and applications". *Journal of Structural Geology*, 27, 2223-2233

Application to gabbronorites of the Bushveld complex

(h)

	A	B	C	$\sqrt{\tilde{F}}$
L. norm	1.113	1.034	0.869	2.5%
trend	284.7	192.9	29.0	
plunge	5.1	19.1	70.2	

A/C	1.282	Flinn	0.405
A/B	1.077	P'	1.291
B/C	1.192	T	0.396

729 combinations

	A	B	C	
L. norm	1.120	1.030	0.867	$\bar{X}$
	0.028	*0.033*	*0.021*	2σ
trend	285.9	194.2	29.1	$\bar{X}$
plunge	4.7	19.0	70.4	$\bar{X}$
	27.4	*27.4*	*8.8*	$2\sigma_1$
	5.6	*8.8*	*5.7*	$2\sigma_2$

	$\bar{X}$	2σ		$\bar{X}$	2σ
A/C	1.292	0.048	$\sqrt{\tilde{F}}$	2.6%	3.5%
A/B	1.087	0.057	P'	1.301	0.050
B/C	1.189	0.060	T	0.352	0.375

(i)

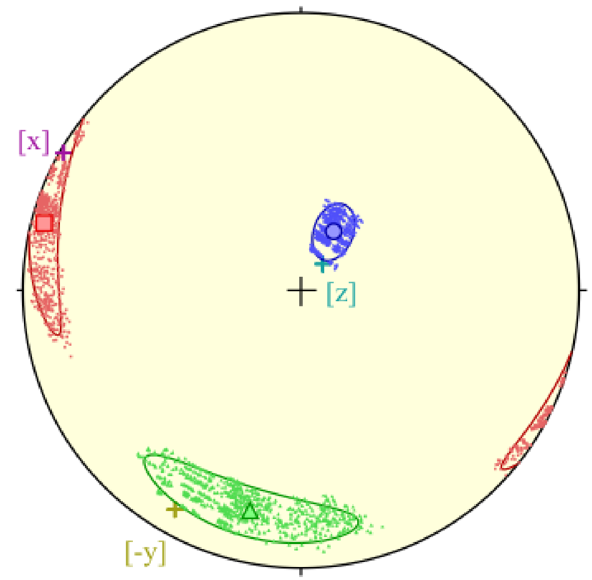

(j)

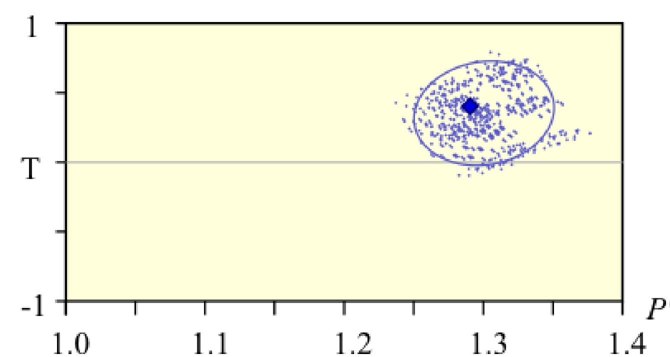

P. Launeau, P.-Y. F. Robin (2005) "Determination of fabric and strain ellipsoids from measured sectional ellipses—implementation and applications". *Journal of Structural Geology*, 27, 2223-2233

Quantitative Image Analysis of Minerals and Rocks

http://www.sciences.univ-nantes.fr/lpgnantes/SPO

Application to gabbronorites of the Bushveld complex

Orthopyroxene

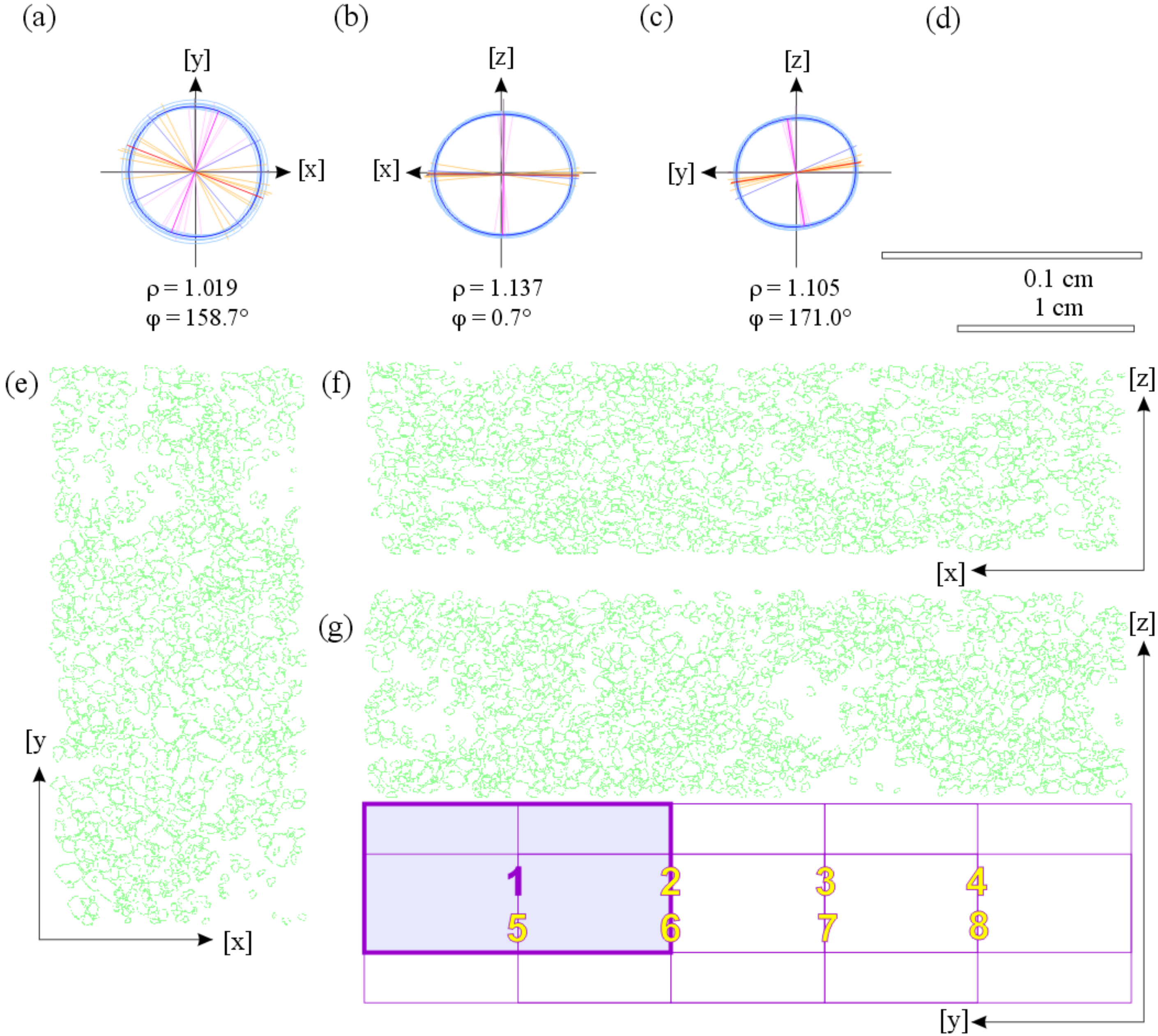

P. Launeau, P.-Y. F. Robin (2005) "Determination of fabric and strain ellipsoids from measured sectional ellipses—implementation and applications". *Journal of Structural Geology*, 27, 2223-2233

Quantitative Image Analysis of Minerals and Rocks

http://www.sciences.univ-nantes.fr/lpgnantes/SPO

UMR 6112 PLANÉTOLOGIE & GÉODYNAMIQUE

Application to gabbronorites of the Bushveld complex

(h)

	A	B	C	$\sqrt{\tilde{F}}$
L. norm	1.113	1.034	0.869	2.5%
trend	284.7	192.9	29.0	
plunge	5.1	19.1	70.2	

A/C	1.282	Flinn	0.405
A/B	1.077	P'	1.291
B/C	1.192	T	0.396

729 combinations

	A	B	C	
L. norm	1.120	1.030	0.867	$\bar{X}$
	0.028	0.033	0.021	2σ
trend	285.9	194.2	29.1	$\bar{X}$
plunge	4.7	19.0	70.4	$\bar{X}$
	27.4	27.4	8.8	$2\sigma_1$
	5.6	8.8	5.7	$2\sigma_2$

	$\bar{X}$	2σ		$\bar{X}$	2σ
A/C	1.292	0.048	$\sqrt{\tilde{F}}$	2.6%	3.5%
A/B	1.087	0.057	P'	1.301	0.050
B/C	1.189	0.060	T	0.352	0.375

(i)

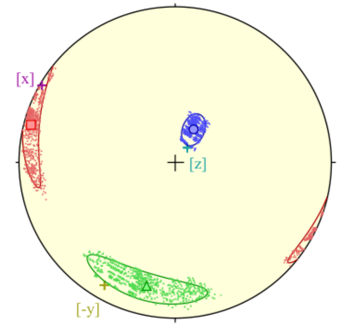

(j)

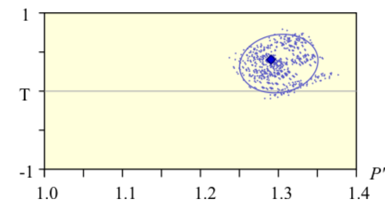

Inertia tensors

(h)

	A	B	C	$\sqrt{\tilde{F}}$
L. norm	1.050	1.029	0.926	1.4%
trend	290.0	197.9	40.8	
plunge	6.8	17.2	71.5	

A/C	1.134	Flinn	0.179
A/B	1.020	P'	1.145
B/C	1.112	T	0.680

512 combinations

	A	B	C	
L. norm	1.052	1.027	0.925	$\bar{X}$
	0.011	0.014	0.015	2σ
trend	289.6	197.6	41.3	$\bar{X}$
plunge	6.9	16.8	71.5	$\bar{X}$
	33.2	33.0	7.8	$2\sigma_1$
	6.8	5.9	4.9	$2\sigma_2$

	$\bar{X}$	2σ		$\bar{X}$	2σ
A/C	1.138	0.027	$\sqrt{\tilde{F}}$	1.7%	2.1%
A/B	1.024	0.018	P'	1.148	0.031
B/C	1.111	0.031	T	0.625	0.268

(i)

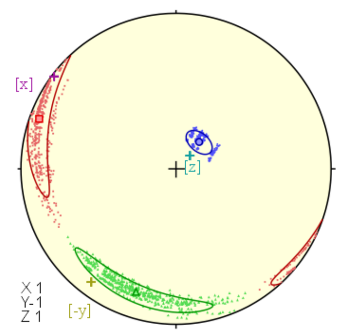

(j)

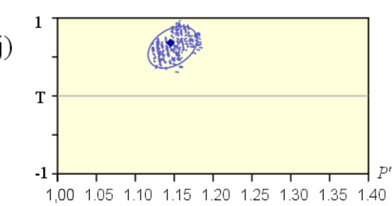

Intercepts

P. Launeau, P.-Y. F. Robin (2005) "Determination of fabric and strain ellipsoids from measured sectional ellipses—implementation and applications". *Journal of Structural Geology*, 27, 2223-2233

Quantitative Image Analysis of Minerals and Rocks

http://www.sciences.univ-nantes.fr/lpgnantes/SPO

Application to gabbronorites of the Bushveld complex

P. Launeau (2004) "Mise en évidence des écoulements magmatiques par analyse d'images 2-D des distributions 3-D d'Orientations Préférentielles de Formes". *Bull. Soc. Géol. Fr* , 175, 331-350

SPO

PO

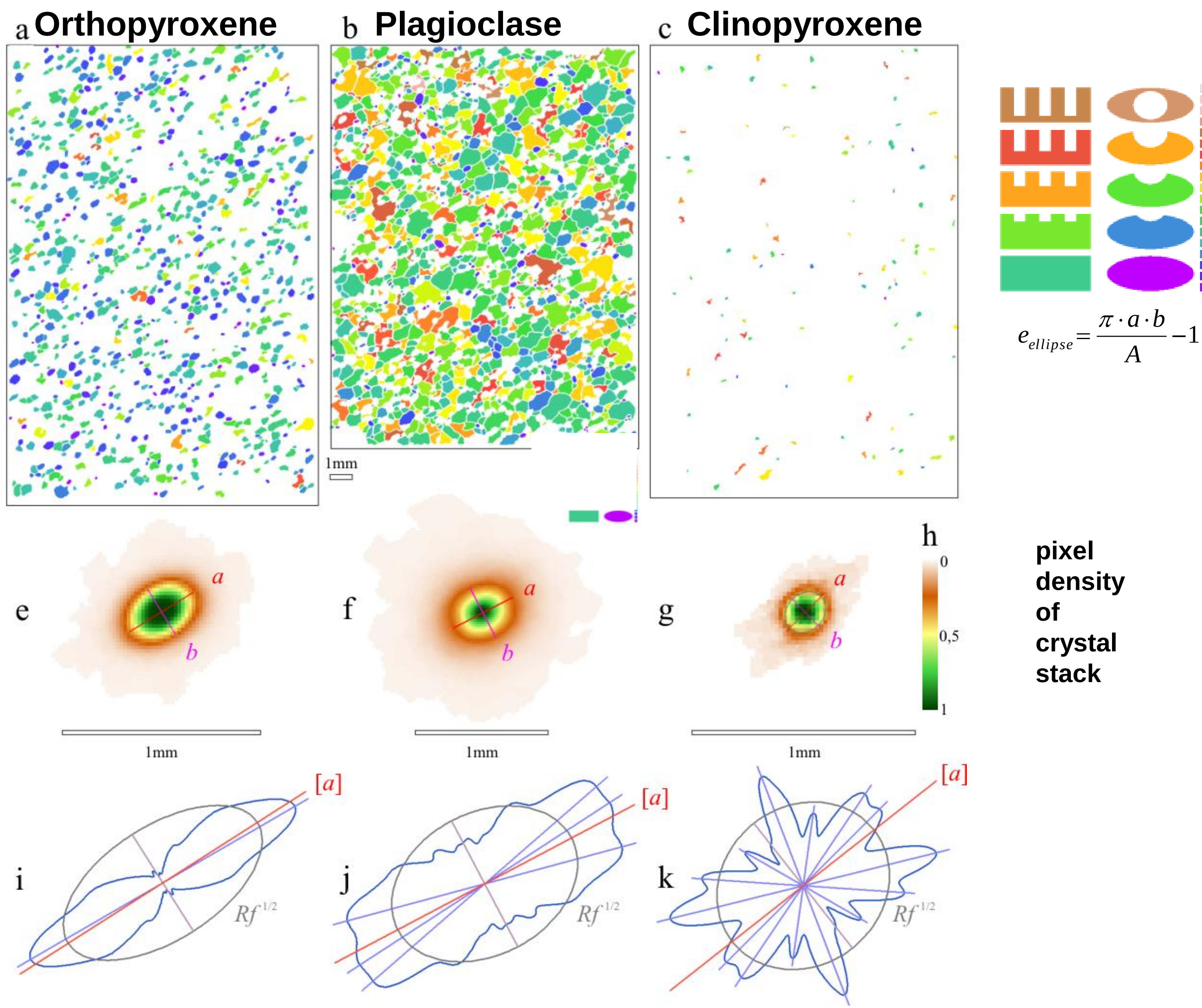

$$e_{ellipse} = \frac{\pi \cdot a \cdot b}{A} - 1$$

Application to gabbronorites of the Bushveld complex

Plagioclase

$$\mathbf{M}_T = \frac{1}{4 \cdot A}\begin{bmatrix} a^2 \cdot \cos^2\varphi + b^2 \cdot \sin^2\varphi & \left(a^2 - b^2\right) \cdot \cos\varphi \cdot \sin\varphi \\ \left(a^2 - b^2\right) \cdot \cos\varphi \cdot \sin\varphi & a^2 \cdot \sin^2\varphi + b^2 \cdot \cos s^2\varphi \end{bmatrix}$$

$$\mathbf{M}_E = A \cdot \begin{bmatrix} \frac{1}{a^2} \cdot \cos^2\varphi + \frac{1}{b^2} \cdot \sin^2\varphi & \left(\frac{1}{a^2} - \frac{1}{b^2}\right) \cdot \cos\varphi \cdot \sin\varphi \\ \left(\frac{1}{a^2} - \frac{1}{b^2}\right) \cdot \cos\varphi \cdot \sin\varphi & \frac{1}{a^2} \cdot \sin^2\varphi + \frac{1}{b^2} \cdot \cos^2\varphi \end{bmatrix}$$

pixel density of crystal stack

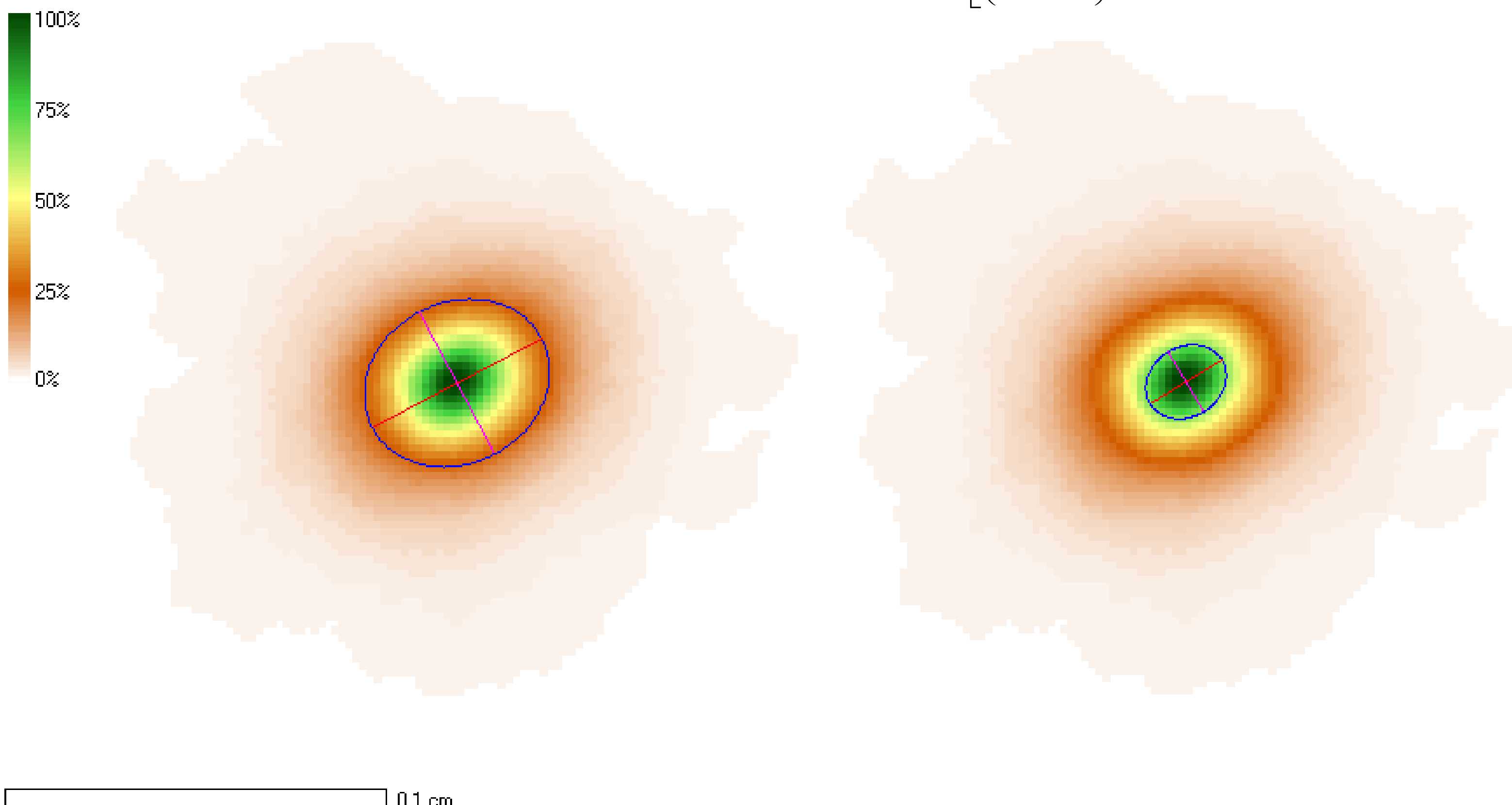

P. Launeau (2004) "Mise en évidence des écoulements magmatiques par analyse d'images 2-D des distributions 3-D d'Orientations Préférentielles de Formes". *Bull. Soc. Géol. Fr* , 175, 331-350

Quantitative Image Analysis of Minerals and Rocks

http://www.sciences.univ-nantes.fr/lpgnantes/SPO

Application to gabbronorites of the Bushveld complex

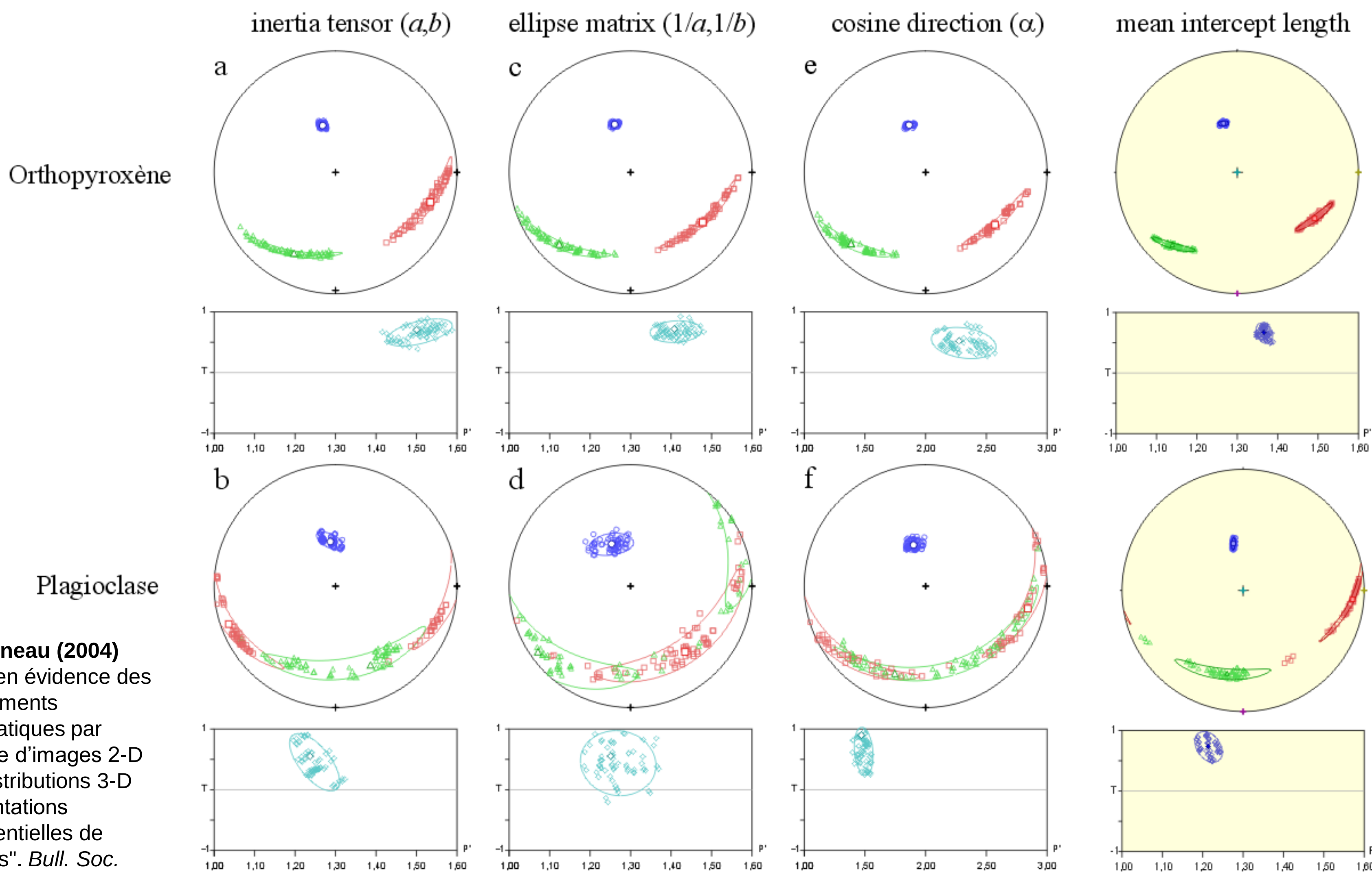

P. Launeau (2004) "Mise en évidence des écoulements magmatiques par analyse d'images 2-D des distributions 3-D d'Orientations Préférentielles de Formes". *Bull. Soc. Géol. Fr* , 175, 331-350

UMR 6112
PLANÉTOLOGIE & GÉODYNAMIQUE

Application to ilmenite-rich norite

SPO with intercepts of one phase made of ilmenite and magnetite (Tellnes, Norway) H. Diot et al. 2003

Grey level threshold on dark minerals

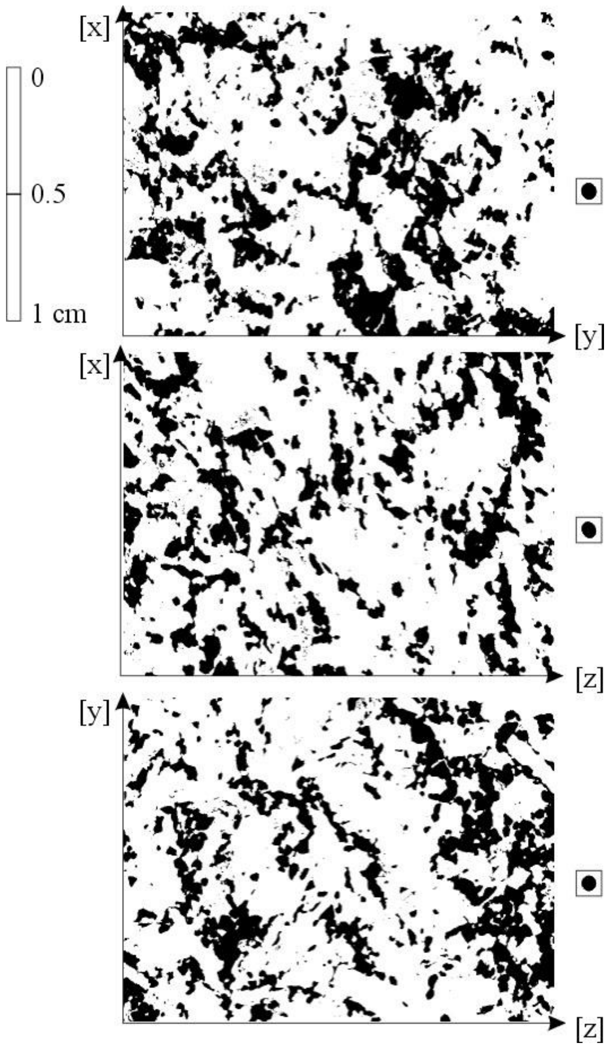

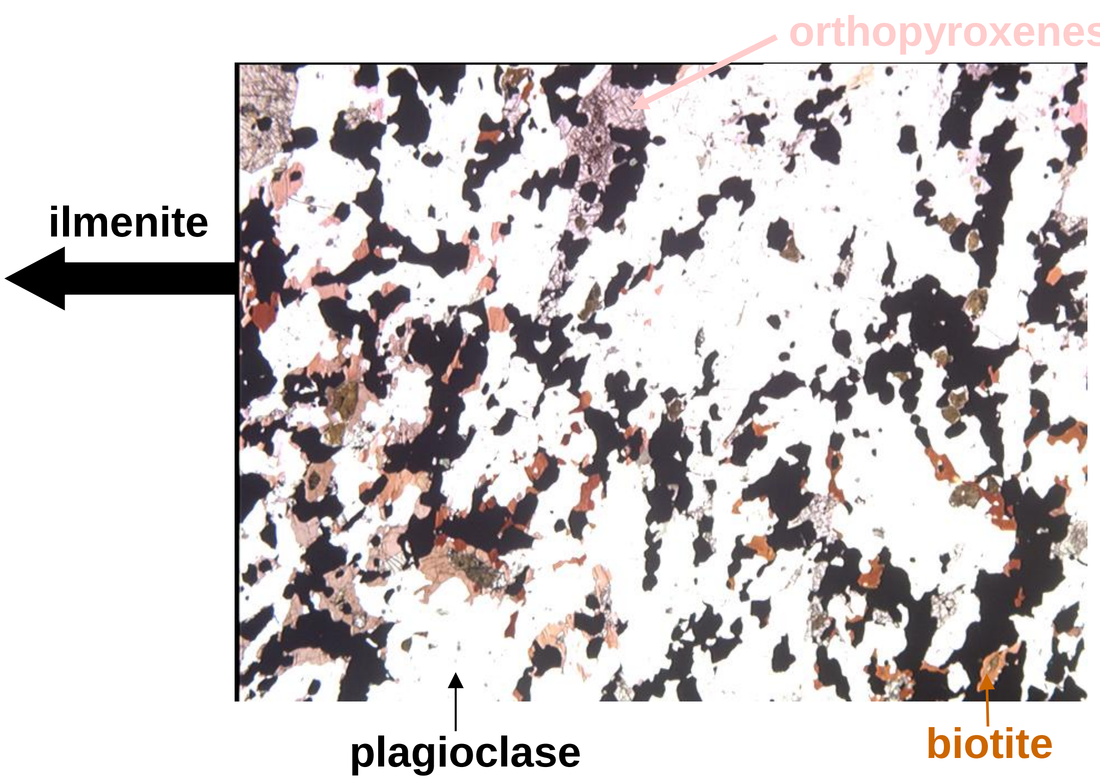

H. Diot, O. Bolle, J.-M. Lambert, P. Launeau and J.-C. Duchesne (2003) The Tellnes ilmenite deposit (Rogaland, South Norway): magnetic and petrofabric evidence for emplacement of a Ti-enriched noritic crystal mush in a fracture zone, *Journal of Structural Geology 25,* 481–501

Application to ilmenite-rich norite

SPO with intercepts of one phase made of ilmenite (Tellnes, Norway) H. Diot et al. 2003

Grey level threshold on dark minerals

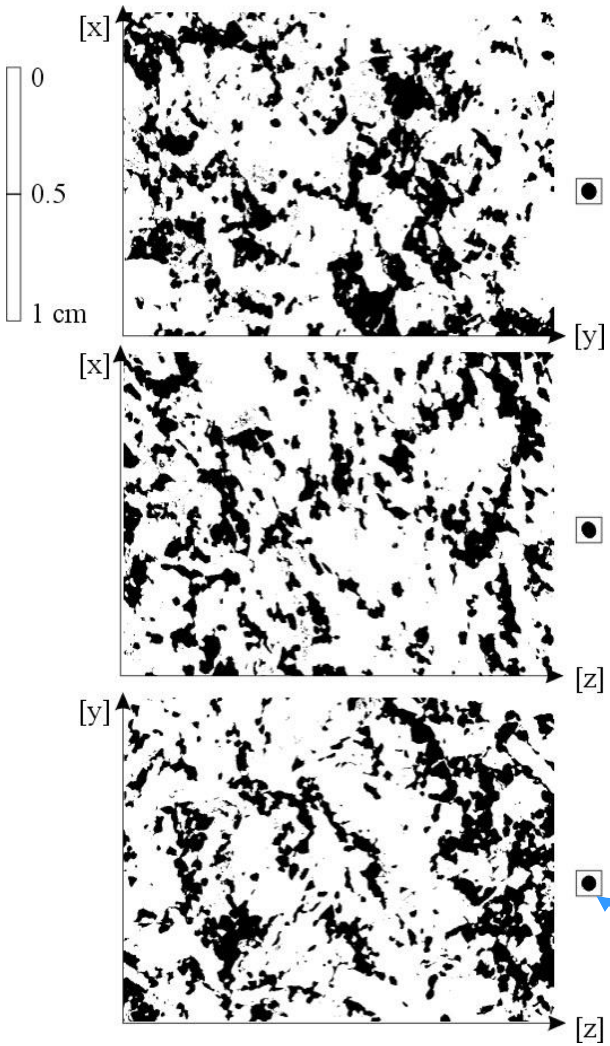

Intercepts of rectangular windows

Intercepts of circular windows

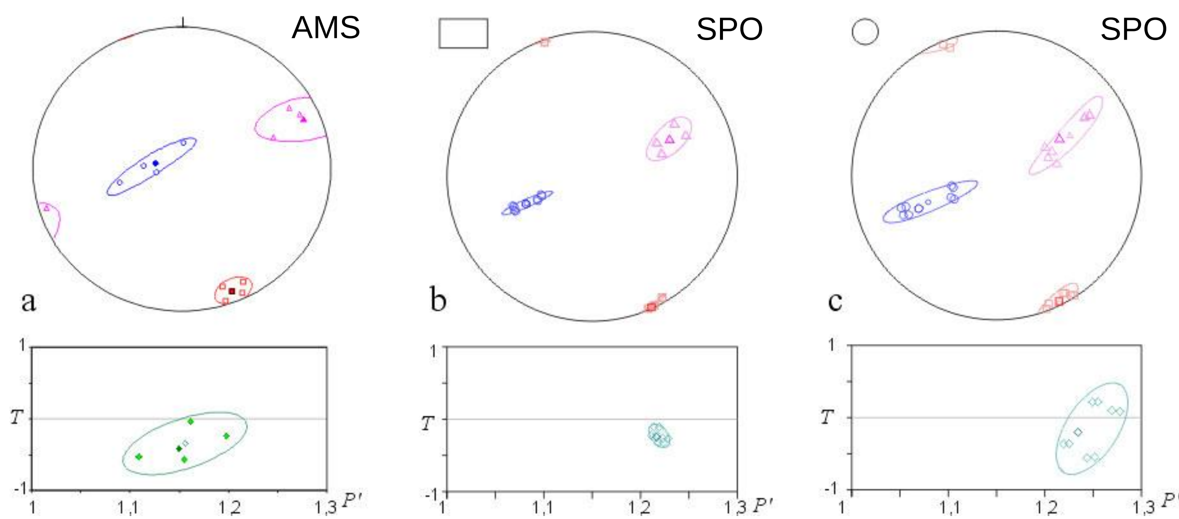

roses of mean intercept length

H. Diot, O. Bolle, J.-M. Lambert, P. Launeau and J.-C. Duchesne (2003) The Tellnes ilmenite deposit (Rogaland, South Norway): magnetic and petrofabric evidence for emplacement of a Ti-enriched noritic crystal mush in a fracture zone, *Journal of Structural Geology 25,* 481–501

Application to ilmenite-rich norite

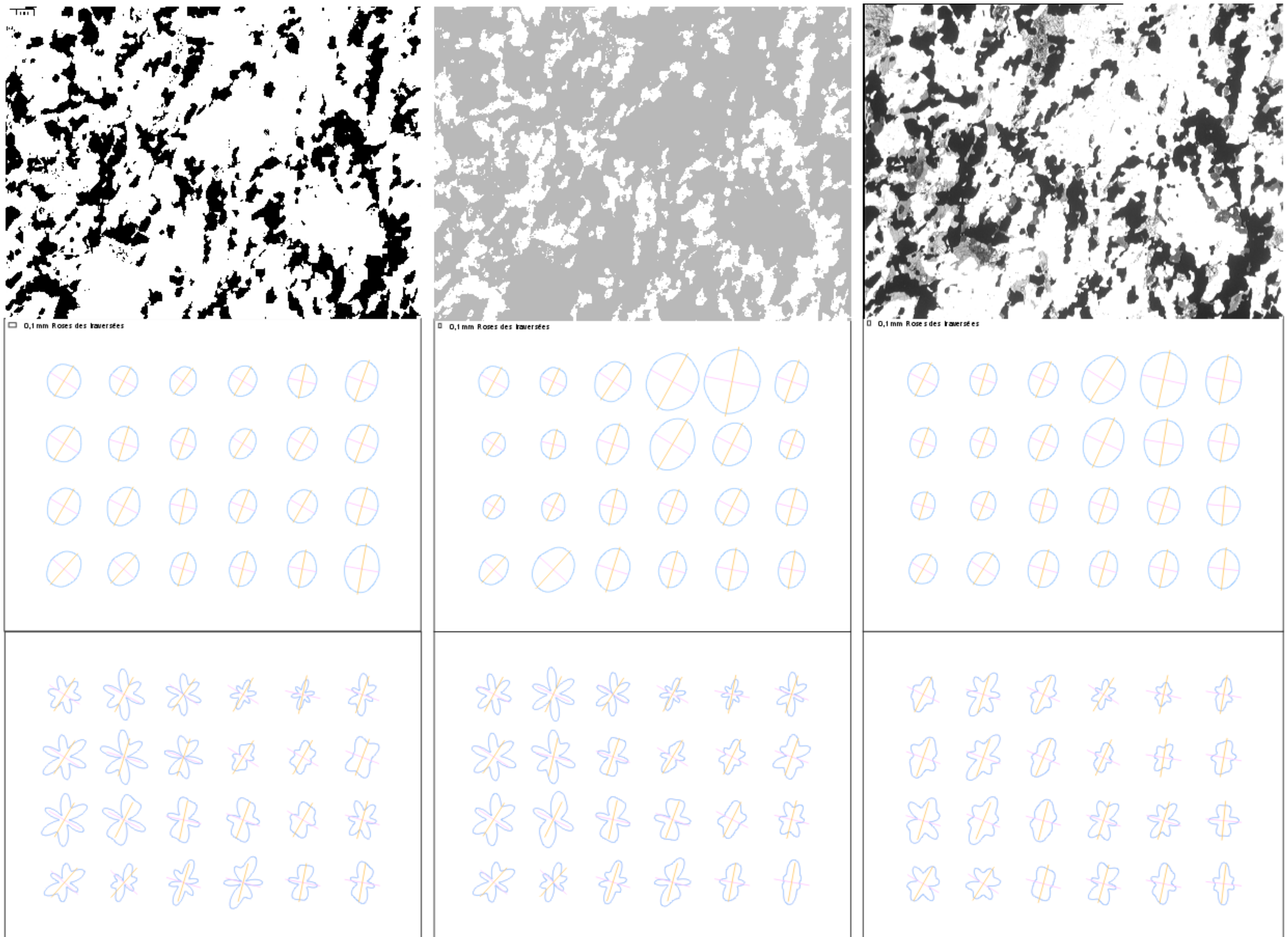

H. Diot, O. Bolle, J.-M. Lambert, P. Launeau and J.-C. Duchesne (2003) The Tellnes ilmenite deposit (Rogaland, South Norway): magnetic and petrofabric evidence for emplacement of a Ti-enriched noritic crystal mush in a fracture zone, *Journal of Structural Geology 25,* 481–501

UMR 6112
PLANÉTOLOGIE &
GÉODYNAMIQUE

Quantitative Image Analysis of Minerals and Rocks

http://www.sciences.univ-nantes.fr/lpgnantes/SPO

Application to ilmenite-rich norite

ilménite

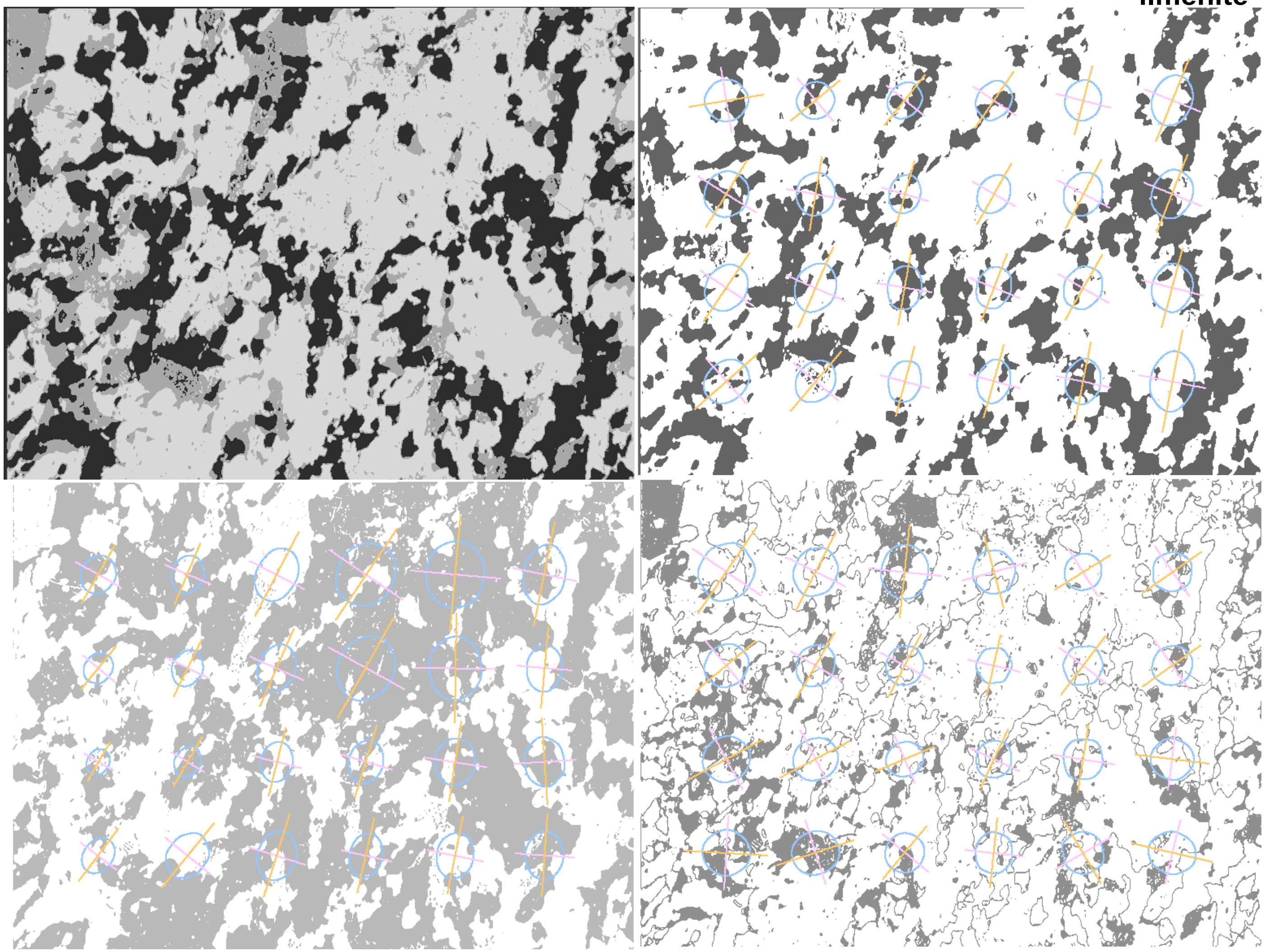

plagioclase **biotite+opx+ ... noise**

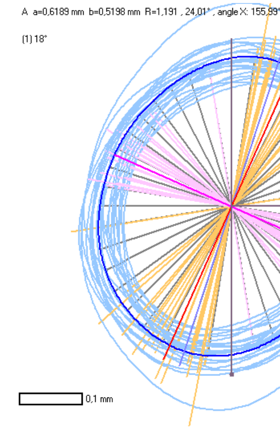

ilménite

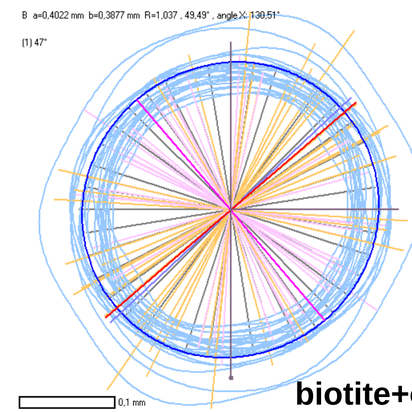

biotite+opx

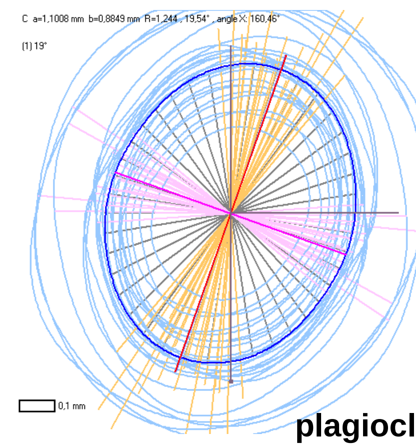

plagioclase

H. Diot, O. Bolle, J.-M. Lambert, P. Launeau and J.-C. Duchesne (2003) The Tellnes ilmenite deposit (Rogaland, South Norway): magnetic and petrofabric evidence for emplacement of a Ti-enriched noritic crystal mush in a fracture zone, *Journal of Structural Geology 25,* 481–501

Application to the Pocinhos granite (Brazil)

RGB

Launeau P., Archanjo C. J., Picard D., Arbaret L., Robin P.Y. (2010). Two- and three-dimensional shape fabric analysis by the intercept method in grey levels. Tectonophysics, Volume 492, Issues 1-4, 20 September 2010, Pages 230-239

Application to the Pocinhos granite (Brazil)

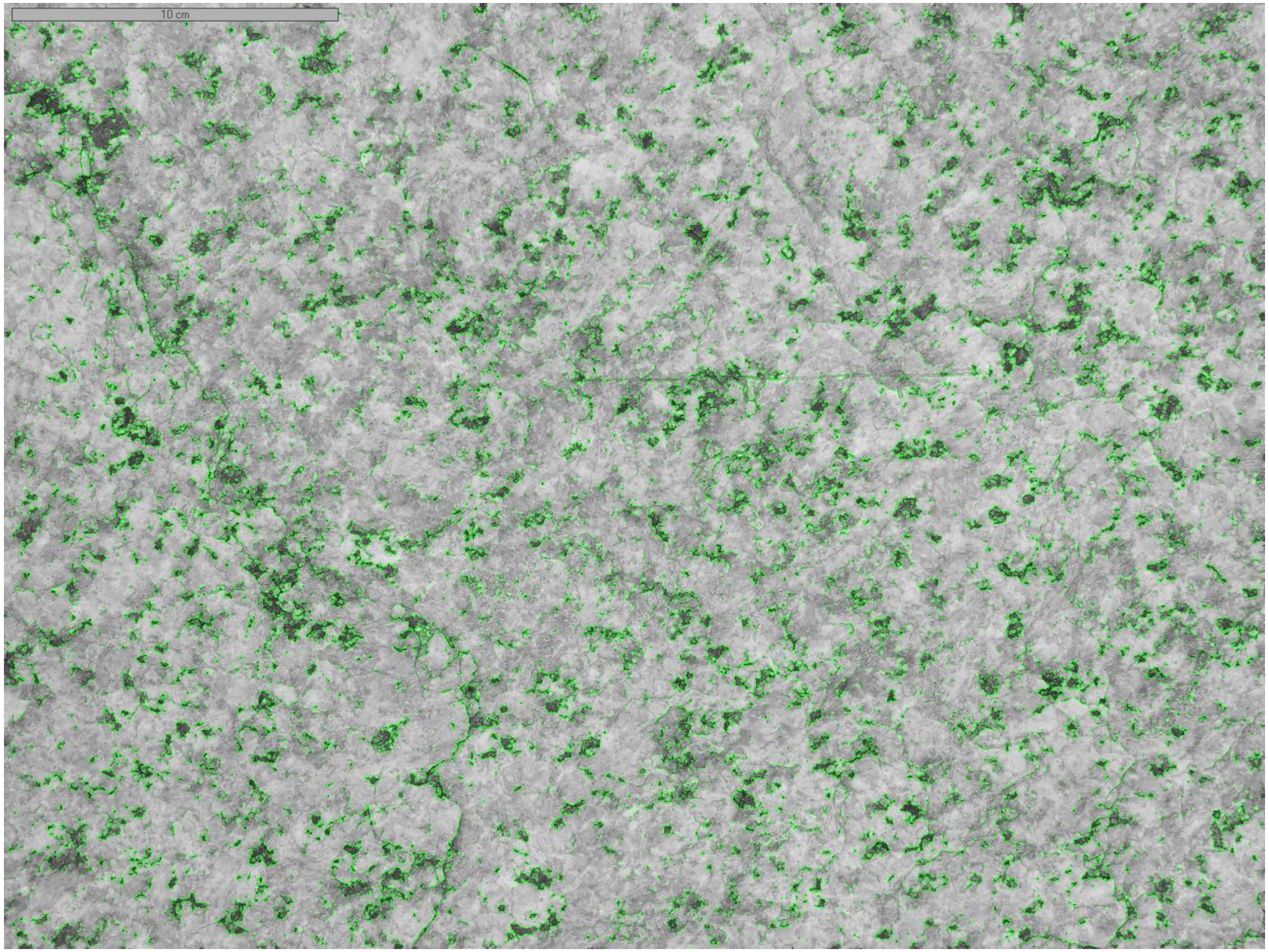

intercepts

Launeau P., Archanjo C. J., Picard D., Arbaret L., Robin P.Y. (2010). Two- and three-dimensional shape fabric analysis by the intercept method in grey levels. Tectonophysics, Volume 492, Issues 1-4, 20 September 2010, Pages 230-239

Application to the Pocinhos granite (Brazil)

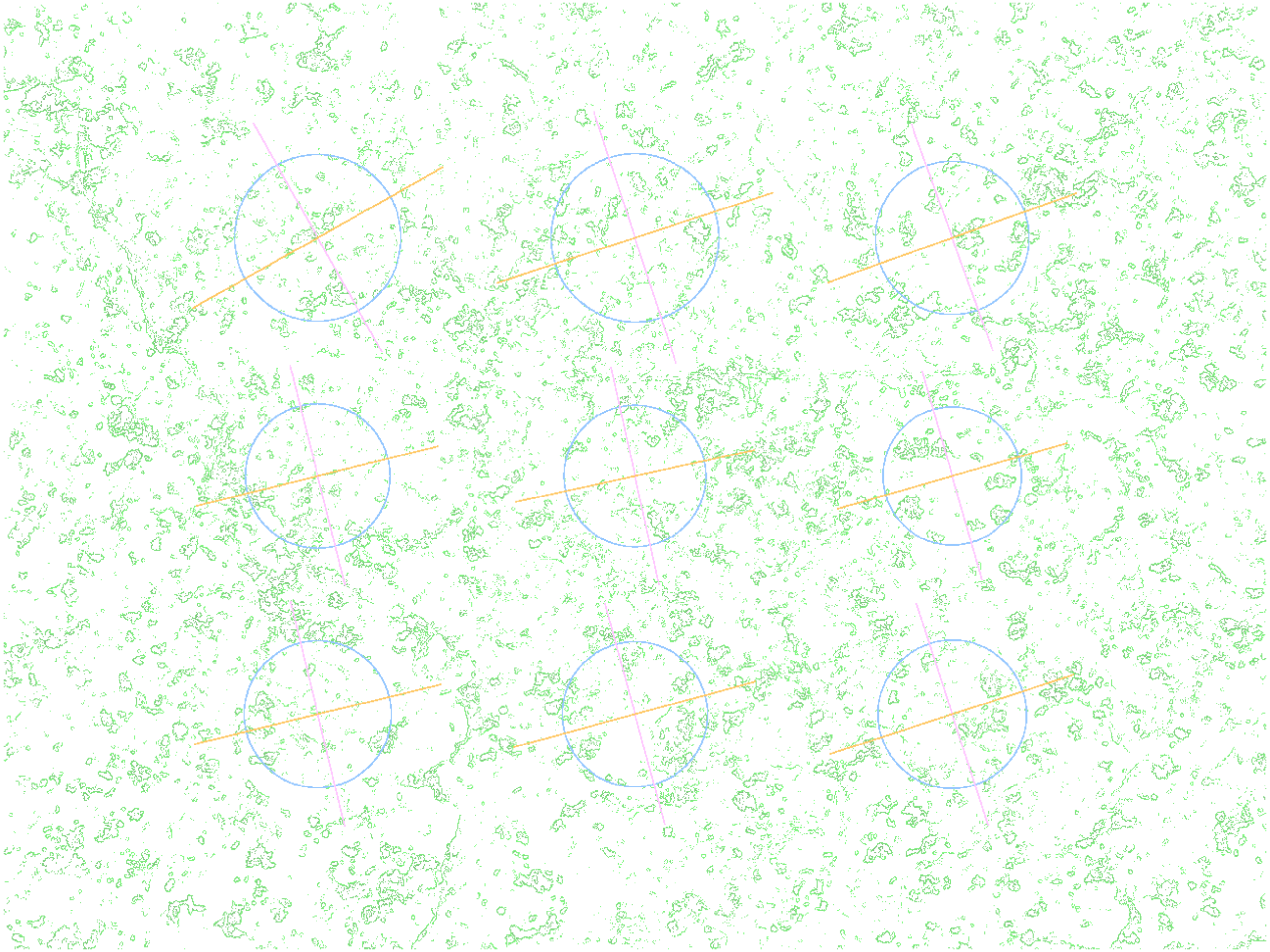

intercepts

Launeau P., Archanjo C. J., Picard D., Arbaret L., Robin P.Y. (2010). Two- and three-dimensional shape fabric analysis by the intercept method in grey levels. Tectonophysics, Volume 492, Issues 1-4, 20 September 2010, Pages 230-239

Application to the Pocinhos granite (Brazil)

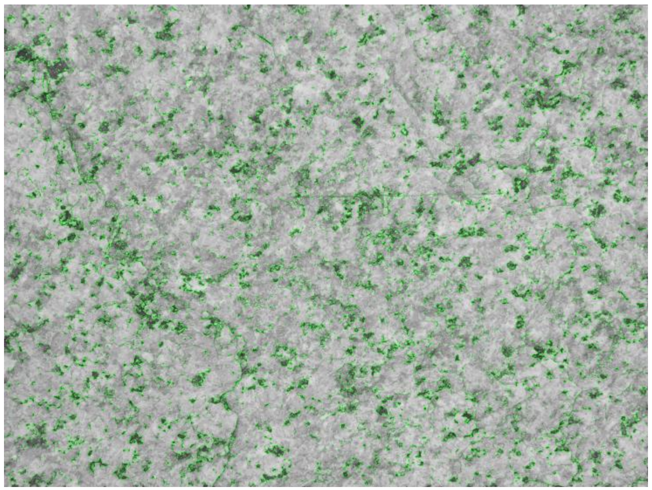

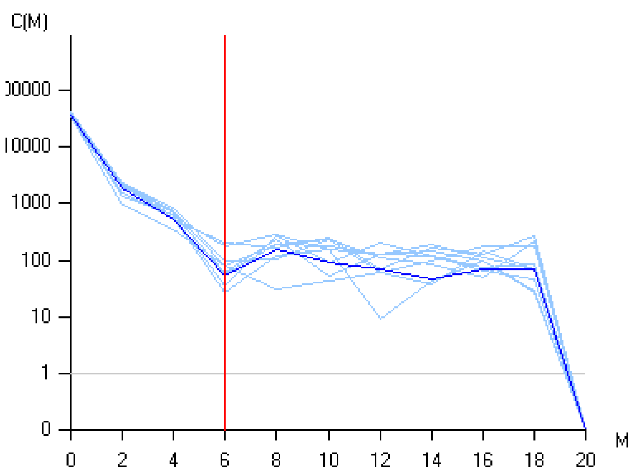

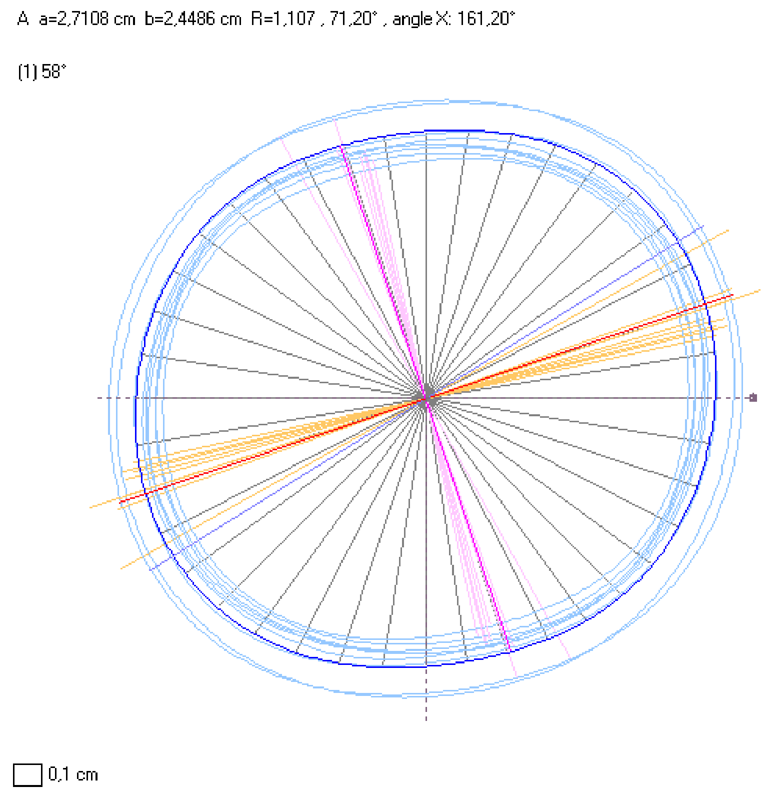

Launeau P., Archanjo C. J., Picard D., Arbaret L., Robin P.Y. (2010). Two- and three-dimensional shape fabric analysis by the intercept method in grey levels. Tectonophysics, Volume 492, Issues 1-4, 20 September 2010, Pages 230-239

Quantitative Image Analysis of Minerals and Rocks

http://www.sciences.univ-nantes.fr/lpgnantes/SPO

UMR 6112 PLANÉTOLOGIE & GÉODYNAMIQUE

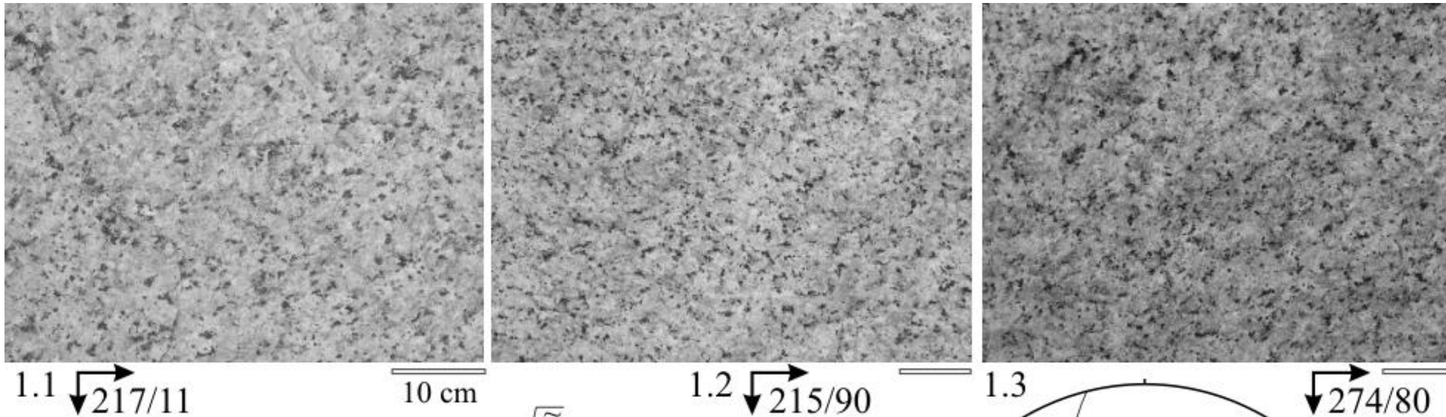

Application to the Pocinhos granite (Brazil)

	A	B	C	$\sqrt{F}$
L. norm	1.095	0.997	0.916	1.4 %
trend	177.6	75.9	311.9	
plunge	26.8	21.9	54.2	

A/C	1.196	Flinn	1.130
A/B	1.099	P'	1.196
B/C	1.088	T	-0.059

	A	B	C	729 combinations
L. norm	1.098	0.995	0.915	$\bar{X}$
	0.030	*0.015*	*0.023*	2σ
trend	177.5	75.9	311.9	$\bar{X}$
plunge	26.6	22.0	54.2	$\bar{X}$
	13.1	*13.4*	*7.1*	$2\sigma_1$
	3.8	*6.5*	*3.7*	$2\sigma_2$

	$\bar{X}$	2σ		$\bar{X}$	2σ
A/C	1.200	*0.061*	$\sqrt{F}$	1.7 %	*2.8 %*
A/B	1.103	*0.040*	P'	1.201	*0.061*
B/C	1.088	*0.035*	T	-0.076	*0.254*

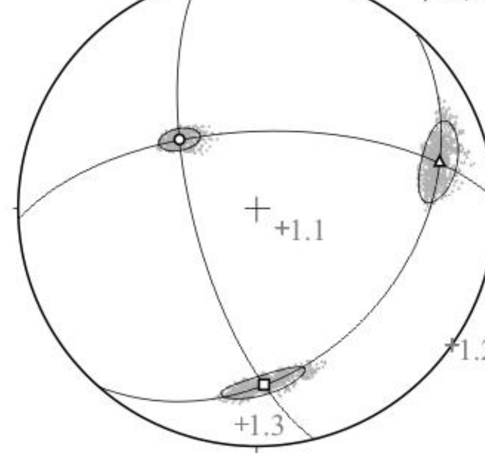

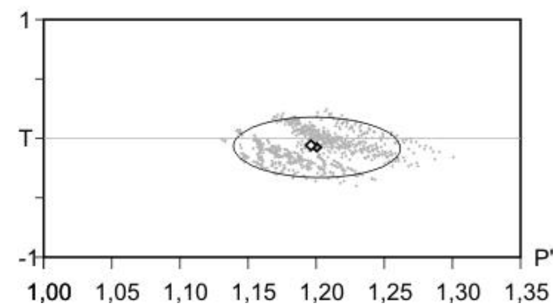

Launeau P., Archanjo C. J., Picard D., Arbaret L., Robin P.Y. (2010). Two- and three-dimensional shape fabric analysis by the intercept method in grey levels. Tectonophysics, Volume 492, Issues 1-4, 20 September 2010, Pages 230-239

Application to the Pocinhos granite (Brazil)

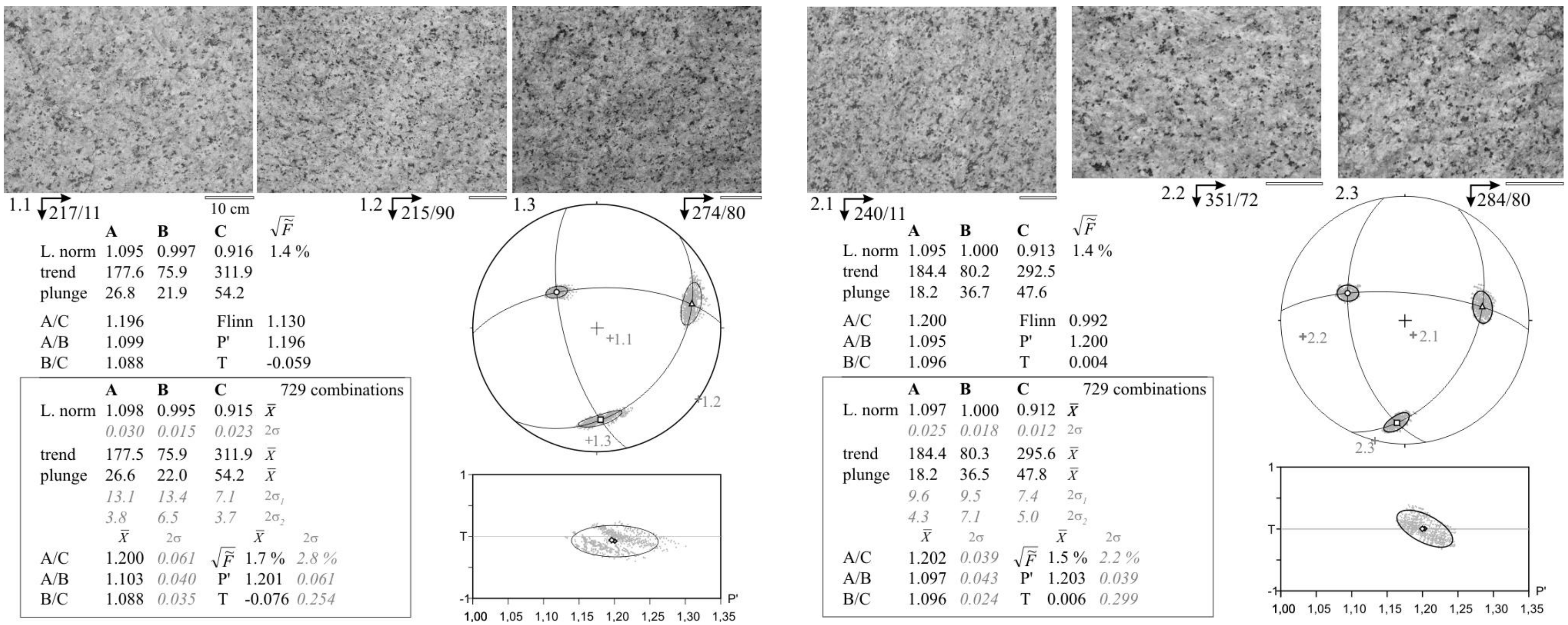

Launeau P., Archanjo C. J., Picard D., Arbaret L., Robin P.Y. (2010). Two- and three-dimensional shape fabric analysis by the intercept method in grey levels. Tectonophysics, Volume 492, Issues 1-4, 20 September 2010, Pages 230-239

Application to sandstones

Application to maximum polarized light, using Fueten and Goodchild (2001) methodology; thin sections of sandstones from the Devonian beds of the Furnas Formation (Brazil)

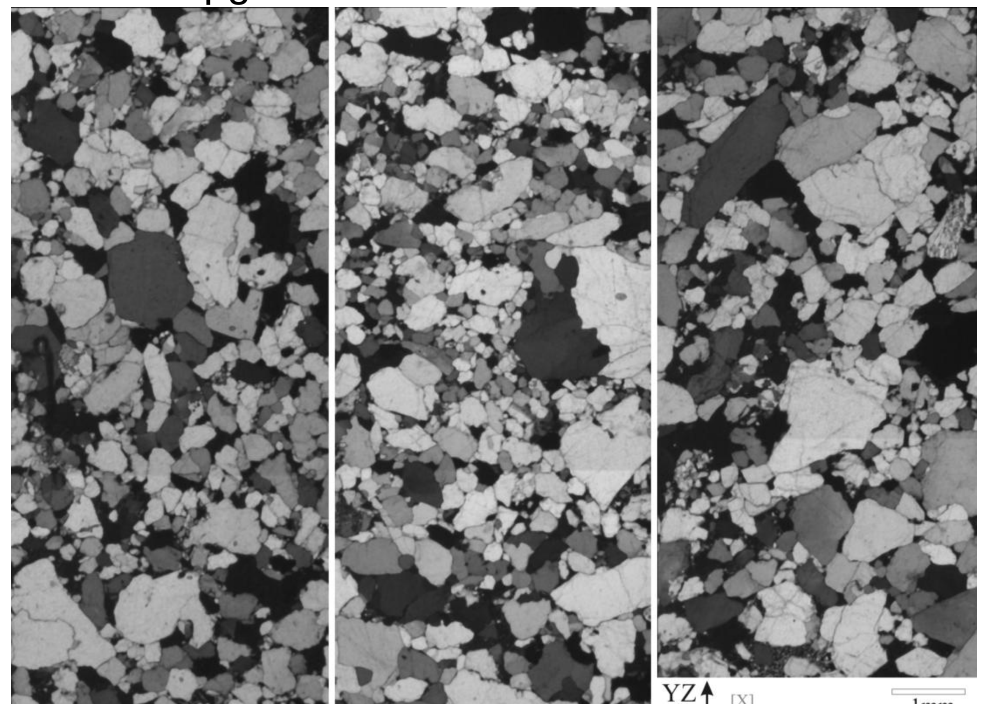

	A	B	C	$\sqrt{F}$
L. norm	1.054	1.014	0.936	2.3%
trend	212.3	312.4	81.7	
plunge	23.0	22.4	56.9	

A/C	1.127	Flinn	0.482
A/B	1.040	P'	1.129
B/C	1.083	T	0.339

	A	B	C	729 combinations
L. norm	1.060	1.011	0.933	$\bar{X}$
	0.024	*0.019*	*0.023*	2σ
trend	214.1	314.2	82.4	$\bar{X}$
plunge	23.5	21.0	57.9	$\bar{X}$
	35.5	*35.8*	*19.1*	$2\sigma_1$
	12.8	*17.0*	*11.1*	$2\sigma_2$

	$\bar{X}$	2σ		$\bar{X}$	2σ
A/C	1.137	*0.050*	$\sqrt{F}$	1.9 %	*2.8 %*
A/B	1.048	*0.035*	P'	1.140	*0.051*
B/C	1.085	*0.042*	T	0.269	*0.457*

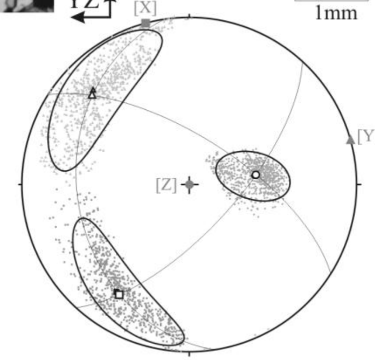

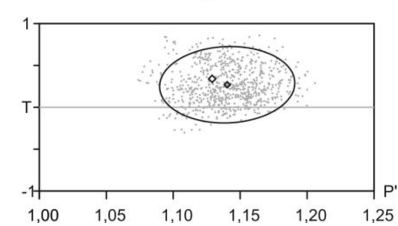

Launeau P., Archanjo C. J., Picard D., Arbaret L., Robin P.Y. (2010). Two- and three-dimensional shape fabric analysis by the intercept method in grey levels. Tectonophysics, Volume 492, Issues 1-4, 20 September 2010, Pages 230-239

Application to a chilled margin of a diabase dike

Application to maximum polarized light, using Fueten and Goodchild (2001) methodology; The specimen comes from about 3 cm from the margin of a Mesozoic diabase dike (Rio Ceará-Mirim swarm, NE Brazil)

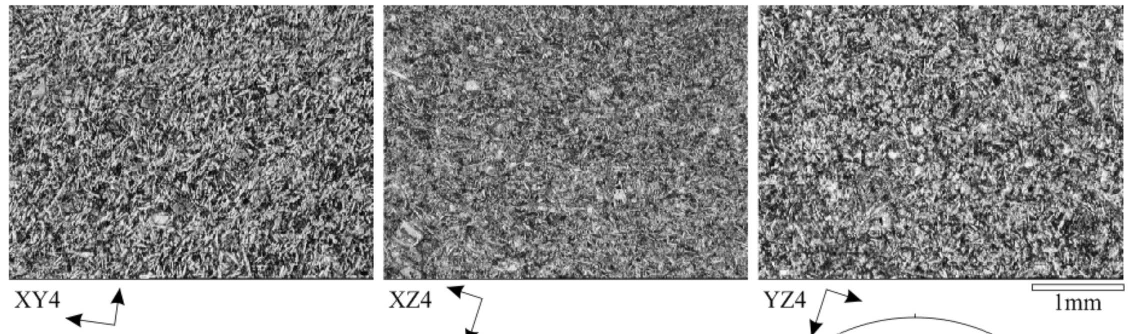

	A	B	C	$\sqrt{\tilde{F}}$
L. norm	1.105	0.960	0.942	2.1%
trend	240.2	338.8	140.3	
plunge	9.4	42.3	46.2	

A/C	1.173	Flinn	7.974
A/B	1.151	P'	1.191
B/C	1.019	T	-0.765

	A	B	C	4096 combinations
L. norm	1.106	0.962	0.941	$\bar{x}$
	0.010	*0.010*	*0.009*	2σ
trend	240.2	339.1	140.6	$\bar{x}$
plunge	9.3	43.3	45.1	$\bar{x}$
	4.5	*33.7*	*33.7*	$2\sigma_1$
	3.2	*4.3*	*3.5*	$2\sigma_2$

	$\bar{x}$	2σ		$\bar{x}$	2σ
A/C	1.176	*0.018*	$\sqrt{\tilde{F}}$	4.6%	*1.8%*
A/B	1.150	*0.019*	P'	1.192	*0.018*
B/C	1.023	*0.019*	T	-0.727	*0.217*

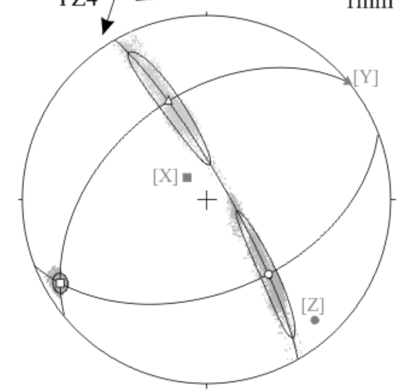

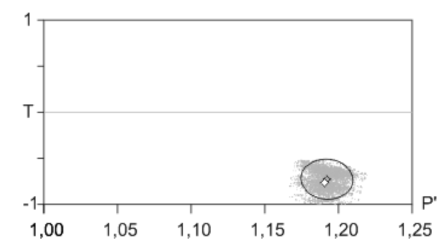

Launeau P., Archanjo C. J., Picard D., Arbaret L., Robin P.Y. (2010). Two- and three-dimensional shape fabric analysis by the intercept method in grey levels. Tectonophysics, Volume 492, Issues 1-4, 20 September 2010, Pages 230-239

Application to a chilled margin of a diabase dike

Application to maximum polarized light, using Fueten and Goodchild (2001) methodology; The specimen comes from about 3 cm from the margin of a Mesozoic diabase dike (Rio Ceará-Mirim swarm, NE Brazil)

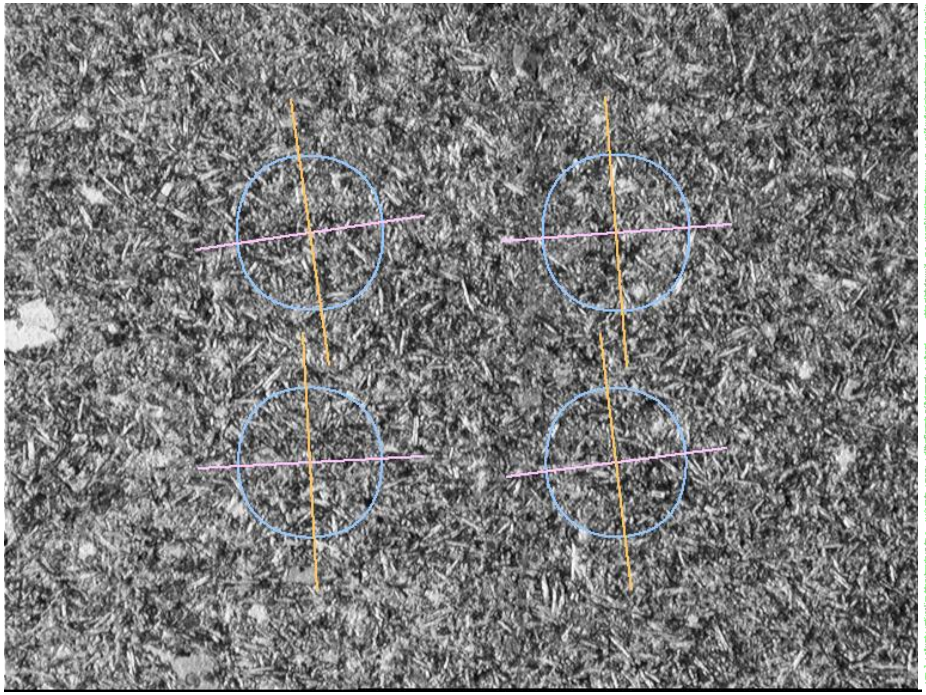

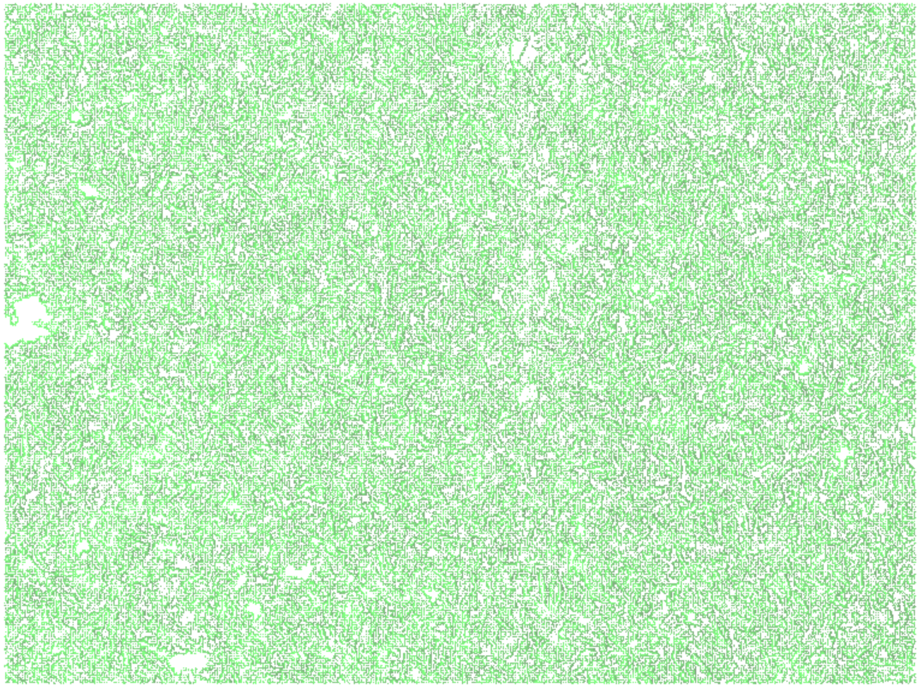

Cm28-3-XZ.bmp

Launeau P., Archanjo C. J., Picard D., Arbaret L., Robin P.Y. (2010). Two- and three-dimensional shape fabric analysis by the intercept method in grey levels. Tectonophysics, Volume 492, Issues 1-4, 20 September 2010, Pages 230-239